

1995

Characterization of PR500 for Use in Resin Transfer Molding

Rhonda Michelle Barksdale
College of William & Mary - Arts & Sciences

Follow this and additional works at: <https://scholarworks.wm.edu/etd>



Part of the [Polymer Chemistry Commons](#), and the [Polymer Science Commons](#)

Recommended Citation

Barksdale, Rhonda Michelle, "Characterization of PR500 for Use in Resin Transfer Molding" (1995).
Dissertations, Theses, and Masters Projects. William & Mary. Paper 1539625975.
<https://dx.doi.org/doi:10.21220/s2-rkfx-gj48>

This Thesis is brought to you for free and open access by the Theses, Dissertations, & Master Projects at W&M ScholarWorks. It has been accepted for inclusion in Dissertations, Theses, and Masters Projects by an authorized administrator of W&M ScholarWorks. For more information, please contact scholarworks@wm.edu.

**CHARACTERIZATION OF PR500
FOR USE IN RESIN TRANSFER MOLDING**

A Thesis

Presented to the Department of Chemistry
The College of William and Mary in Virginia

In Partial Fulfillment
of the Requirements for the Degree of
Master of Arts

by

Rhonda Michelle Barksdale
1995

APPROVAL SHEET

This thesis is submitted in partial fulfillment
of the requirements for the degree of
Master of Arts

Rhonda Michelle Burkholder

Approved, August 1995

David E. Kranbuehl
David E. Kranbuehl

Gary W. Rice
Gary W. Rice

David W. Thompson
David W. Thompson

TABLE OF CONTENTS

	Page
ACKNOWLEDGEMENTS	v
LIST OF FIGURES	vi
ABSTRACT	xii
CHAPTER I. INTRODUCTION	1
CHAPTER II. THEORY AND INSTRUMENTATION	4
A. Capacitance and Permittivity	4
B. Frequency Dependent Electromagnetic Sensing	5
C. Differential Scanning Calorimetry	11
D. Kinetics	12
E. Rheology	13
F. Resin Transfer Molding	13
CHAPTER III. INTRODUCTION TO EPOXY SYNTHESIS	16
A. Properties	16
B. Synthesis	17
CHAPTER IV. CHARACTERIZING THE KINETICS AND VISCOSITY OF PR500	21
A. Kinetics Analysis	21
B. Calibrations	36
CHAPTER V. MONITORING OF RESIN TRANSFER MOLDING EXPERIMENTS	46
A. Correlations	46
B. First RTM Run - DH071394	48
C. Second RTM Run - DH012795	59
D. Third RTM Run - DH032495	67
E. Fourth RTM Run - DH032995	77

F. Fifth RTM Run - DH033195	87
CHAPTER IV. CONCLUSIONS	94
VITA	97

ACKNOWLEDGEMENTS

I would like to thank Dr. Kranbuehl for his understanding and guidance during my graduate research. I would also like to thank David Hood and Leslie McCullough for their friendship and support.

This thesis is dedicated to my father and in loving memory of my mother. Thank you for the encouragement and support I received for many years.

LIST OF FIGURES

<u>Figure</u>	<u>Page</u>
2.1 Illustration of Polarization Due to an Induced Electric Field	4
2.2 Schematic Diagram of the FDEMS Apparatus	6
2.3 Pictorial Representation of DekDyne Sensor	6
2.4 Illustration of FDEMS Isothermal Cure	10
2.5 Schematic Diagram of Sample Cells in the Perkin-Elmer DSC	11
3.1 Reaction of Epoxy	16
3.2 Diglycidyl Ether of Fluorene Bisphenol	17
3.3 Epichlorohydrin and Bisphenol	18
3.4 Diglycidyl Ether of Bisphenol	18
3.5 Reaction of Epoxy Systems	19
4.1a DSC Isothermal Cure of PR500 @ 160°C	22
4.1b DSC Isothermal Cure of PR500 @ 170°C	22
4.1c DSC Isothermal Cure of PR500 @ 180°C	23
4.1d DSC Isothermal Cure of PR500 @ 190°C	23
4.1e DSC Isothermal Cure of PR500 @ 200°C	24
4.2 Ln K versus 1/T for PR500	26
4.3a Experimental and Theoretical α versus Time at 160°C	27
4.3b Experimental and Theoretical α versus Time at 170°C	27
4.3c Experimental and Theoretical α versus Time at 180°C	28
4.3d Experimental and Theoretical α versus Time at 190°C	28
4.3e Experimental and Theoretical α versus Time at 200°C	29
4.4a Proposed Theoretical Fit, α versus Time at 160°C, Maussy	31
4.4b Proposed Theoretical Fit, α versus Time at 180°C, Maussy	31
4.4c Proposed Theoretical Fit, α versus Time at 200°C, Maussy	32
4.5a Proposed Theoretical Fit, α versus Time at 160°C, Loos	33
4.5b Proposed Theoretical Fit, α versus Time at 170°C, Loos	33
4.5c Proposed Theoretical Fit, α versus Time at 180°C, Loos	34
4.5d Proposed Theoretical Fit, α versus Time at 190°C, Loos	34
4.5e Proposed Theoretical Fit, α versus Time at 200°C, Loos	35
4.6a FDEMS Isothermal Cure of PR500 @ 160°C	38
4.6b FDEMS Isothermal Cure of PR500 @ 170°C	38
4.6c FDEMS Isothermal Cure of PR500 @ 180°C	39
4.7a Alpha and Eta versus $\log e''w$ for 160°C Calibration	40
4.7b Alpha and Eta versus $\log e''w$ for 170°C Calibration	40
4.8 Slope ($de''/dt/e''$) and alpha versus time for 180°C Calibration using One Point Method at 5 Khz	41

LIST OF FIGURES (continued)

4.9a Slope ($de'/dt/e'$) and alpha versus Time for 180°C Calibration using One Point Method at 500 Hz	42
4.9b Slope ($de'/dt/e'$) and alpha versus Time for 180°C Calibration using One Point Method at 5 Khz	42
4.10a Eta versus Time for Isothermal Cure of PR500 @ 160°C	43
4.10b Eta versus Time for Isothermal Cure of PR500 @ 170°C	43
4.10c Eta versus Time for Isothermal Cure of PR500 @ 180°C	44
4.11 $\log e''*w$ versus Eta for 160°C, 170°C, 180°C	45
5.1a FDEMS output for RTM run at NASA Langley 07/13/94 Probe #1	50
5.1b FDEMS output for RTM run at NASA Langley 07/13/94 Probe #2	50
5.1c FDEMS output for RTM run at NASA Langley 07/13/94 Probe #3	51
5.1d FDEMS output for RTM run at NASA Langley 07/13/94 Probe #4	51
5.1e FDEMS output for RTM run at NASA Langley 07/13/94 Probe #5	52
5.1f FDEMS output for RTM run at NASA Langley 07/13/94 Probe #6	52
5.2a Viscosity Correlation with RTM at NASA Langley DH071394 Probe #1	53
5.2b Viscosity Correlation with RTM at NASA Langley DH071394 Probe #2	53
5.2c Viscosity Correlation with RTM at NASA Langley DH071394 Probe #3	54
5.2d Viscosity Correlation with RTM at NASA Langley DH071394 Probe #4	54
5.2e Viscosity Correlation with RTM at NASA Langley DH071394 Probe #5	55
5.2f Viscosity Correlation with RTM at NASA Langley DH071394 Probe #6	55
5.2g Degree of Cure Correlation with RTM at NASA Langley dh071394 Probe #1	56
5.2h Degree of Cure Correlation with RTM at NASA Langley dh071394 Probe #2	56
5.2i Degree of Cure Correlation with RTM at NASA Langley dh071394 Probe #3	57

LIST OF FIGURES (continued)

5.2j	Degree of Cure Correlation with RTM at NASA Langley dh071394 Probe #4	57
5.2k	Degree of Cure Correlation with RTM at NASA Langley dh071394 Probe #5	58
5.2l	Degree of Cure Correlation with RTM at NASA Langley dh071394 Probe #6	58
5.3	Diagram of RTM Plate Used in Experiment DH071394	49
5.4a	FDEMS output for RTM run at NASA Langley 01/27/95 Probe #1	61
5.4b	FDEMS output for RTM run at NASA Langley 01/27/95 Probe #2	61
5.4c	FDEMS output for RTM run at NASA Langley 01/27/95 Probe #3	62
5.4d	FDEMS output for RTM run at NASA Langley 01/27/95 Probe #4	62
5.4e	FDEMS output for RTM run at NASA Langley 01/27/95 Probe #5	63
5.4f	FDEMS output for RTM run at NASA Langley 01/27/95 Probe #6	63
5.5a	Viscosity Correlation with RTM at NASA Langley DH012795 Probe #1	64
5.5b	Viscosity Correlation with RTM at NASA Langley DH012795 Probe #6	64
5.5c	Degree of Cure Correlation with RTM at NASA Langley DH012795 Probe #1 - Maussy	65
5.5d	Degree of Cure Correlation with RTM at NASA Langley DH012795 Probe #1 - Loos	65
5.5e	Degree of Cure Correlation with RTM at NASA Langley DH012795 Probe #6 - Maussy	66
5.5f	Degree of Cure Correlation with RTM at NASA Langley DH012795 Probe #6 - Loos	66
5.6	Diagram of RTM Plate Used in Experiment DH012795	60
5.7a	FDEMS output for RTM run at NASA Langley 03/24/95 Probe #1 & #5	69
5.7b	FDEMS output for RTM run at NASA Langley 03/24/95 Probe #2 & #6	69

LIST OF FIGURES (continued)

5.7c	FDEMS output for RTM run at NASA Langley 03/24/95 Probe #3	70
5.7d	FDEMS output for RTM run at NASA Langley 03/24/95 Probe #4	70
5.8a	Viscosity Correlation with RTM at NASA Langley DH032495 Probe #3	71
5.8b	Viscosity Correlation with RTM at NASA Langley DH032495 Probe #4	71
5.8c	Viscosity Correlation with RTM at NASA Langley DH032495 Probe #5	72
5.8d	Viscosity Correlation with RTM at NASA Langley DH032495 Probe #6	72
5.8e	Degree of Cure Correlation with RTM at NASA Langley DH032495 Probe #3 - Maussy	73
5.8f	Degree of Cure Correlation with RTM at NASA Langley DH032495 Probe #3 - Loos	73
5.8g	Degree of Cure Correlation with RTM at NASA Langley DH032495 Probe #4 - Maussy	74
5.8h	Degree of Cure Correlation with RTM at NASA Langley DH032495 Probe #4 - Loos	74
5.8i	Degree of Cure Correlation with RTM at NASA Langley DH032495 Probe #5 - Maussy	75
5.8j	Degree of Cure Correlation with RTM at NASA Langley DH032495 Probe #5 - Loos	75
5.8k	Degree of Cure Correlation with RTM at NASA Langley DH032495 Probe #6 - Maussy	76
5.8l	Degree of Cure Correlation with RTM at NASA Langley DH032495 Probe #6 - Loos	76
5.9	Diagram of RTM Plate Used in Experiment DH032495	68
5.10a	FDEMS output for RTM run at NASA Langley 03/29/95 Probe #1 & #5	79
5.10b	FDEMS output for RTM run at NASA Langley 03/29/95 Probe #2 & #6	79
5.10c	FDEMS output for RTM run at NASA Langley 03/29/95 Probe #3	80
5.10d	FDEMS output for RTM run at NASA Langley 03/29/95 Probe #4	80

LIST OF FIGURES (continued)

5.11a Viscosity Correlation with RTM at NASA Langley DH032995 Probe #3	81
5.11b Viscosity Correlation with RTM at NASA Langley DH032995 Probe #4	81
5.11c Viscosity Correlation with RTM at NASA Langley DH032995 Probe #5	82
5.11d Viscosity Correlation with RTM at NASA Langley DH032995 Probe #6	82
5.11e Degree of Cure Correlation with RTM at NASA Langley DH032995 Probe #3 - Maussy	83
5.11f Degree of Cure Correlation with RTM at NASA Langley DH032995 Probe #3 - Loos	83
5.11g Degree of Cure Correlation with RTM at NASA Langley DH032995 Probe #4 - Maussy	84
5.11h Degree of Cure Correlation with RTM at NASA Langley DH032995 Probe #4 - Loos	84
5.11i Degree of Cure Correlation with RTM at NASA Langley DH032995 Probe #5 - Maussy	85
5.11j Degree of Cure Correlation with RTM at NASA Langley DH032995 Probe #5 - Loos	85
5.11k Degree of Cure Correlation with RTM at NASA Langley DH032995 Probe #6 - Maussy	86
5.11l Degree of Cure Correlation with RTM at NASA Langley DH032995 Probe #6 - Loos	86
5.12 Diagram of RTM Plate Used in Experiment DH032995	78
5.13a FDEMS output for RTM run at NASA Langley 03/31/95 Probe #1	89
5.13b FDEMS output for RTM run at NASA Langley 03/31/95 Probe #2	89
5.13c FDEMS output for RTM run at NASA Langley 03/31/95 Probe #3	90
5.14a Viscosity Correlation with RTM at NASA Langley DH033195 Probe #1	91
5.14b Viscosity Correlation with RTM at NASA Langley DH033195 Probe #2	91
5.14c Degree of Cure Correlation with RTM at NASA Langley DH033195 Probe #1 - Maussy	92

LIST OF FIGURES (continued)

5.14d Degree of Cure Correlation with RTM at NASA Langley DH033195 Probe #1 - Loos	92
5.14e Degree of Cure Correlation with RTM at NASA Langley DH033195 Probe #2 - Maussy	93
5.14f Degree of Cure Correlation with RTM at NASA Langley DH033195 Probe #2 - Loos	93
5.15 Diagram of RTM Plate Used in Experiment DH033195	88

ABSTRACT

In this study, PR500, an epoxy resin, was characterized. The resin's dielectric, thermal and rheometric properties were measured. Calibration curves were developed to predict viscosity and degree of cure. Frequency dependent electromagnetic sensing was used to monitor the wetout, viscosity, and degree of cure during five different RTM experiments. The flow rate, frame style, and port of injecting the resin were varied to determine models for different injection conditions. The wetout time, viscosity, and degree of cure were then compared for all five runs to predict the optimal conditions for the fabrication of the PR500 composite part using RTM.

CHARACTERIZATION OF PR500
FOR USE IN RESIN TRANSFER MOLDING

I. Introduction

Composites are composed of two or more different materials. Alone, each of these materials may not exhibit durability to pressure, temperature, or time. However, when these materials are mixed together, they possess new properties that can contribute to greater durability. There are several types of composites including the following: fiber composites, flake composites, particulate composites, filled composites, and laminar composites.¹

Composites made by resin transfer molding (RTM) are laminar composites. Laminar composites, also called layered composites, are strategically placed with the orientation of each layer differing from the one above it. The resulting composite then has more strength and an overall balance of properties. Therefore, the woven carbon fibers used in the RTM process reinforce the structure of the part.

For this study, frequency dependent electromagnetic sensors were placed in the bottom RTM plate. The sensors were used to monitor wetout, degree of cure, and viscosity during the entire RTM fabrication process. By monitoring dielectric behavior, the composite's properties were characterized in situ, in the mold. The

effectiveness of the injection pattern and the flow rate were evaluated from this characterization. Using this information it is possible to determine the best method for producing the composite. It is also possible to determine physical and chemical properties of PR500 in its final composite form.

References

1. Schwartz, M. M., *Composite Materials Handbook*, McGraw-Hill, New York, 1984.
2. Dusek, K., *Epoxy Resins and Composites II*, Springer - Verlag, New York, 1986.

Chapter II. Theory and Instrumentation

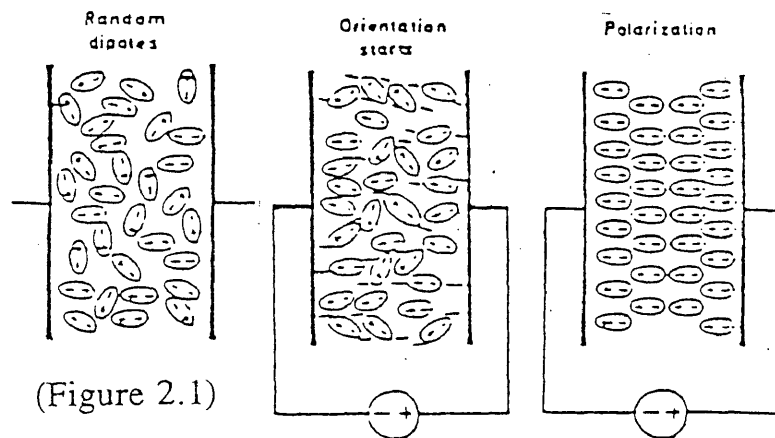
A. Capacitance and Permittivity

Capacitance (C) is the charge (q) on two parallel plates divided by the voltage (V_0) applied to the plates.

$$C_0 = \frac{q}{V_0}$$

[1]

If there is dielectric material between the plates, polarization of the molecules will occur due to the electrical field induced by the potential difference^{5,7}. When the material is first put between the plates, the orientation of the dipoles is random. Upon application of an external (electric) field, the positive and negative charges attempt to align themselves with the oppositely charged plate. Thus, the molecules become polarized. (Figure 2.1)



The dielectric constant, ϵ , also known as permittivity, can be defined as the ratio of the capacitance of a capacitor filled with dielectric material, C , divided by the capacitance of a capacitor in a vacuum, C_0 .

$$\epsilon = \frac{C}{C_0}$$

[2]

When an alternating electric field is applied, the direction of the dipolar molecules oscillates. At low frequencies, the dipoles are able to align themselves with the orientation of the field. At higher frequencies, the current of the electric field is faster, therefore one hundred percent alignment is more difficult.

B. Frequency Dependent Electromagnetic Sensing

Frequency dependent electromagnetic sensing (FDEMS) is a convenient method for measuring physical and chemical properties of polymeric systems. Impedance measurements are taken over the hertz to megahertz range. A Hewlett-Packard 4192A LF Impedance Analyzer and a Schlumberger-Solartron 1260 Impedance Gain-Phase Analyzer are used to take measurements. An illustration of the system used is given below. (Figure 2.2) FDEMS is able to measure various resin states and properties: solid, liquid, viscoelastic, T_g , etc. The ionic and dipolar mobility change with a change in state and as the viscoelastic properties change within a given state due to polymerization or temperature effects.

Therefore, changes in the state or properties of the resin may be studied from a oligomeric liquid to a crosslinked, insoluble, high temperature solid.¹

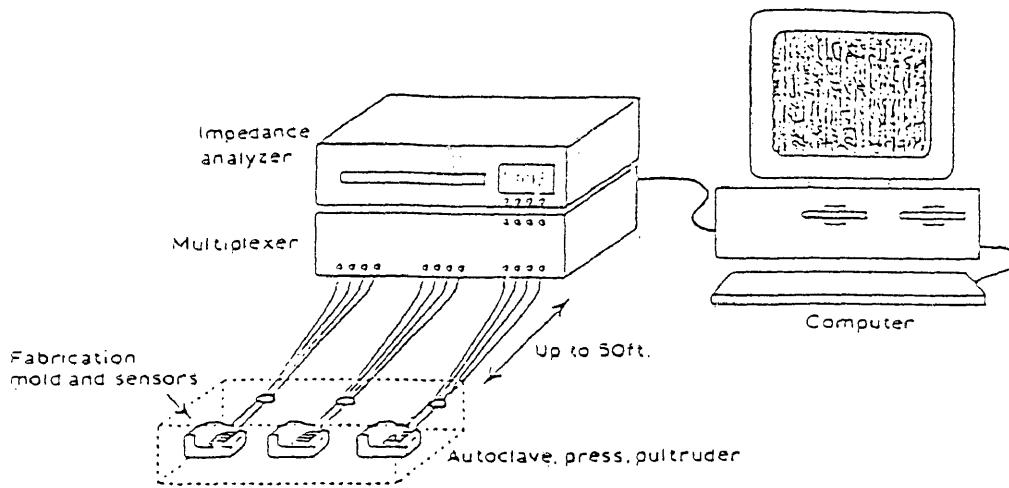


Figure 2.2

A flat DekDyne sensor is used to measure the capacitance and conductance from the dielectric impedance. This geometry independent microsensor consists of a fine array of two interdigitated comb electrodes. The sensor is inert and able to withstand temperatures exceeding 400°C, and pressures up to 1000 psi.⁶(Figure 2.3) The impedance with relation to capacitance and conductance is as follows:

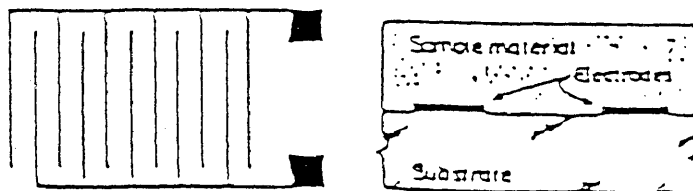


Figure 2.3

$$Z^{-1} = G + i\omega C$$

[3]

where

$$\omega = 2\pi f$$

[4]

Z is the electrode impedance induced by the ions, G is conductance, C is capacitance, and f is frequency.

The intensive geometry independent complex permittivity, $\epsilon^* = \epsilon' - i\epsilon''$, can be determined from both capacitance and conductance which are sample geometry dependent.

$$\epsilon' = \frac{C_{material}}{C_o}$$

[5]

$$\epsilon'' = \frac{G_{material}}{C_o \omega}$$

[6]

where C_o is the air replaceable capacitance value.

The real and imaginary parts of ϵ^* have dipolar and ionic components.

$$\epsilon' = \epsilon'_d + \epsilon'_i$$

[7]

$$\epsilon'' = \epsilon''_d + \epsilon''_i$$

[8]

The dipolar component arises from rotational diffusion of bound charge of molecular dipole moments. This term is most prevalent at high frequencies and in highly viscous media.^{1,2} The Cole-Davidson function is used to represent the frequency dependence of the polar component

$$\epsilon_d^* = \frac{(\epsilon_r - \epsilon_u)}{(1 - i2\pi f\tau)^{\beta + \epsilon_u}}$$

[9]

where ϵ_r and ϵ_u are the limiting low and high frequency values of ϵ_d , τ is the dipolar relaxation time and β is the relaxation time distribution ($0 < \beta < 1$) which is the Cole-Davidson parameter. The parameter is one if there is only one variable. If there are a variety of constants such as a multiplicity of rate constants and rate controlling mechanisms, the parameter will be less than one.

The ionic component ϵ_i^* , which results from translational diffusion of charge, dominates at lower frequencies, low viscosities, and high temperatures.² Johnson and Cole derived equations for the ionic contribution to ϵ^*

$$e' = C_o Z_o \sin \frac{(n\pi)}{2} \omega^{-(n+1)} \left(\frac{\sigma}{8.85 \times 10^{-14}} \right)^2$$

[10]

$$e_i = \frac{\sigma}{8.85 \times 10^{-14} \omega} - C_o Z_o \cos \frac{(n\pi)}{2} \omega^{-(n+1)} \left(\frac{\sigma}{8.85 \times 10^{-14}} \right)^2$$

[11]

where σ is the conductivity ($\text{ohm}^{-1} \text{cm}^{-1}$). The first term in equation 11 expresses the conductance of ions translating through the medium. The second term is due to the charge polarization effects. The second term makes frequency measurements increasingly difficult to use and interpret at lower frequencies.²

An illustration of a dielectric run is given in Figure 2.4. The region where all of the frequency bands converge is dominated by ionic translational diffusion. The region where the bands diverge represents dipolar rotational diffusion. When the frequencies begin to separate, the crosslinking network of the epoxy-amine resin increases along with the viscosity and degree of cure.

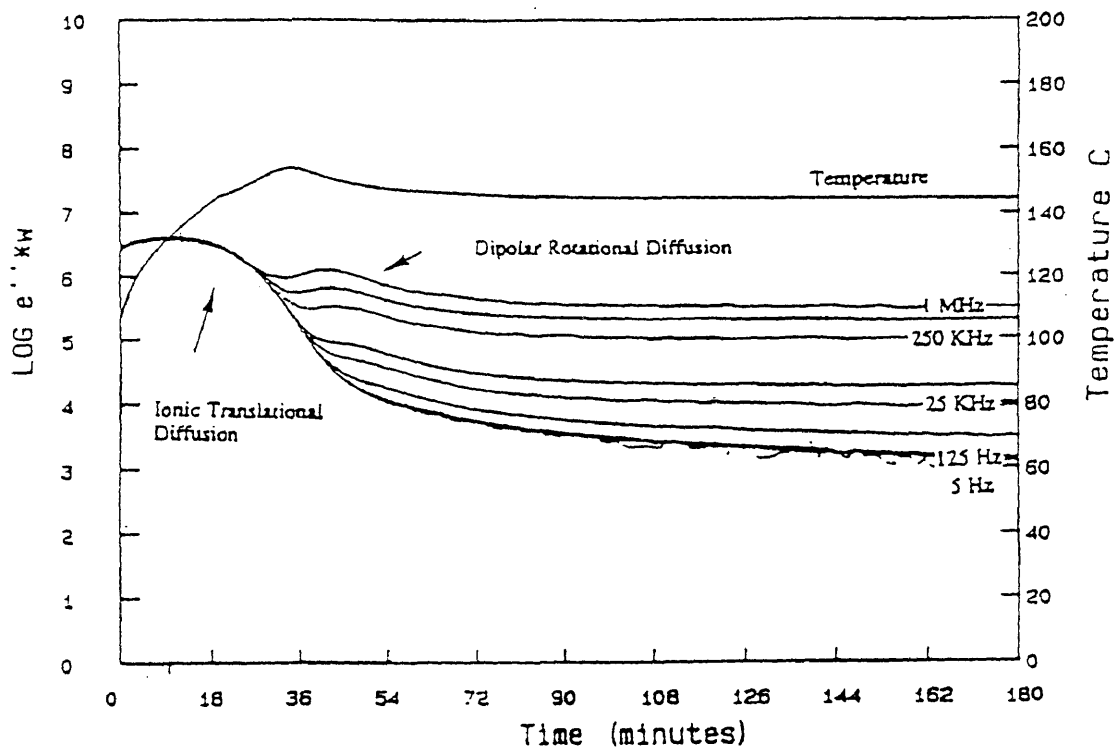


Figure 2.4

C. DSC

The differential scanning calorimeter is used to investigate first and second order phase transitions in amorphous, and semi-crystalline polymers. First order transition is T_m , melting temperature, and second order transitions refer to T_g , glass transition temperatures. A Perkin-Elmer DSC-7 is used to take DSC measurements. The DSC measures the heat required to maintain the same temperature in the sample and the appropriate reference material as both are heated. The reference material undergoes no thermal transitions in the selected temperature range. An empty pan is the reference material. Aluminum pans are used both as reference and to hold approximately six milligrams of the epoxy resin.

Electric resistance heating is applied independently to the sample and reference material in two calorimetric cells. (Figure 2.5)

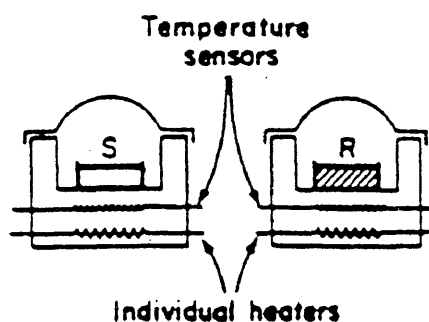


Figure 2.5

The difference in electrical power required to keep both pans at the same temperature is recorded and plotted as a function of temperature. Endothermic and

exothermic peaks may be seen depending on the amount of energy the sample may need to be maintained at the same temperature as the reference pan.

The area under the exothermic curve is the total heat used to give 100% cure.

$$H_R = \int \frac{dQ}{dt} dt$$

[12]

H_R is the heat of reaction and dQ/dt is the rate of heat generation. Degree of cure,

α_c , is expressed as

$$\alpha_c = \frac{H}{H_R}$$

[13]

H is the enthalpy of the sample.

D. Kinetics

In order to relate dielectric measurements and degree of cure, an appropriate kinetic model must be chosen. The rate of the chemical reaction depends on the reaction rate of the epoxide and amine groups.³ Because these groups can react in more than one way, the model is an approximation. Once a theoretical fit is generated from laboratory data, these curves are used to predict degree of cure in large samples during a RTM experiment.

E. Rheology

The rheometer is used to study the flow and deformation of an epoxy resin. A Rheometrics Dynamic Analyzer 700 is used in this study. Both stress and strain are measured as a function of time or temperature. From these measurements, other mechanical properties, such as G' and G'' , can be determined. G' is the measurement of the amount of energy that is stored in a material while being placed under strain. G'' is the stress 90° out of phase with the strain divided by the strain.

Gel point occurs when G' and G'' are equivalent. Gel point, which normally occurs around 1000 poise, is important because it reflects the time at which either the molecular weight or the crosslinked network is infinite.¹

F. Resin Transfer Molding

Composite fabrication by resin transfer molding (RTM) is accomplished by injecting resin into an enclosed fiber preform. Some advantages of RTM are higher production rates, more consistent parts, little or no worker exposure to toxic materials, and cost efficiency⁹.

The RTM process begins by degassing the resin to remove any entrapped air. Several layers of woven carbon fiber are then placed inside a mold cavity. The bottom plate contains strategically placed plugs with holes enabling the resin to

flow onto the sensors. The mold is heated. Pressure and vacuum are then applied to the mold. The degassed resin is injected into the enclosed preform. The mold is then heated to a higher temperature. At higher temperatures, the resin is advanced until it reaches full cure. Once the mold cools, it is opened, and the part can be removed.

References

1. Kranbuehl, D. E., "Cure Monitoring", *International Encyclopedia of Composites*, Vol. 1, VCH Publishers Inc., New York, 1990.
2. Kranbuehl, D. E., "Frequency - Dependent Dielectric Analysis", *Cross-Linked Polymers*, American Chemical Society, Washington, D. C., 1988.
3. M. G. Parthun and G. P. Johari, "Relaxations in Thermosets. 23. Dielectric Studies of Curing Kinetics of an Epoxide with Diamines of Varying Chain Lengths", *Macromolecules*, Vol. 25, 1992.
4. Kranbuehl, D. E., et al., "Dielectric properties of the polymerization of an aromatic polyimide", *Polymers*, Vol. 27, 1986.
5. Hart, Sean, Masters Thesis, "Intelligent Processing of PMR-15", College of William and Mary, 1992.
6. Short, Christina K., Masters Thesis, "Characterization of Epoxy Resins for Use in the Resin Transfer Molding Process", College of William and Mary, 1993.
7. Argiriadi, Maria A., Masters Thesis, "Characterization and Modeling of Amine Epoxide Resins", College of William and Mary, 1994.
8. Mallick, P. K., *Fiber-Reinforced Composites*, Second Edition, 1993.
9. Schwartz, M. M., *Composites Materials Handbook*, McGraw-Hill, New York, 1984.

Chapter III - Introduction to epoxy synthesis

An epoxy is a compound that has an oxygen atom bonded to two carbon atoms in a ring structure. An epoxy resin is any molecule that contains two or more alpha epoxy groups which can react to form a thermoset system.¹(Figure 3.1) A polymer is classified as a thermoset if it does not flow upon heating. A thermoset is the result of crosslinking the polymeric chains together to form a network.²

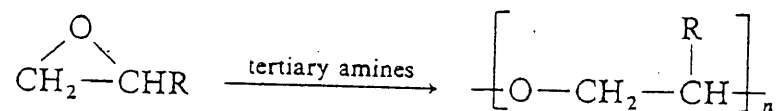


Figure 3.1

Properties

Epoxy resins have many useful properties. Liquid epoxy resins have low viscosity, quick and easy cure at a wide range of temperatures, and low shrinkage during the cure process. Epoxy resins also exhibit high adhesive strength which

during the cure process. Epoxy resins also exhibit high adhesive strength which helps to minimize the weakening of the resin. Furthermore, fully cured solid epoxy resins have good adhesion, thermal stability, and mechanical strength.³

Epoxy resins have many uses including adhesives, caulking, and aerospace technology.³ PR500 has been proposed for use in aerospace technology.

The exact structure of PR500 can not be disclosed because of its proprietary nature. The structure is based on diglycidyl ether of fluorene bisphenol.(Figure 3.2)⁷ It uses an amine of a similar structure plus a linear diamine. This study shows that PR500 reaches full cure after being held at 180°C for at least 90 minutes. Under these conditions, it is a thermoset.

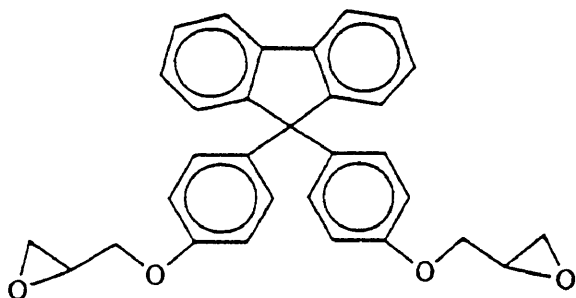


Figure 3.2

Synthesis

Epoxide polymerizations may occur by anionic or cationic catalysts.

Epichlorohydrin, an epoxide, and bisphenol A, a polyhydroxy compound, are the most common reactants in an epoxide synthesis. (Figure 3.3) The product formed is diglycidyl ether of bisphenol A (DGEBA).^{4,5} (Figure 3.4)

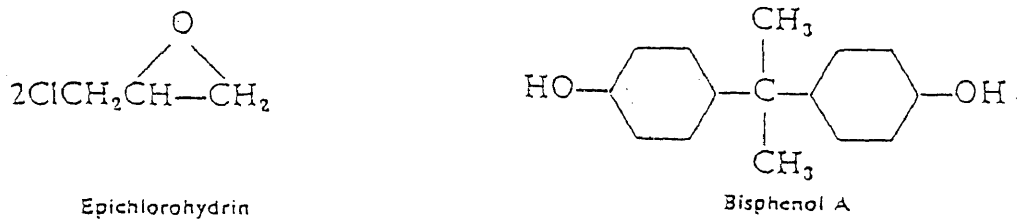


Figure 3.3

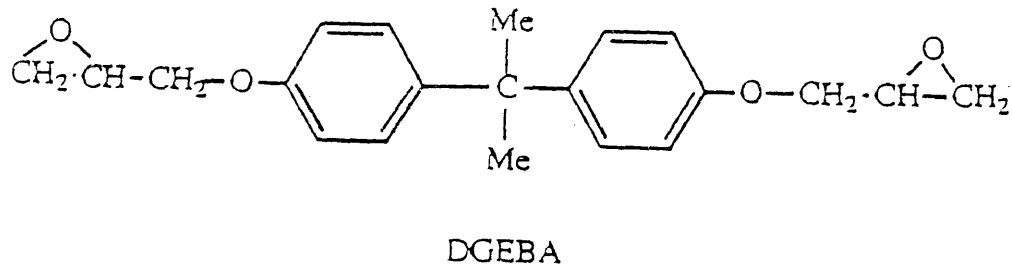


Figure 3.4

First, the chlorohydrin intermediate is formed in the presence of NaOH . Then the intermediate is dehydrohalogenated to DGEBA. (Figure 3.5)

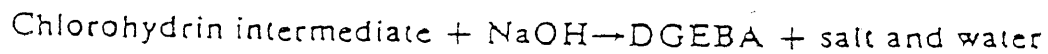
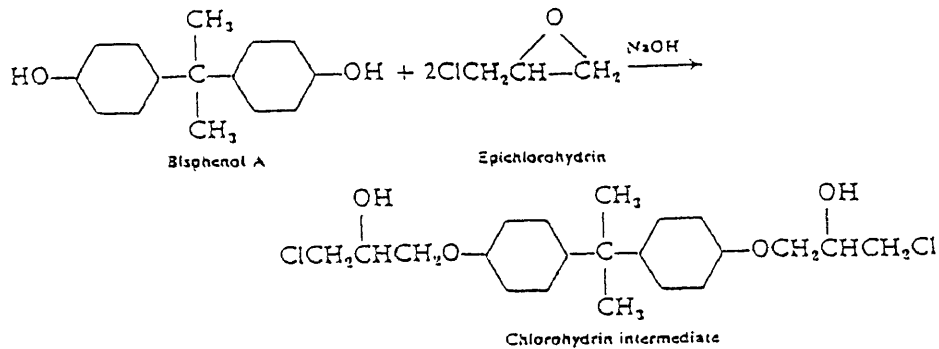


Figure 3.5

In order to have a high purity of DGEBA, there must be an excess of epichlorohydrin. Without the excess of epichlorohydrin, the bisphenol A compound will attack DGEBA instead of the epichlorohydrin resulting in the incorrect product.³

References

1. Dusek, K., *Epoxy Resins and Composites II*, Springer - Verlag, New York, 1986.
2. Sperling, H. L., *Introduction to Physical Polymer Science*, John Wiley & Sons, New York, 1986.
3. Lee and Neville, *Handbook of Epoxy Resins*, McGraw - Hill, New York, 1967.
4. Allcock, Harry R. and Lampe, Frederick W., *Contemporary Polymer Chemistry*, Second Edition, Prentice Hall Inc., New Jersey, 1990.
5. Short, Christina K., Master Thesis, "Characterization of Epoxy Resins for Use in the Resin Transfer Molding Process", College of William and Mary, 1993.
6. *Epoxy Resin Chemistry*, American Chemical Society, Washington, D. C., 1979.
7. 3M Aerospace Materials Department, "Material Safety Data Sheet."

Chapter IV. Characterizing the Kinetics and Viscosity of PR500

PR500 is a one-part epoxy resin developed by 3M to be manufactured for use in aerospace technology. The pre-mixed solid state of the epoxy allows the resin to be analyzed without the possibility of error due to mixing. The catalyst in PR500 melts at 145°C. In order to characterize PR500, the resin's dielectric, thermal, and rheometric properties were measured using Frequency Dependent Electromagnetic Sensing (FDEMS), differential scanning calorimetry (DSC), and rheometry, respectively. Calibration curves were developed for degree of cure and viscosity. Dielectric data was obtained during RTMs using Dekdyne sensors. Once data was obtained, degree of cure and viscosity were predicted.

Kinetic Analysis

Because of alpha's time and temperature dependency, several models were used to find theoretical values for degree of cure. First, experimental values of alpha and $d\alpha/dt$ were determined at isotherms of 160°C, 170°C, 180°C, 190°C, and 200°C, using the differential scanning calorimeter. (Figures 4.1a-4.1e) The autocatalytic equation $d\alpha/dt = k * \alpha^m(1-\alpha)^n$ was selected. Using a program

DSC Data File: prn15
Sample Weight: 8.900 mg
Wed Aug 04 15:46:54 1993
pr500 lot#214a3r NASA-LaRC

PERKIN-ELMER
7 Series Thermal Analysis System

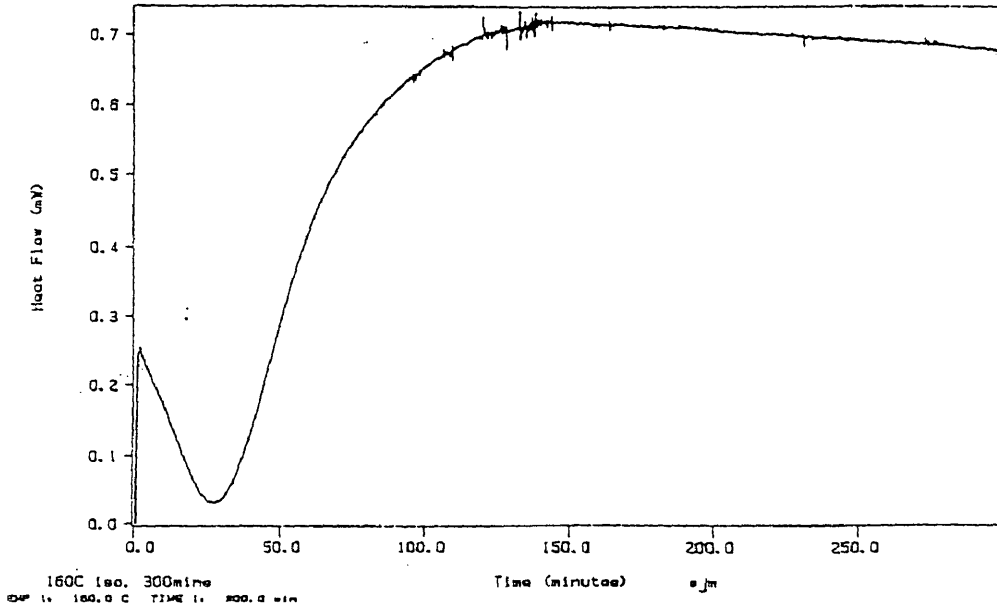


Figure 4.1a

DSC Data File: prn29
Sample Weight: 7.000 mg
Tue Nov 02 14:19:53 1993
pr500 lot # 214a3r

PERKIN-ELMER
7 Series Thermal Analysis System

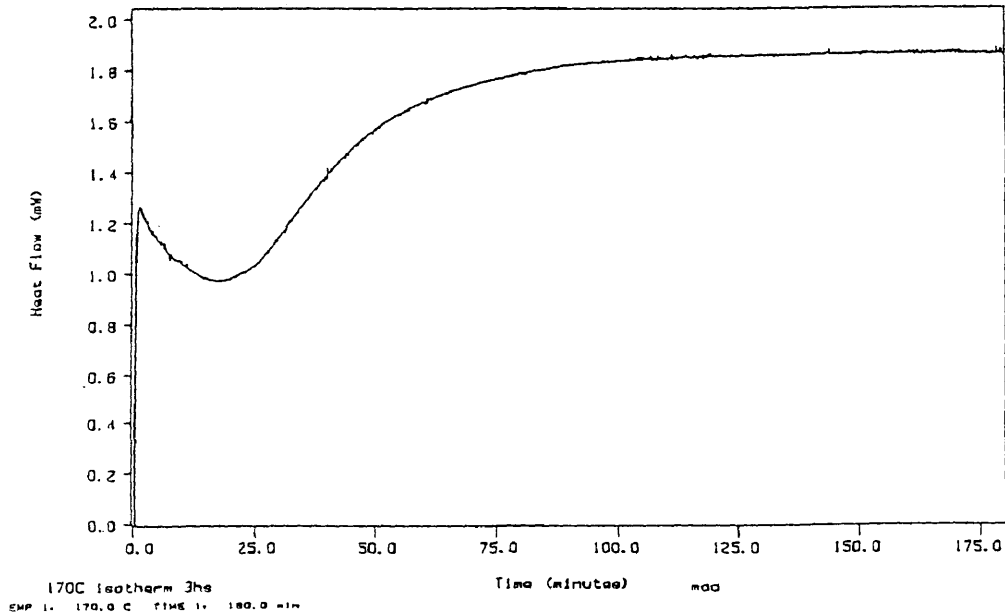


Figure 4.1b

DSC Data File: prn17
Sample Weight: 8.100 mg
Thu Aug 05 08:25:08 1993
pr500 lot#214a3r rec'd 2/25/93

PERKIN-ELMER

7 Series Thermal Analysis System

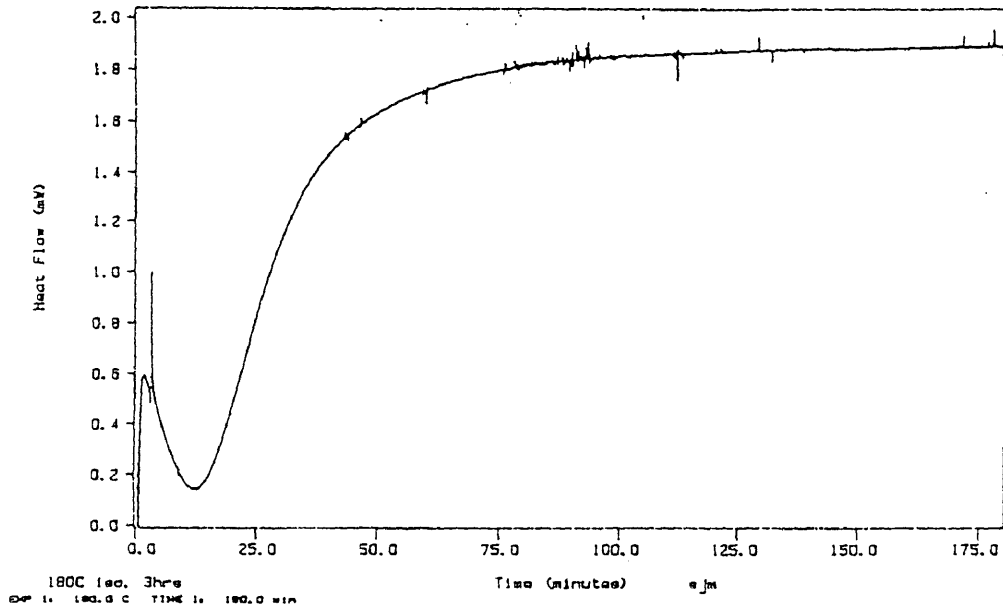


Figure 4.1c

DSC Data File: prn27
Sample Weight: 7.300 mg
Tue Nov 02 02:32:18 1993
pr500 lot#214a3r

PERKIN-ELMER

7 Series Thermal Analysis System

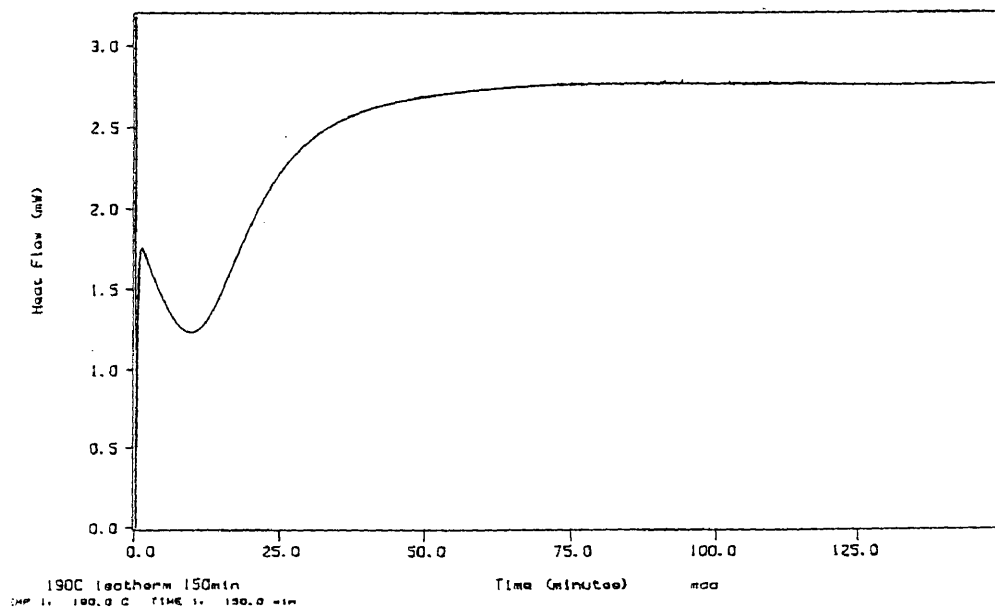


Figure 4.1d

DSC Data File: prn21
Sample Weight: 7.200 mg
Tue Aug 10 09:01:32 1993
pr500 lot#21403r rec'd 2/25/93

PERKIN-ELMER
7 Series Thermal Analysis System

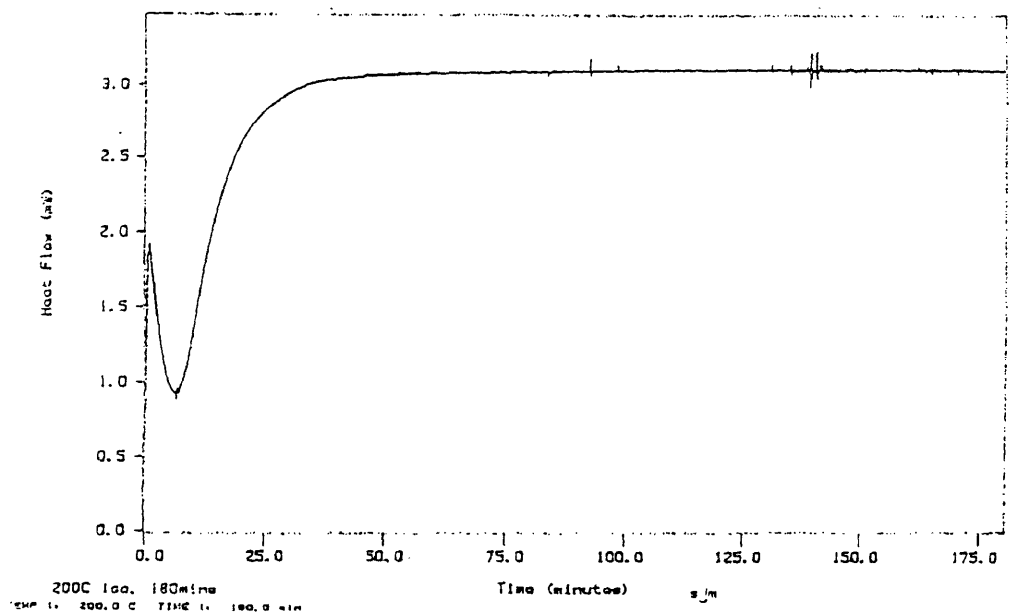


Figure 4.1e

created for SYSTAT®, values of k, M, and N were calculated at all five temperatures. A wide range of temperatures must be used because M and N are temperature dependant. A least square fit was used to generate these parameters. Optimal fits were generated for all five temperatures. The Arrhenius equation, $k = Ae^{-E/RT}$, or $\ln(k) = (-E/R) * 1/T + \ln(A)$, was used to backcalculate k where R is the ideal gas constant (1.987 cal/K-mol), A is a pre-exponential factor, and E is the activation energy constant. The natural log of the rate constants and 1/T were plotted to find the slope and the y-intercept.(Figure 4.2) A is the y-intercept and (-E/R) or B, is the slope. K was backcalculated using the average of A and B at all temperatures. The final equation used to calculate the desired parameters was $d\alpha/dt = (k * e^{-B/T}) * \alpha^M * (1-\alpha)^N$.(Figure 4.3a-4.3e) The parameters of the equation are as follows: B=501204; M=0.33; N=1.07 (Since M and N did not vary much over all temperatures, averaged values of M and N were used.)

<u>temperature(°C)</u>	<u>k (kJ/kmol)</u>
160	.042
170	.055
180	.070
190	.089
200	.110

The equation, $d\alpha/dt = (k1 + k2 * \alpha^M * (1-\alpha)^N)$, which was also used by Dr. Maussy at Georgia Tech, was then used. k1 yields the initial reaction rate assuming α equals zero when time equals zero. Again SYSTAT® and the

Ln K versus 1/T

Pr500 our fit

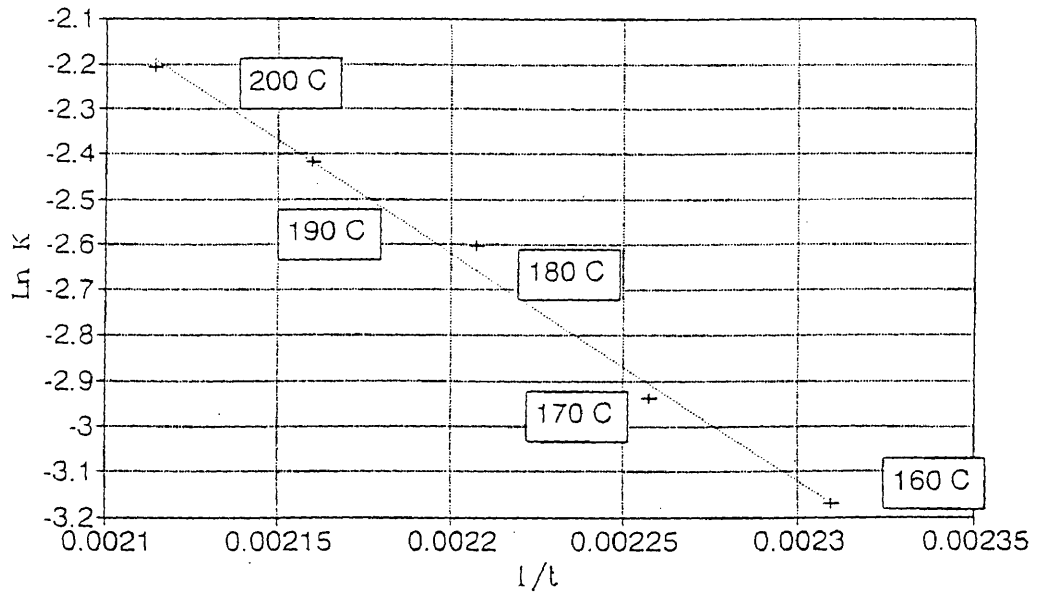


Figure 4.2

PR500 160C prn15
exp vs. theo alpha

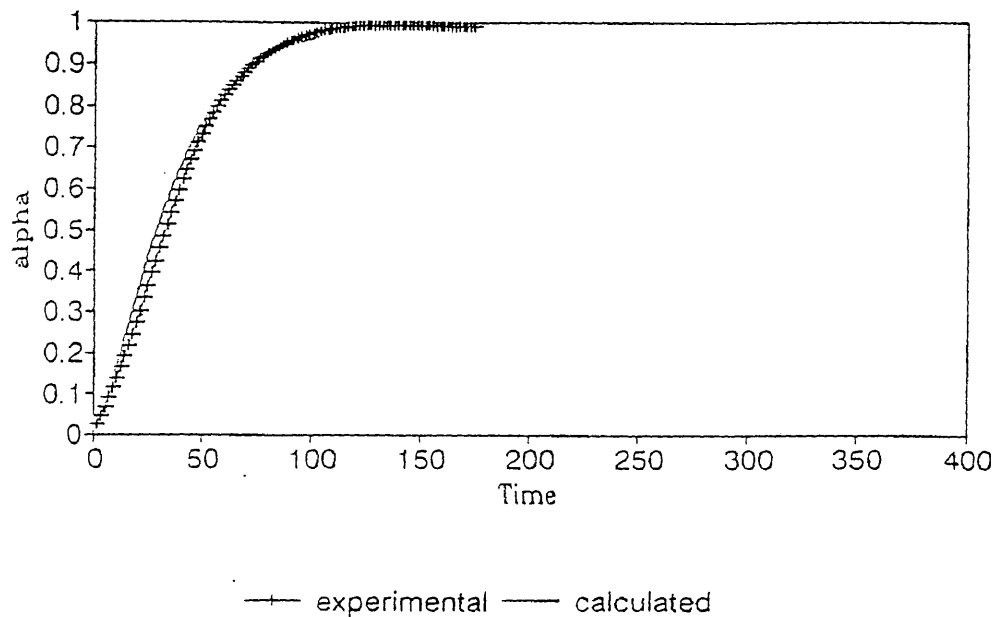


Figure 4.3a

PR500 170C prn29
exp vs. theo alpha

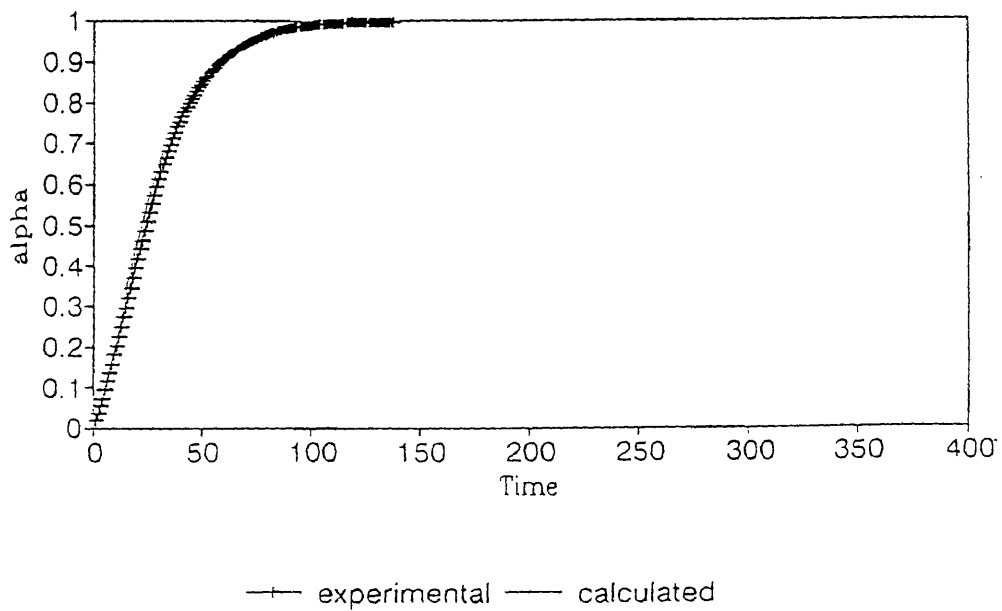


Figure 4.3b

PR500 180C prn17
exp vs. theo alpha

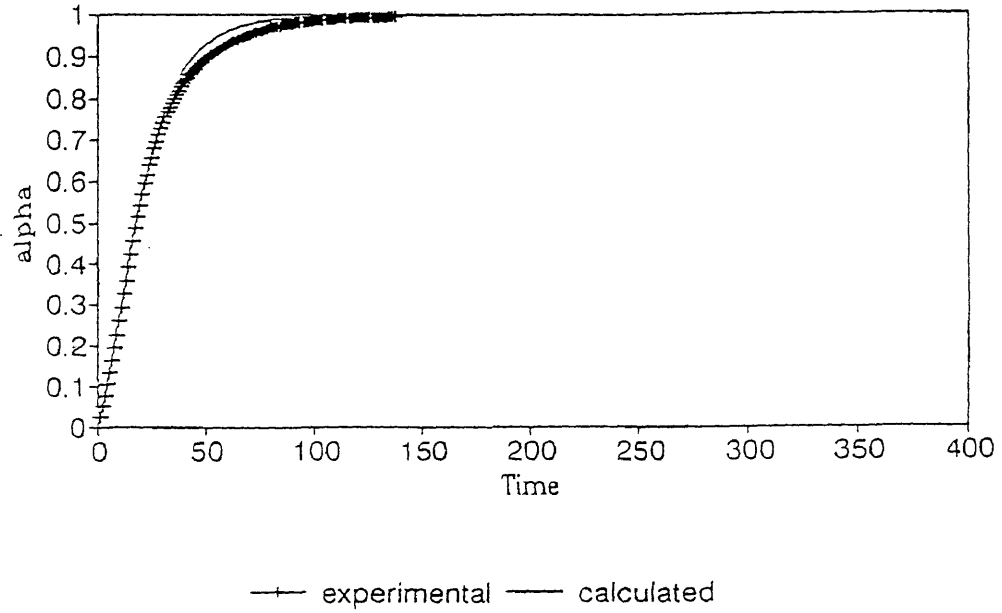


Figure 4.3c

PR500 190C prn27
exp vs. theo alpha

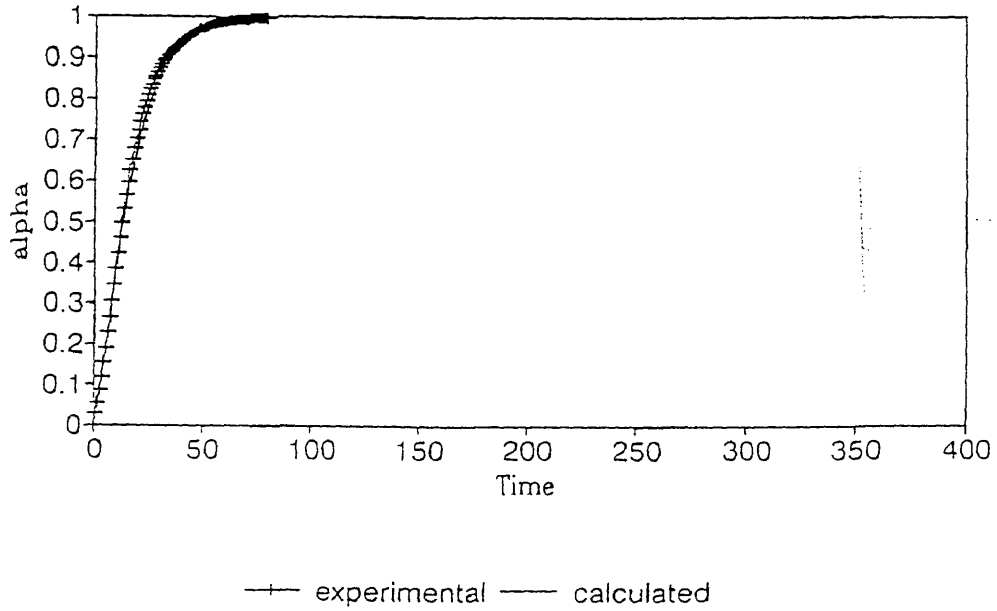


Figure 4.3d

PR500 200C prn21
exp vs. theo alpha

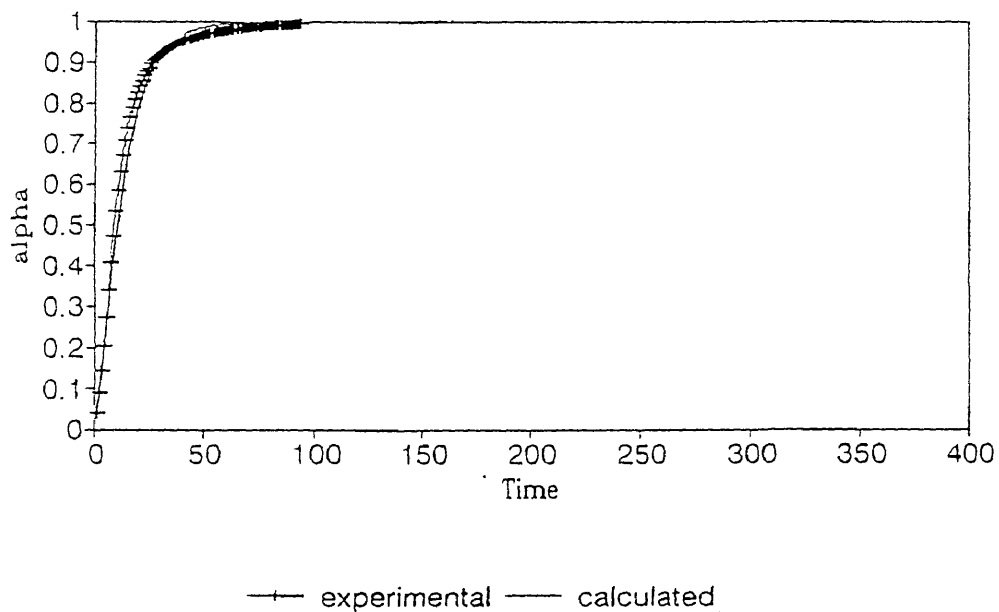


Figure 4.3e

Arrhenius equation were used to calculate the parameters k_1 , k_2 , M , and N . (Figure 4.4a-4.4c) $M = 0.70$ and $N = 1.10$

<u>temperature(°C)</u>	<u>k₁</u>	<u>k₂</u>
160	3.07E-3	0.0464
180	7.80E-3	0.0870
200	0.0183	0.154

Finally A. C. Loos from Virginia Polytechnical Institute who independently characterized the resin suggests the following parameters be used to generate k_1 and k_2 :

$$A_1 = 3.122 \times 10^6; \quad -E_1/R = -8.6016 \times 10^3 \text{ 1/K};$$

$$A_2 = 2.286 \times 10^4; \quad -E_2/R = -5.6005 \times 10^6 \text{ 1/K};$$

$$M = .9993 \quad N = 1.352$$

Loos' model was used to create our small sample calibration curve in addition to Maussy's model. (Figure 4.5a-4.5e) The curve was necessary because of variations from small and large samples.

The parameters used are the following:

<u>temperature(°C)</u>	<u>k₁</u>	<u>k₂</u>
160	.012316	.038418
170	.016192	.067298
180	.021031	.115010
190	.027010	.192040
200	.034240	.313800

Alpha vs. time

PR500 lot#214A3R rec'd 2/25/93 @LaRC

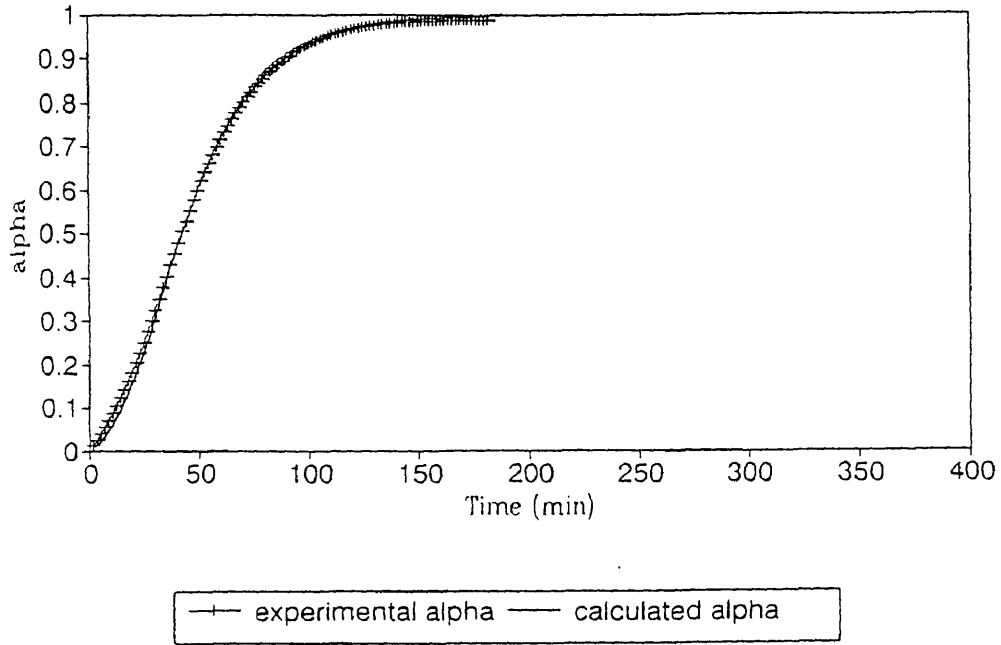


Figure 4.4a

Alpha vs. time

PR500 lot#214A3R rec'd 2/25/93 @LaRC

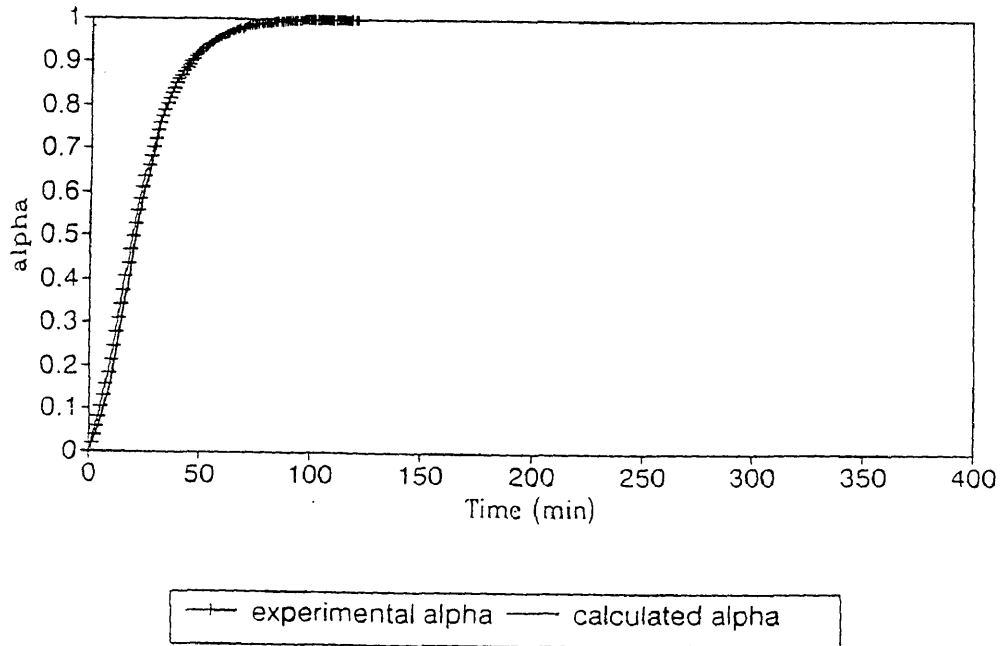


Figure 4.4b

Alpha vs. Time

PR500 lot#214A3R rec'd 2/25/93 @LaRC

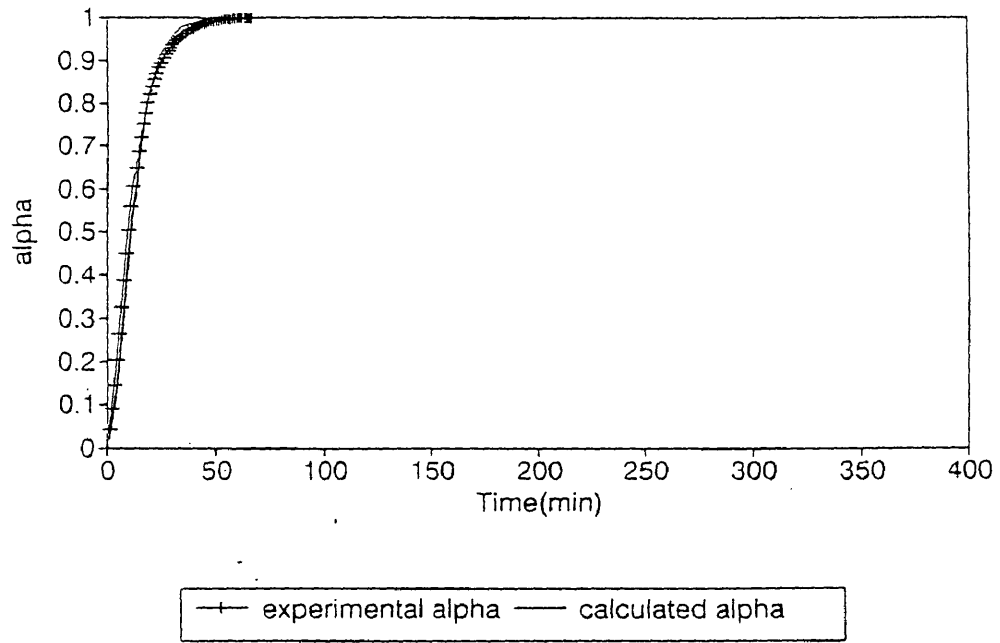


Figure 4.4c

PR500 exp fit vs Loos fit (95)

160 C

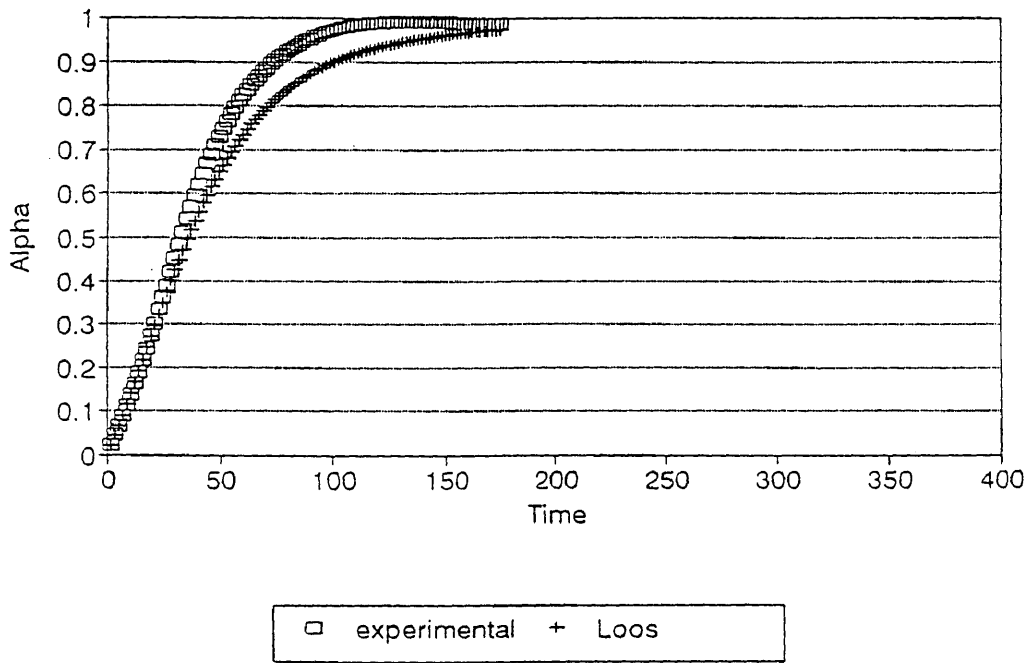


Figure 4.5a

PR500 exp fit vs Loos fit (95)

170 C

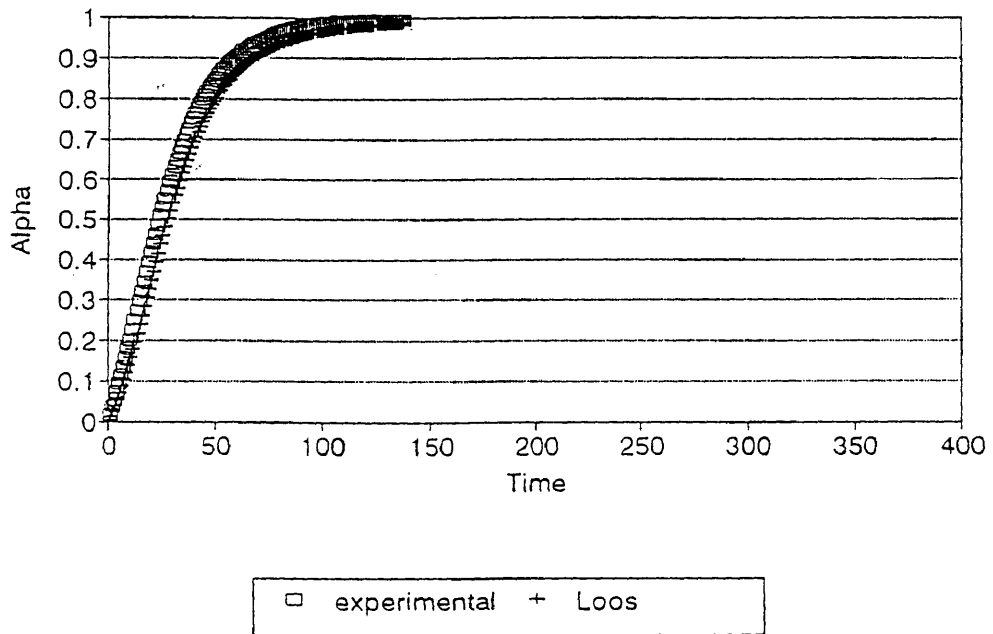


Figure 4.5b

PR500 exp fit vs Loos fit (95)
180 C

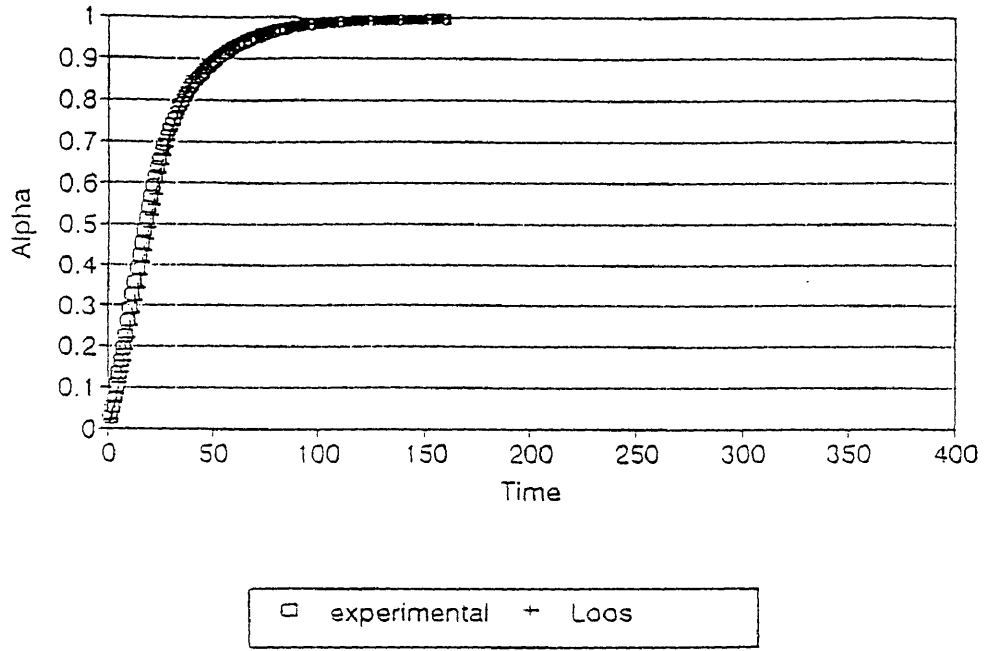


Figure 4.5c

PR500 exp fit vs Loos fit (95)
190 C

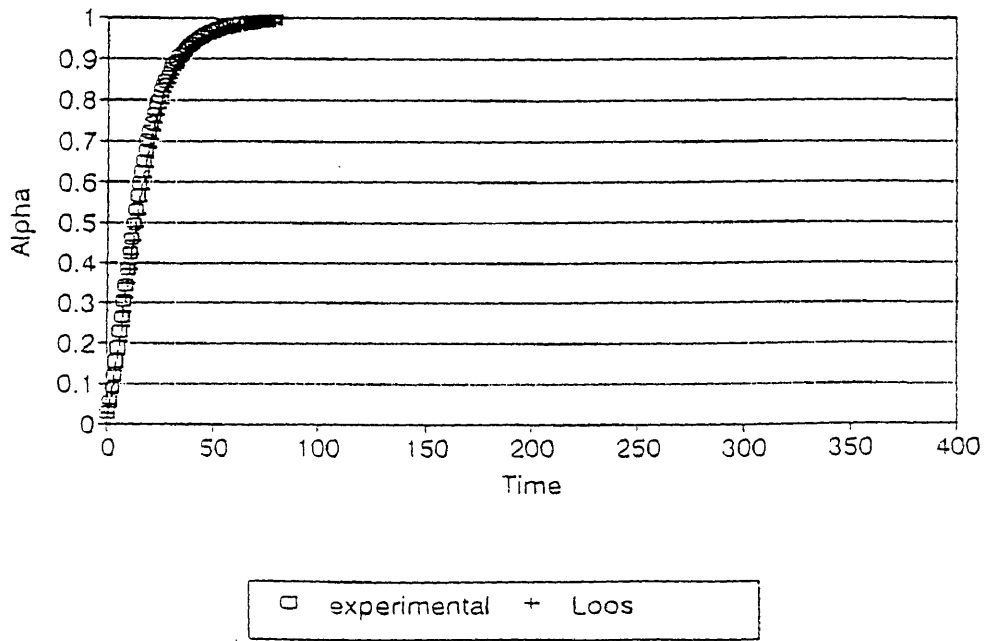


Figure 4.5d

PR500 exp fit vs Loos fit (95)
200 C

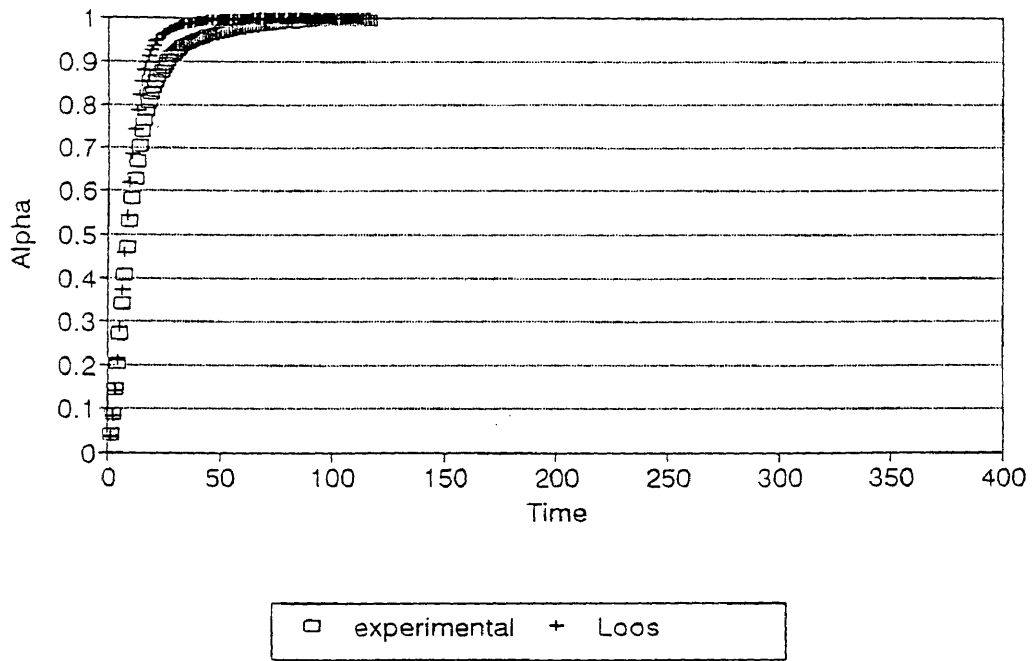


Figure 4.5e

Calibrations

In order to create the calibration curves, dielectric experiments on PR500 were performed at isotherms of 160°C, 170°C, and 180°C.(Figures 4.6a-4.6c) To predict degree of cure, experiments were also done on the DSC at the same temperatures.(Figures 4.1a-4.1c) Time zero was determined when the various isothermal dielectric experiments were within 4°C of desired temperature. Time zero was then subtracted from the rest of the times. The new times were matched with alphas (degree of cure) from Loos' model and Maussy's model. This data was used to model the calibration curves.(Figures 4.7a-4.7b)

At high temperatures, such as 180°C, the dielectric measurements at different frequencies begin to separate; therefore, the general ionic calibration curves can not be used to calculate alpha. Consequently, alpha was determined by the slope formula $(de''/dt)/e''$ at 5kHz.(Figure 4.8) The slope formula $(de'/dt)/e'$ was also used to calculate alpha for 500 Hz and 5 kHz. (Figures 4.9a-4.9b).

To predict viscosity, runs were done at 160°C, 170°C, 180°C on the rheometer. (Figures 4.10a-4.10c) Time zero was determined when temperature is within 4°C of desired temperature. Eta, η , (viscosity) was calibrated in the same manner as degree of cure. The dielectric data and the rheometer data corresponding to eta were used to calibrate the viscosity curves. Eta was measured from zero to 1000 poise.(Figures 4.7a-4.7c) Any information over 1000 poise was not relevant to the monitoring of viscosity. PR500 gels at about 1000

poise (units of eta). Gel point is when the viscous liquid transforms to a rubbery gel. The gel point is determined as the point when G' and G'' cross. Once gelation occurs, viscosity data is not a useful concept. The gelation times of the rheometric runs are as follows:

<u>Temperature</u>	<u>Time of Gelation (min)</u>
160	66
170	50
180	37

Once the viscosity calibration curves were generated, all temperatures were plotted on one graph yielding a slope of approximately -1.(Figure 4.11) This slope suggests an inverse linear relationship between the decreasing dielectric ionic mobility and increasing viscosity.

Data file: b:ar090894

Probe: 1

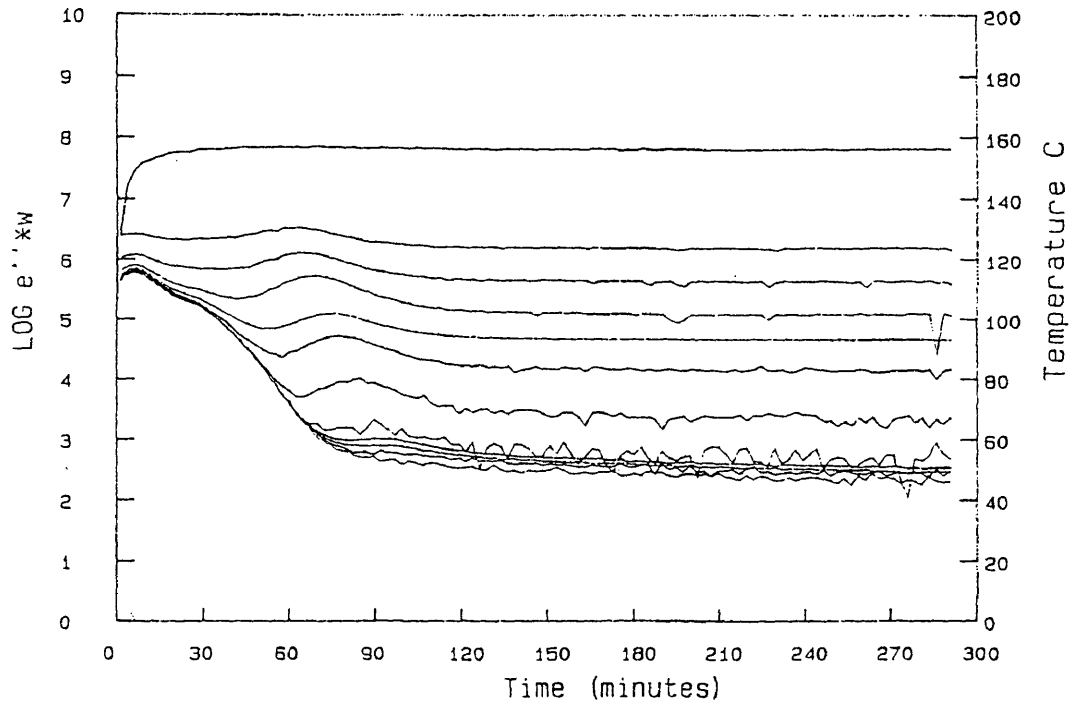


Figure 4.6a

Data file: b:rb091294.a

Probe: 1

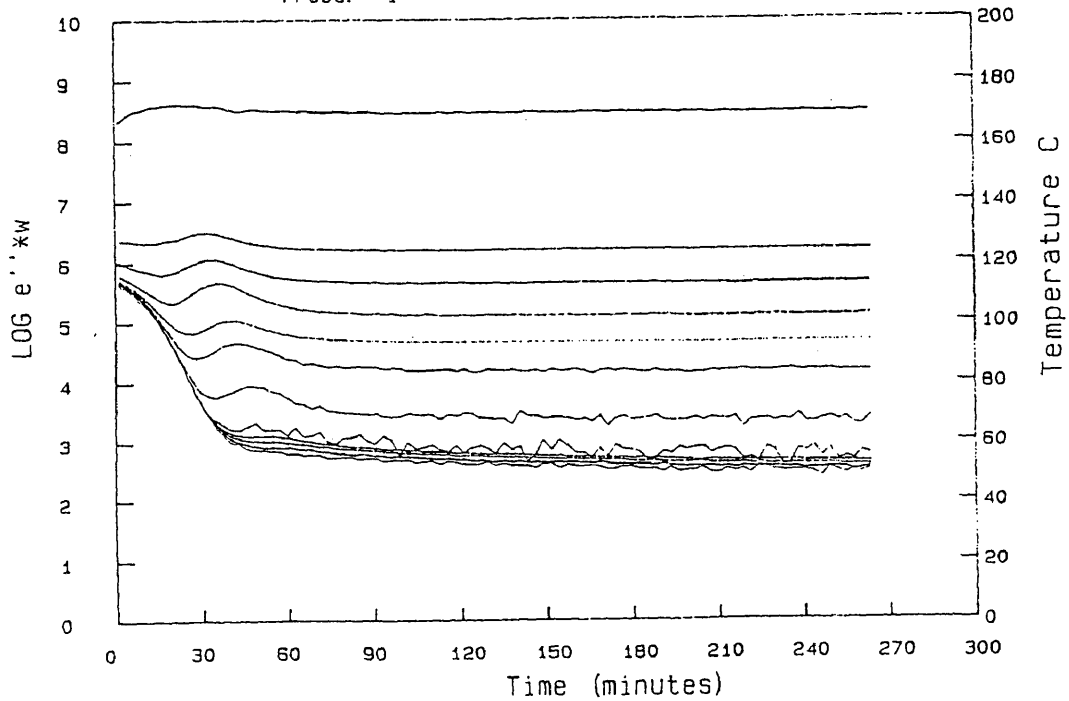


Figure 4.6b

Data file: b:ar090794
Probe: 1

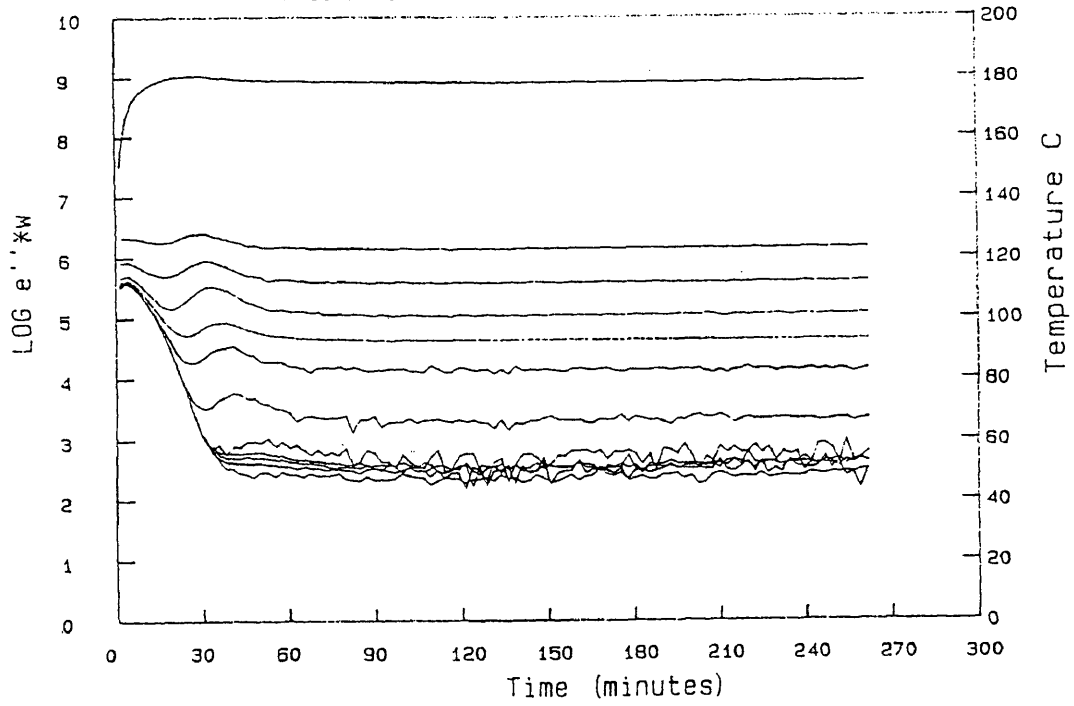


Figure 4.6c

PR500 160C isotherm (95)

Alpha and Eta vs. $\log(e''*w)$

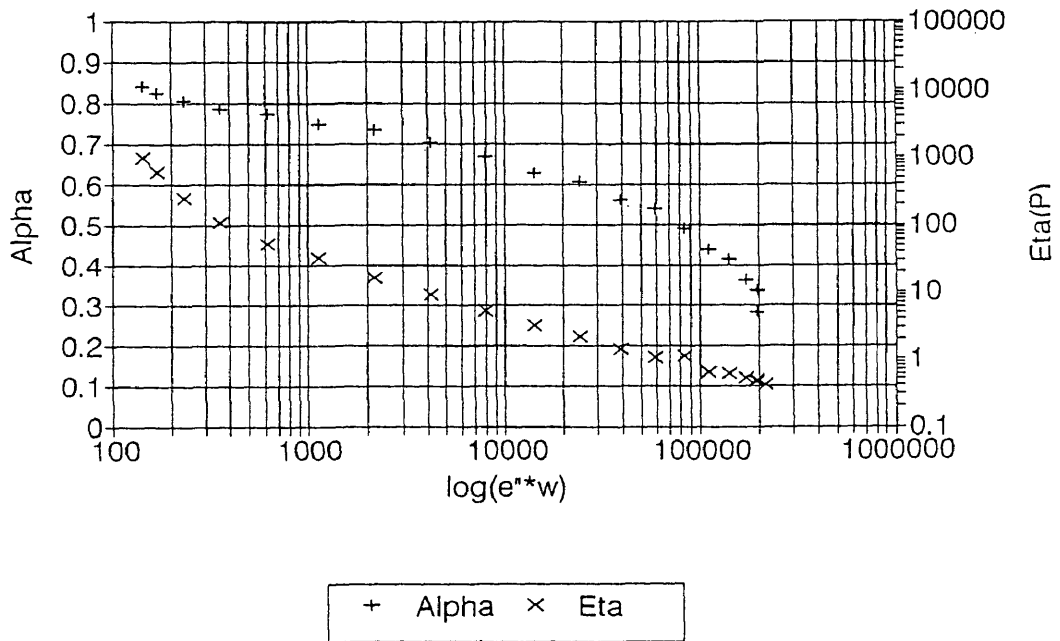


Figure 4.7a

PR500 170C isotherm (95)

Alpha and Eta vs. $\log(e''*w)$

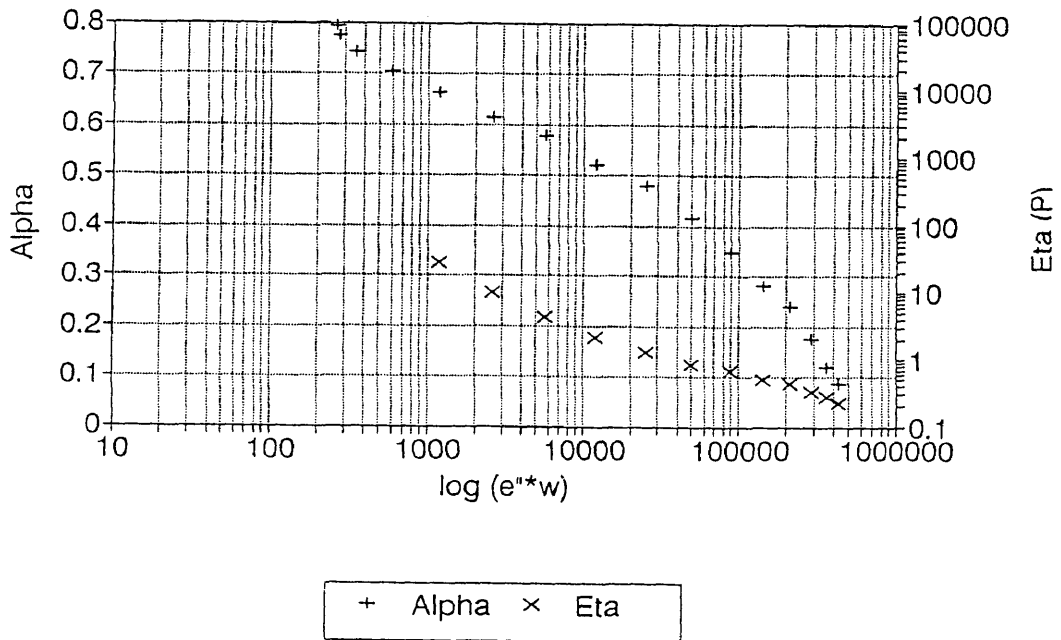


Figure 4.7b

PR500 180C Isotherm (5kHz) ('95)
 (de"/dtime)/e" and alpha vs time - 1 pt

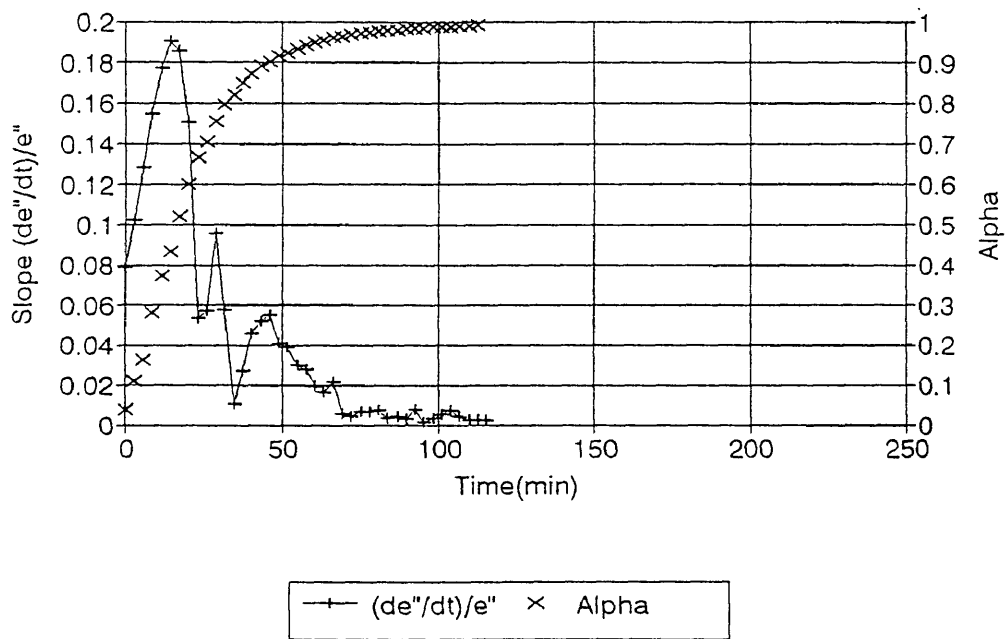


Figure 4.8

PR500 180C Isotherm (500Hz)

(de'/dtime)/e' and alpha vs time

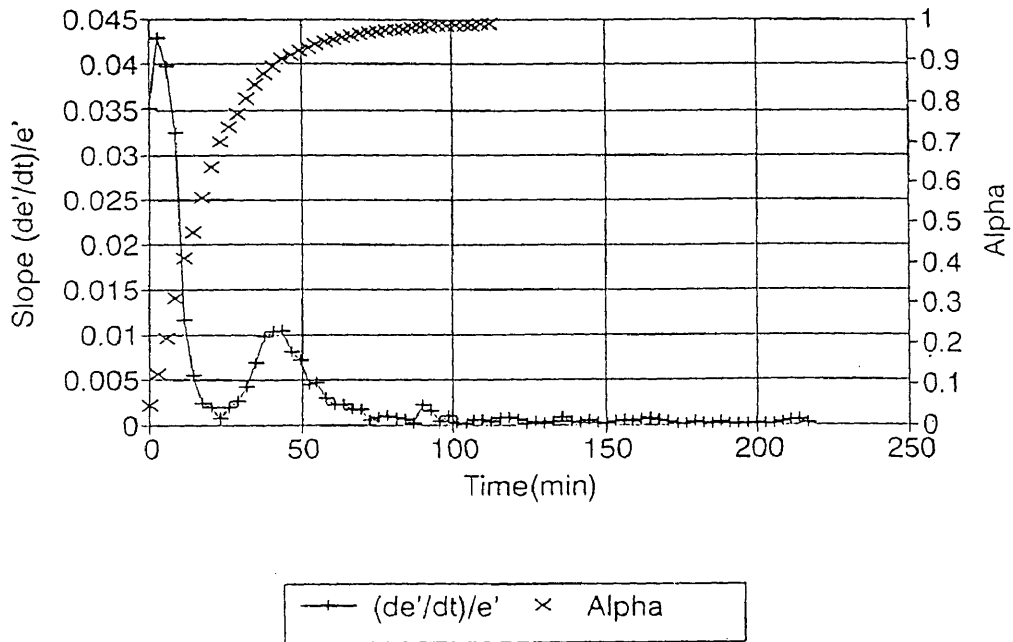


Figure 4.9a

PR500 180C Isotherm (5kHz)

(de'/dtime)/e' and alpha vs time

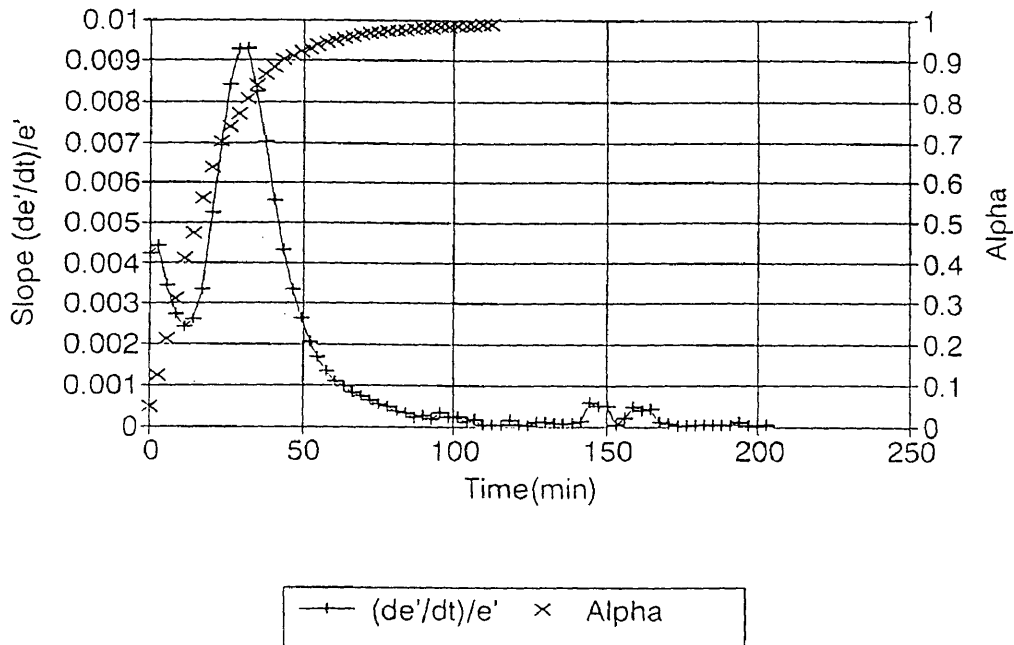


Figure 4.9b

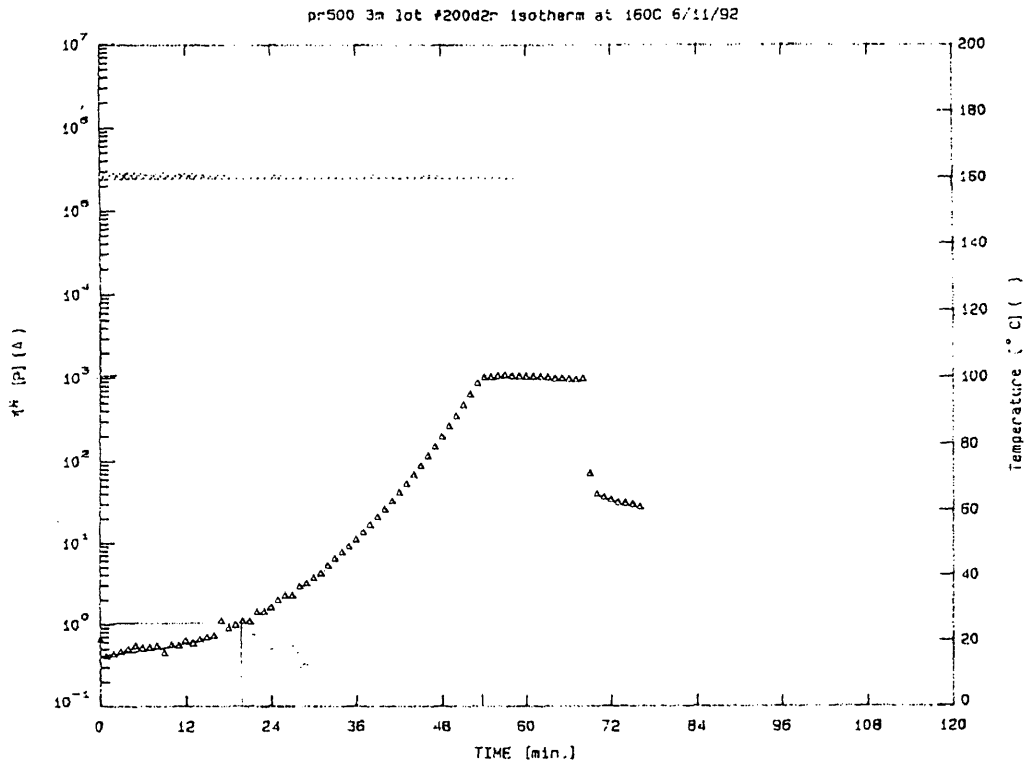


Figure 4.10a

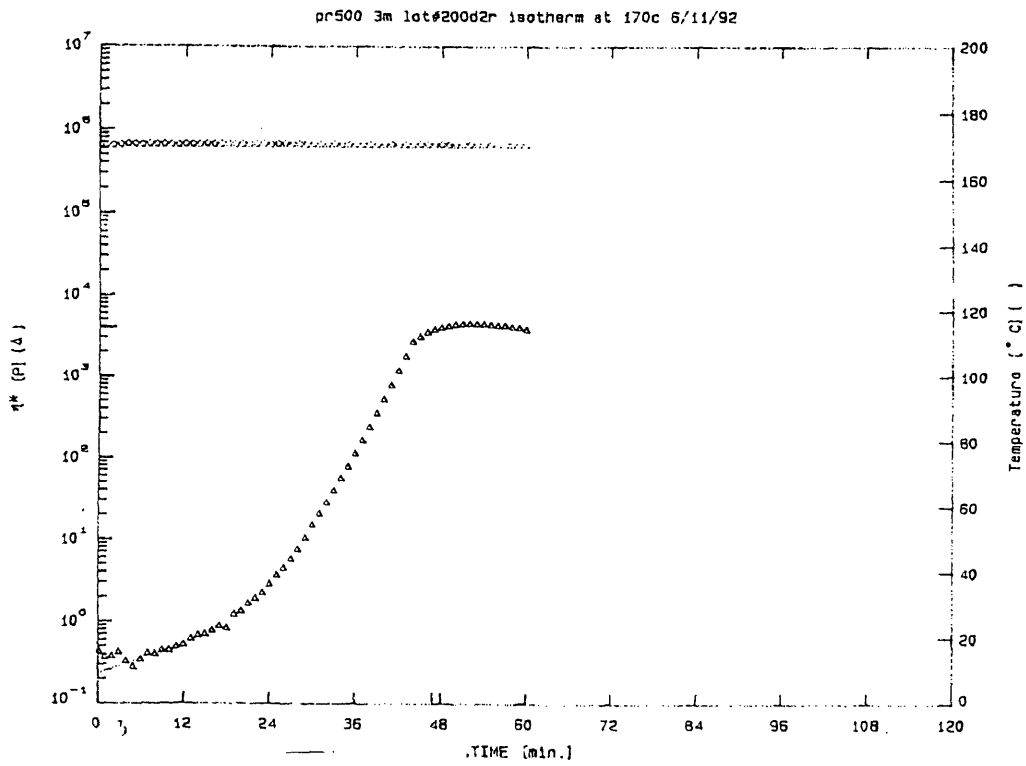


Figure 4.10b

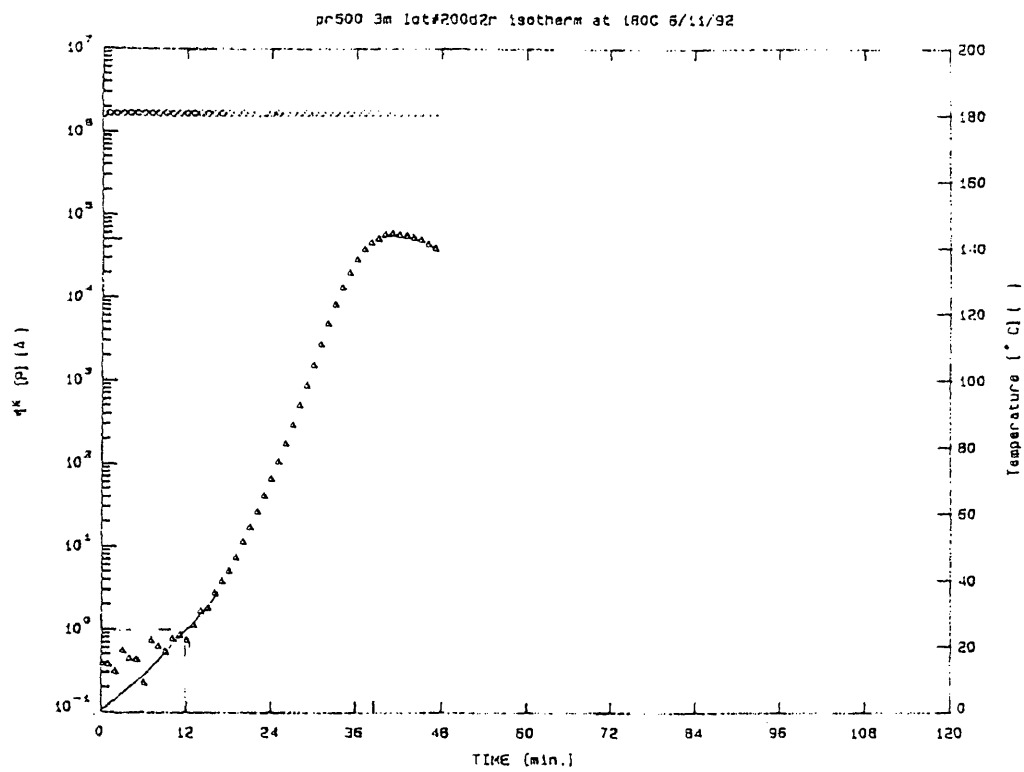


Figure 4.10c

PR500
e''*w vs. Eta

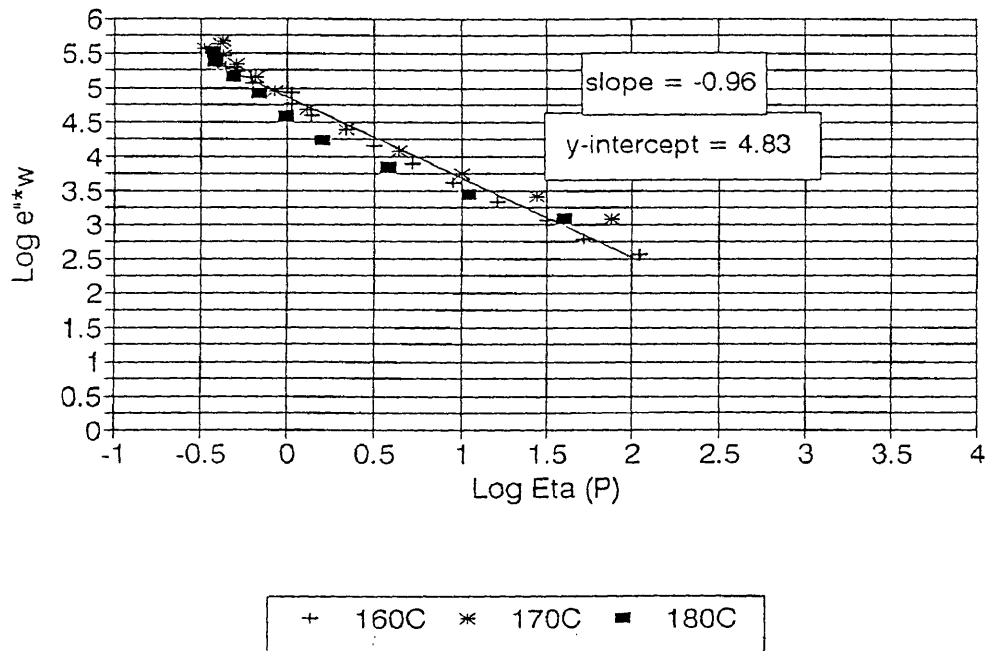


Figure 4.11

V. Monitoring of Resin Transfer Molding Experiments

Correlations

The cure processing properties of PR500 resin were analyzed using the calibration curves described. For the experiments DH071394, DH012795, DH032495, and DH032995, six kapton sensors in aluminum plugs and two thermocouples were placed in the bottom plate of a mold. For the experiment DH033195, three kapton sensors in aluminum plugs and two thermocouples were placed in the bottom plate of a mold. The mold cavity was filled with sixteen plies of carbon fiber. The enclosed mold was then placed into a temperature controlled hydraulic press. The mold has an inlet and exit line. The exit line was connected to a vacuum pump, which degassed the mold to eliminate entrapped air. The inlet was connected to a Radius Floware RTM 2100 injector gun which injected the resin into the mold. The sensors were monitored to determine degree of cure, viscosity, and wetout time. Wetout is the time when the resin reaches the sensor.

In this study, five experiments were analyzed. The objective of this study was to determine how different variables would effect the wetout time, viscosity, and

cure of the composite. This variation of conditions was necessary to verify models for different injection conditions. The conformation of injection, flow rate, and frame type were varied in the experiments. The resin was either injected in the front port of the plate or the exit port of the plate. There were two different frame types used. Frame II has a groove around the top. The resin first fills the groove and then flows into the preform. Frame I does not have this groove. Therefore, the resin flows into the channel and then the preform. The advantage of frame II is that there should be an even flow of resin. Wetout would then take longer than in frame I. Table 5.1 lists flow rates, conformation of injection, and frame type.

Experiment	Flow Rate (cc/min)	Injection Pattern	Frame Type
DH071394	20	Front	II
DH012795	20	Front	I
DH032495	20	Front	I
DH032995	10	Exit	I
DH033195	10	Exit	I

Table 5.1

First RTM Run - DH071394

The wetout times for DH071394 are listed in Table 5.2.

Sensor #	Wetout Time (min)
1	16
2	29
3	32
4	18
5	29
6	17

Table 5.2

The flow rate for this experiment was 20 cc/min. The resin was injected at the front of the plate. Dielectric measurements of the sensors were started approximately five minutes before injection. The part fabrication was monitored for approximately 120 minutes. (Figures 5.1a-5.1f) The data was correlated using $\log \epsilon'' * \omega$. This was calculated by multiplying ϵ'' by $2\pi * f$, f is frequency in Hertz. For the correlations, a frequency of 5 kHz was used for degree of cure and 125 Hz was used for viscosity. For this experiment, the Maussy model was used to correlate degree of cure. Degree of cure and viscosity were predicted by using the calibration curves described earlier. All probes in the experiment reach near full cure (α approximately .99) by 100 minutes. The viscosity curves of all

six probes show an exponential relation to time. (Figures 5.2a-5.2l) A diagram of the RTM plate used is shown in Figure 5.3.

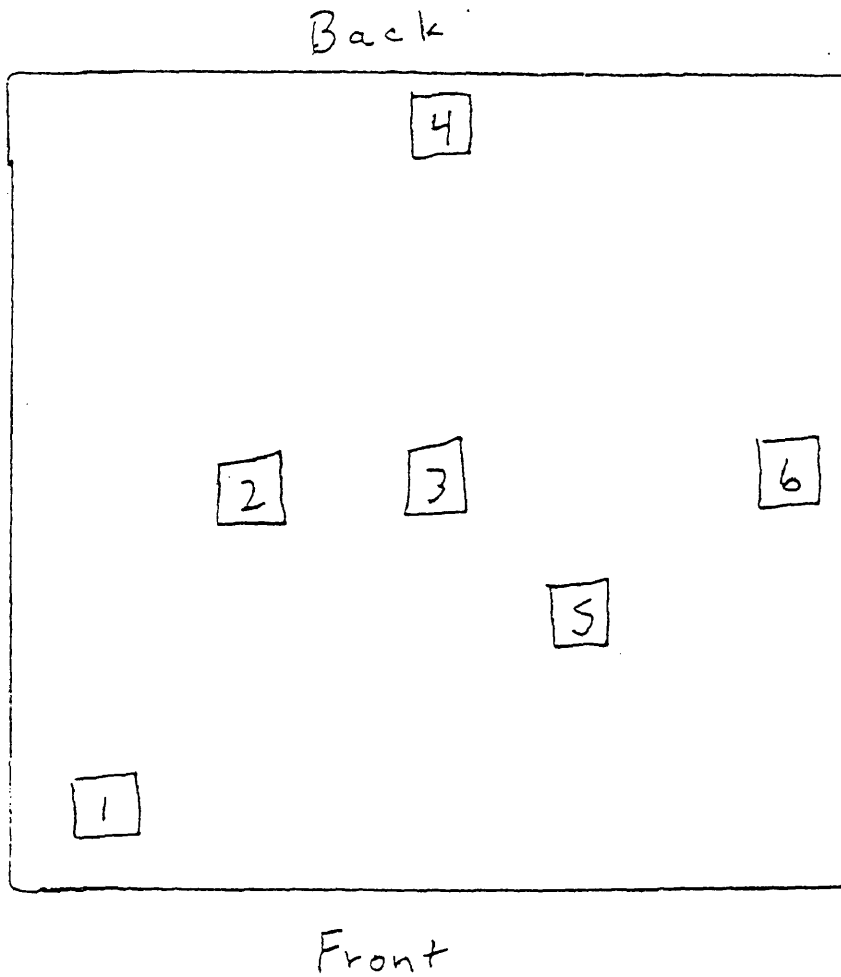


Figure 5.3

Data file: a: dh071394

Probe: 1

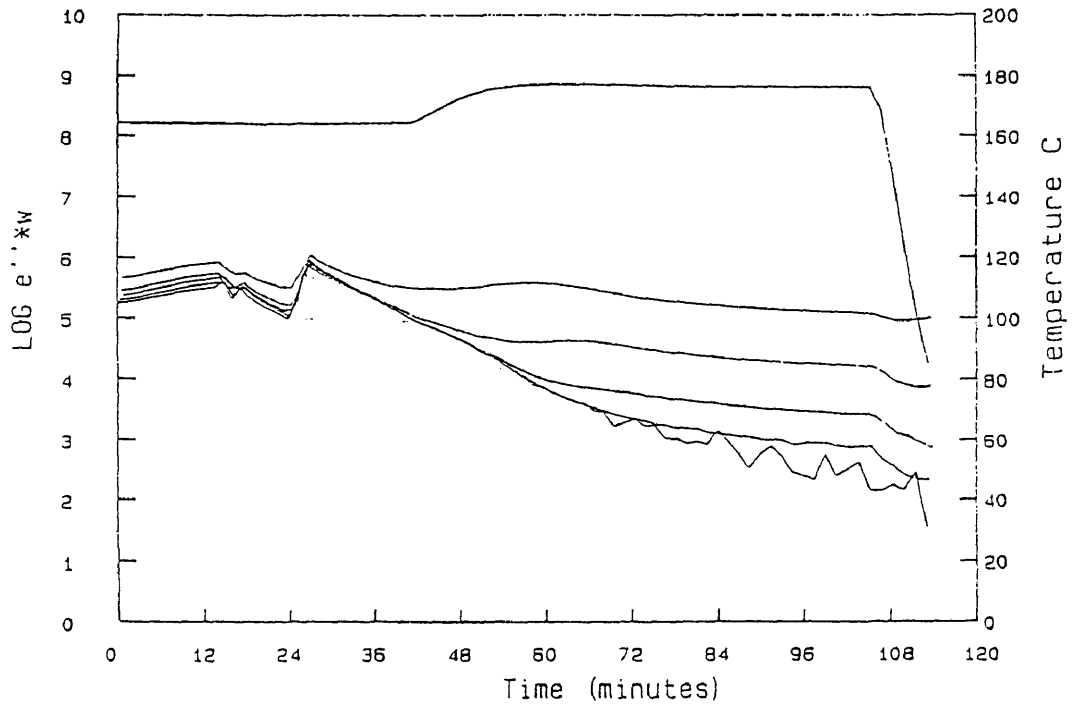


Figure 5.1a

Data file: a: dh071394

Probe: 2

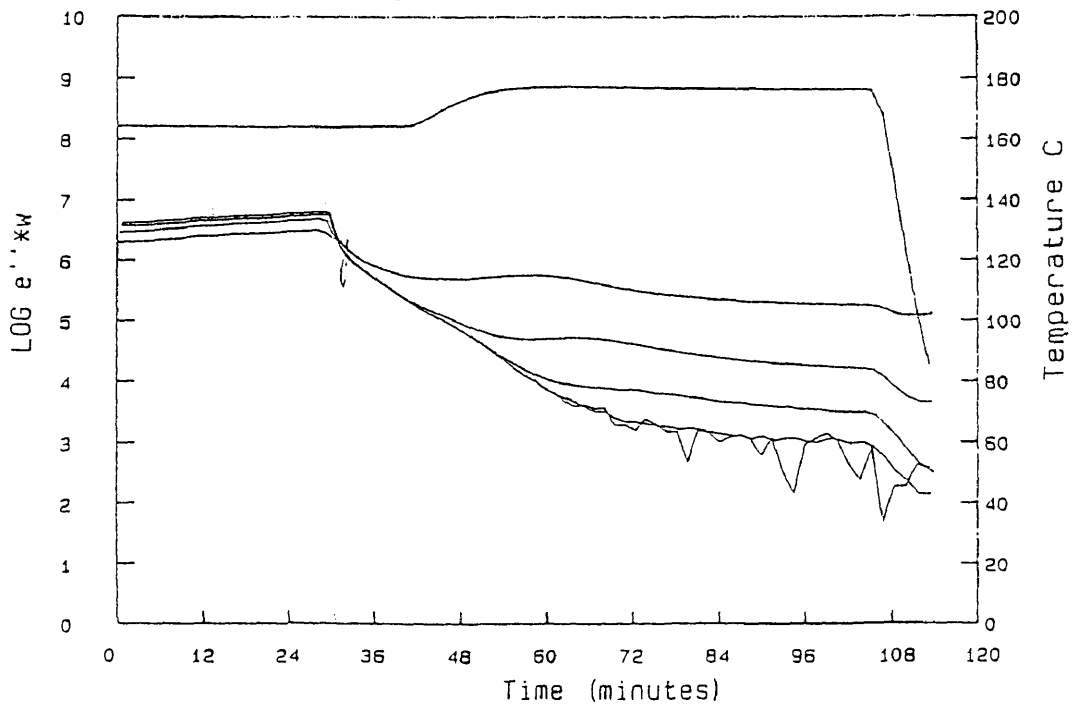


Figure 5.1b

Data file: a: dh071394
Probe: 3

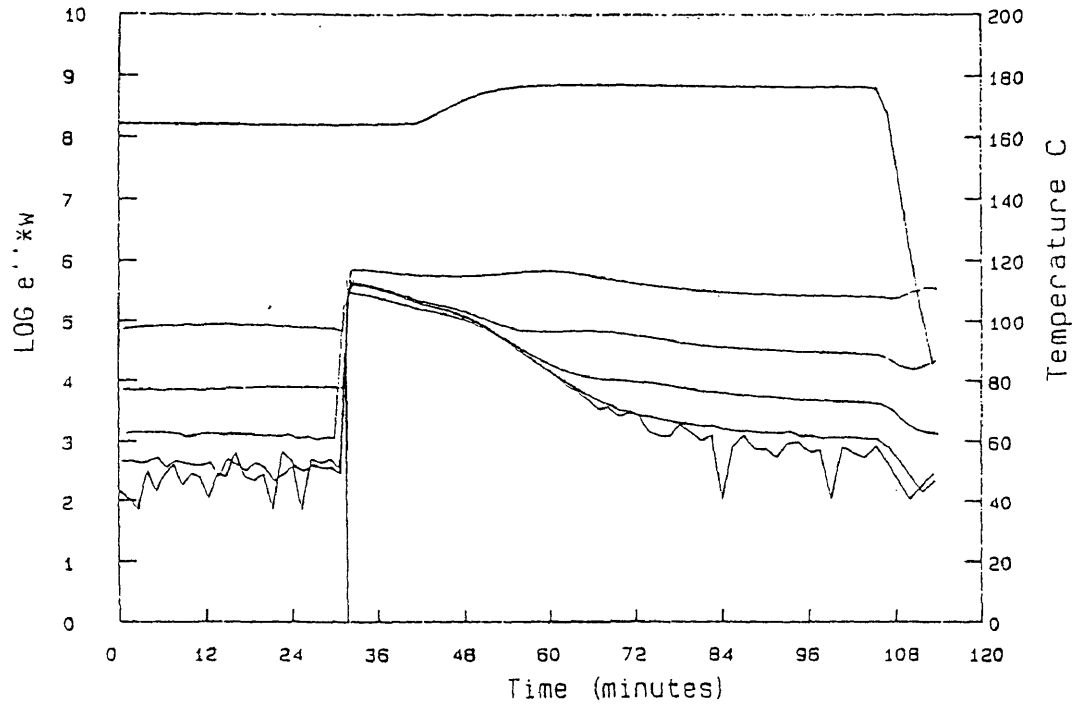


Figure 5.1d

Data file: a: dh071394
Probe: 4

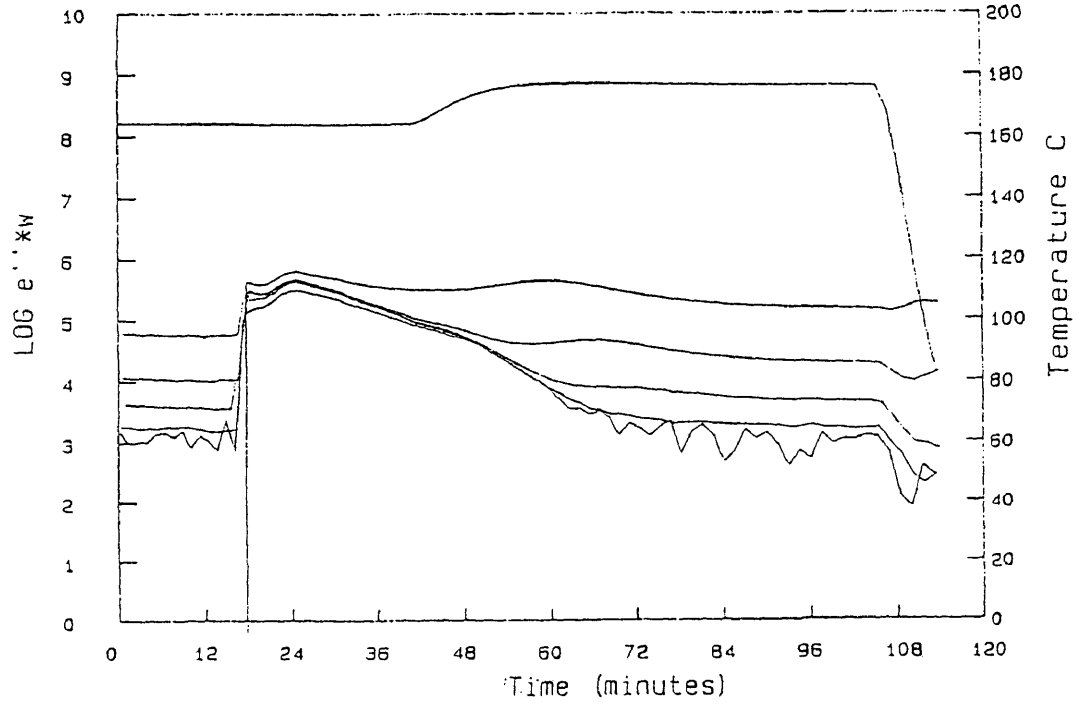


Figure 5.1c

Data file: a: dh071394
Probe: 5

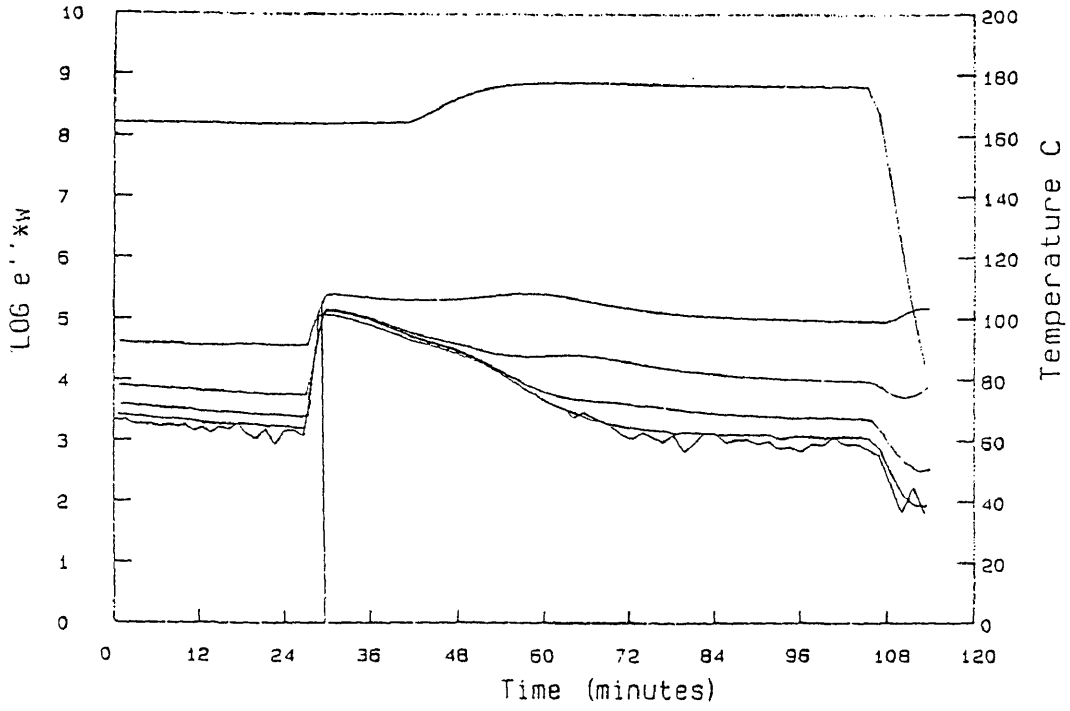


Figure 5.1e

Data file: a: dh071394
Probe: 5

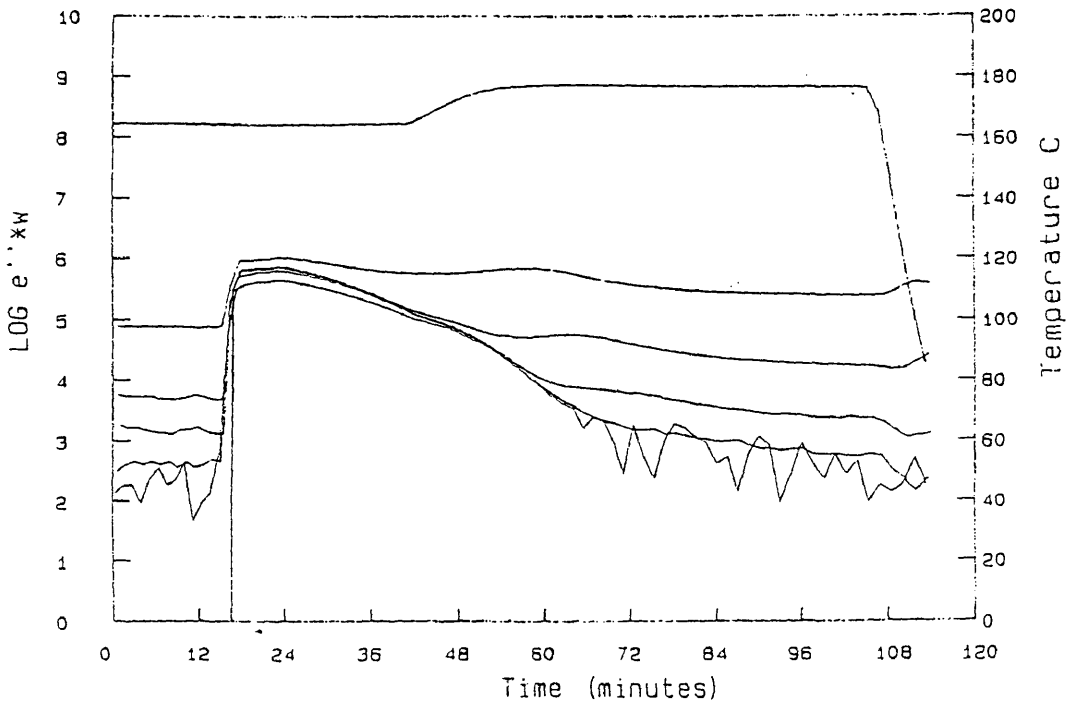


Figure 5.1f

PR500 run dh071394 probe#1
Correlated Viscosity

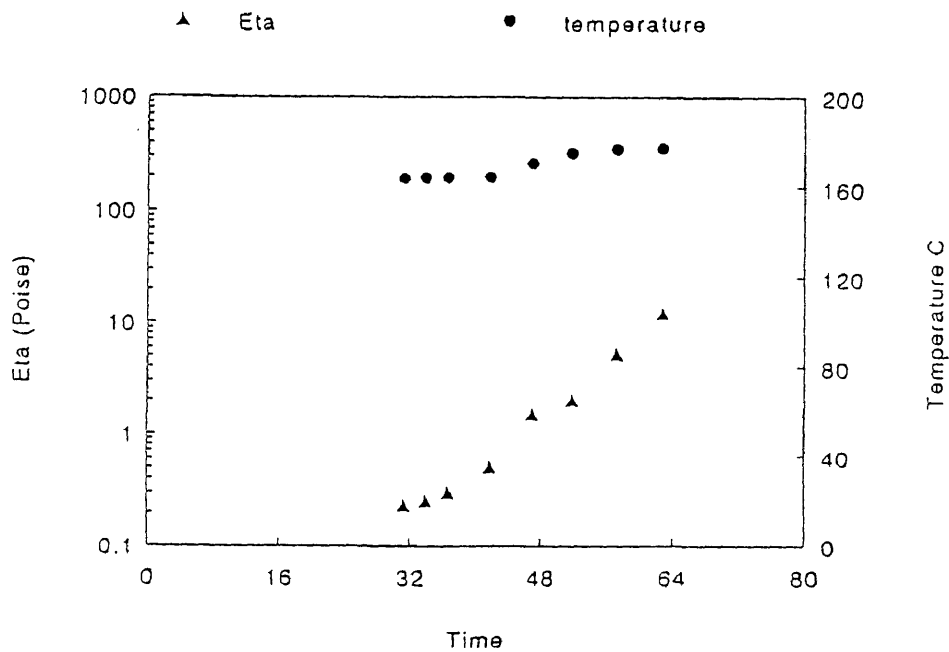


Figure 5.2a

PR500 run dh071394 Probe#2
Correlated Viscosity

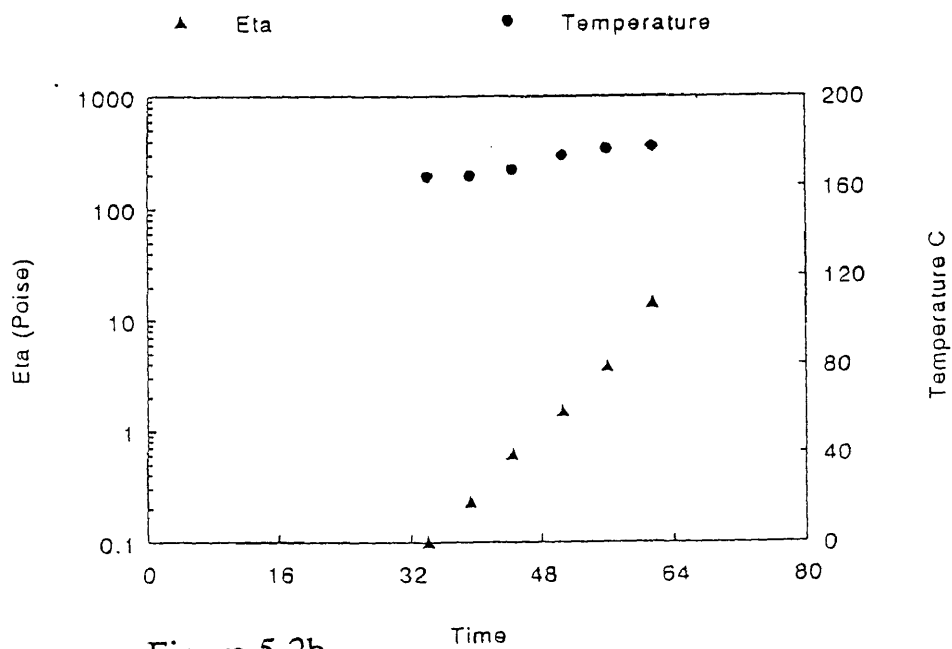


Figure 5.2b

PR500 run dh071394 Probe#3
Correlated Viscosity

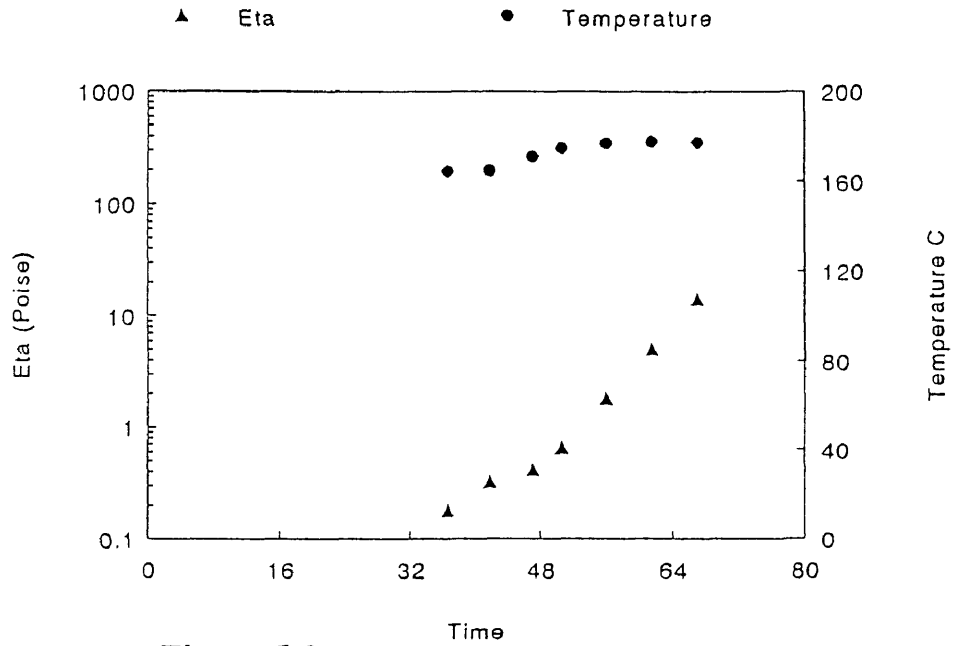


Figure 5.2c

PR500 run dh071394 Probe#4
Correlated Viscosity

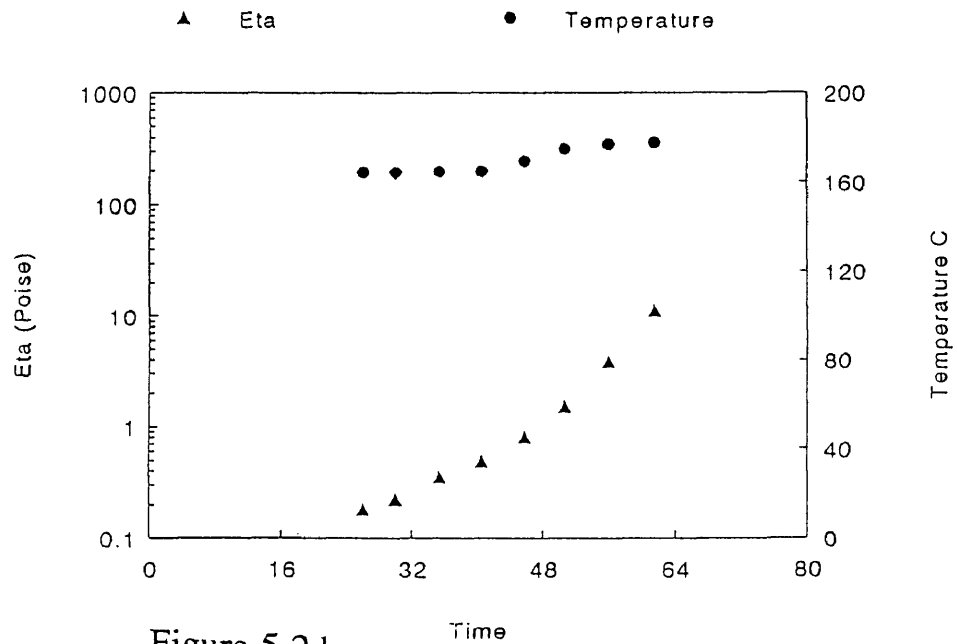


Figure 5.2d

PR500 run dh071394 Probe#5
Correlated Viscosity

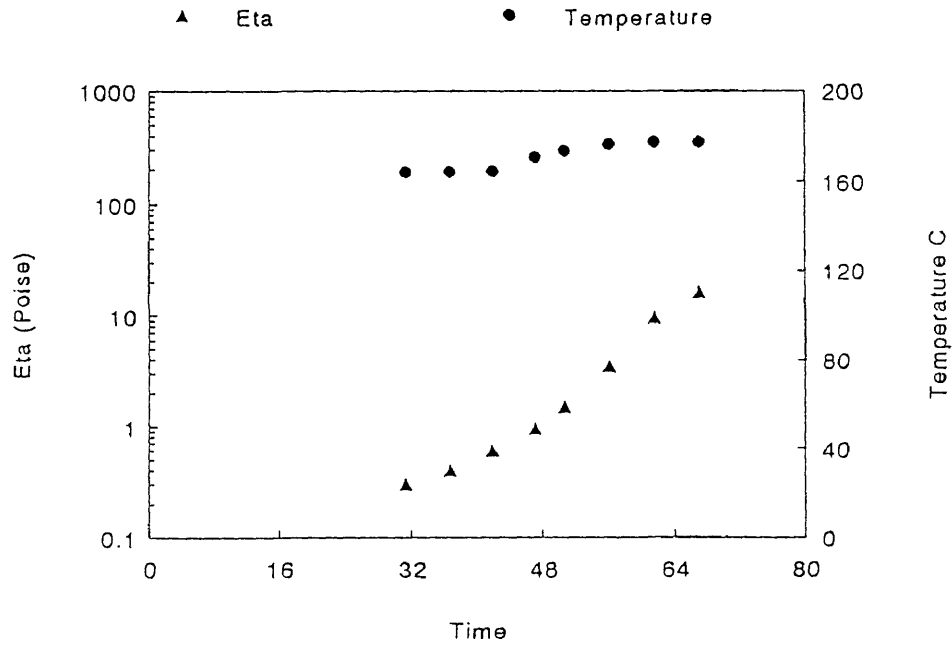


Figure 5.2e

PR500 run dh071394 Probe#6
Correlated Viscosity

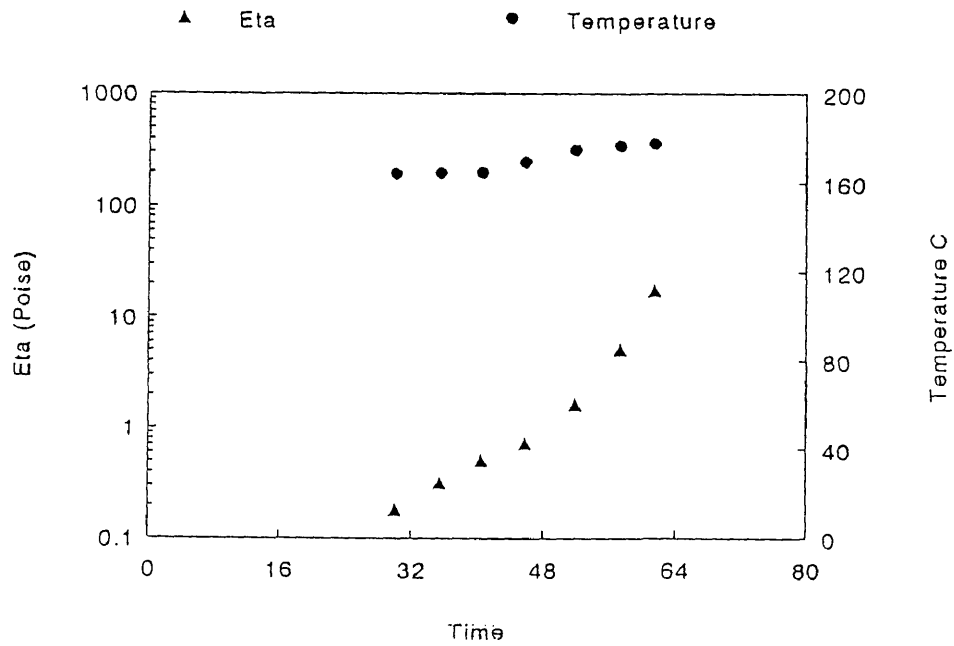


Figure 5.2f

PR500 run dh071394 probe#1

Degree of Cure (alpha)-M

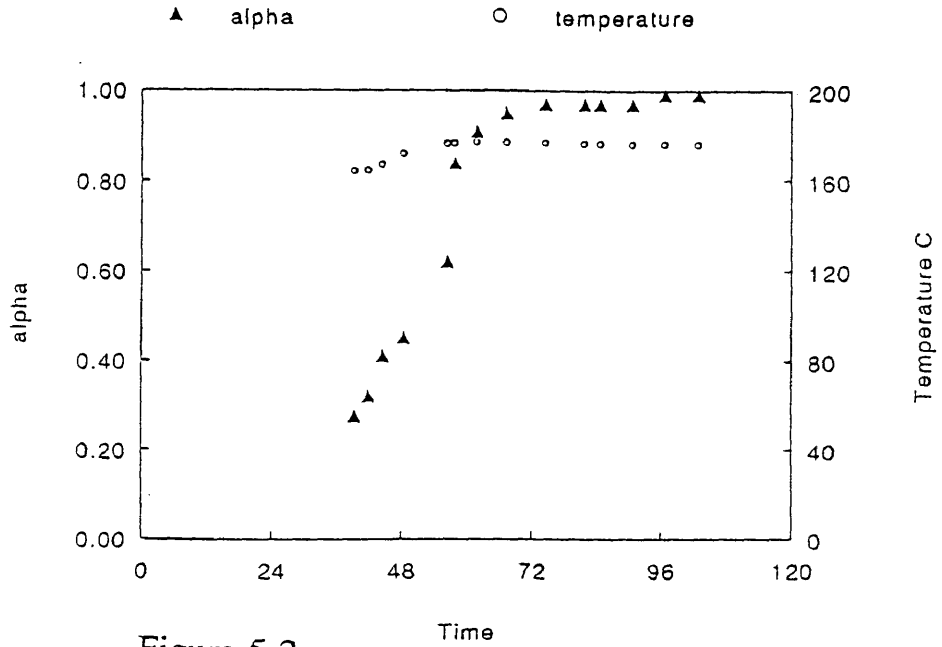


Figure 5.2g

PR500 run dh071394 Probe#2

Degree of Cure (alpha)-M

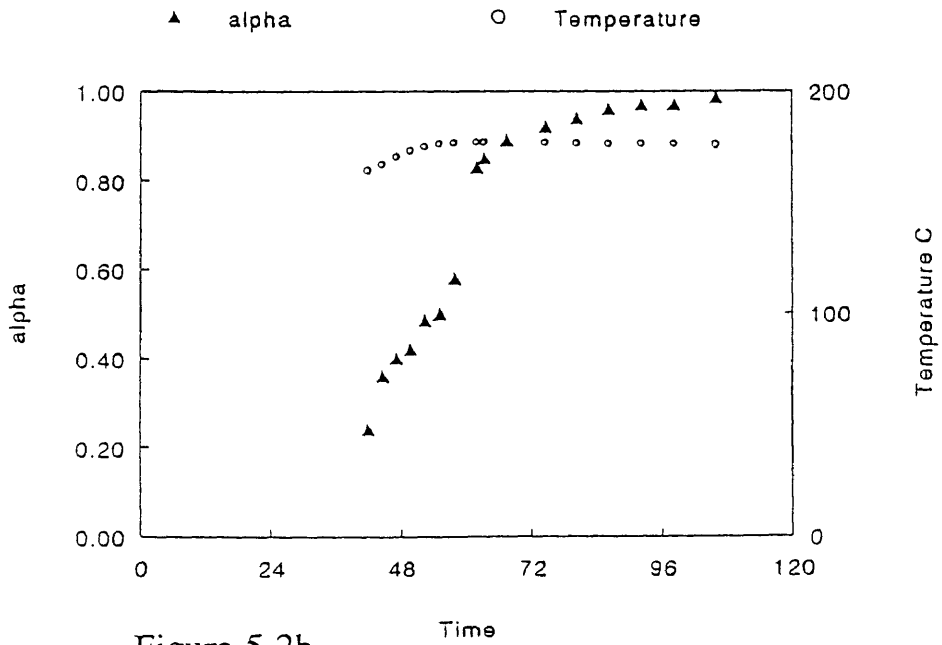


Figure 5.2h

PR500 run dh071394 Probe#3

Degree of Cure (alpha)-M

▲ alpha ○ Temperature

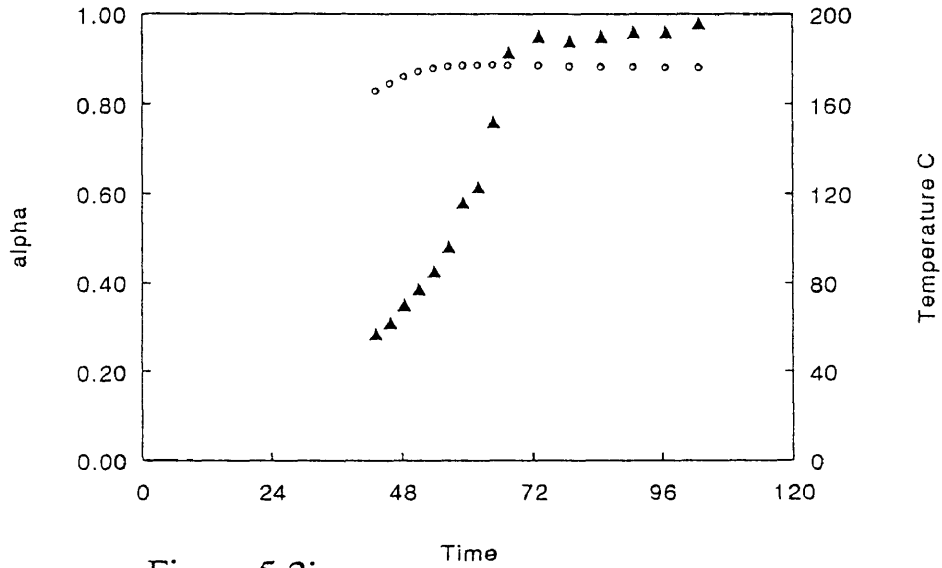


Figure 5.2i

PR500 run dh071394 Probe#4

Degree of Cure (alpha)-M

▲ alpha ○ Temperature

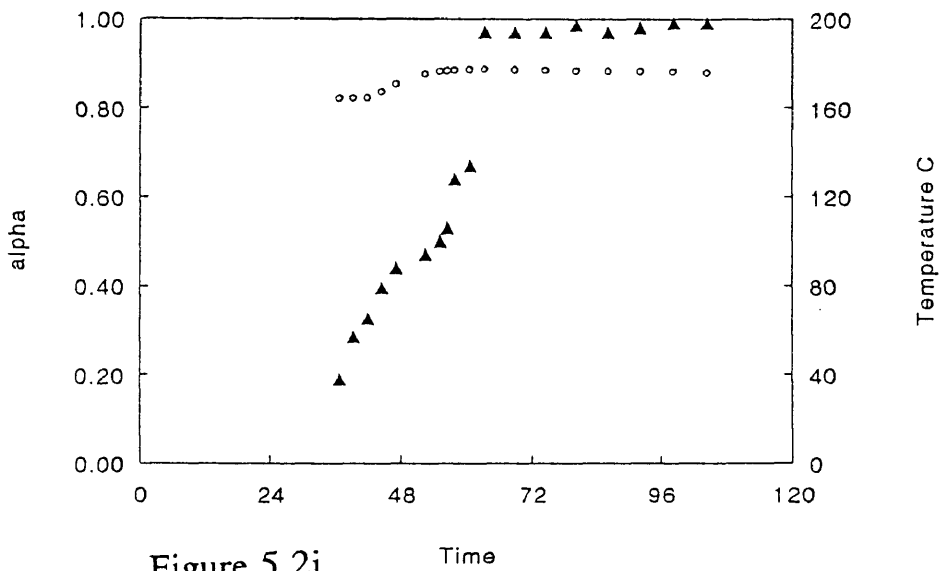


Figure 5.2j

PR500 run dh071394 Probe#5

Degree of Cure (alpha)-M

▲ alpha ○ Temperature

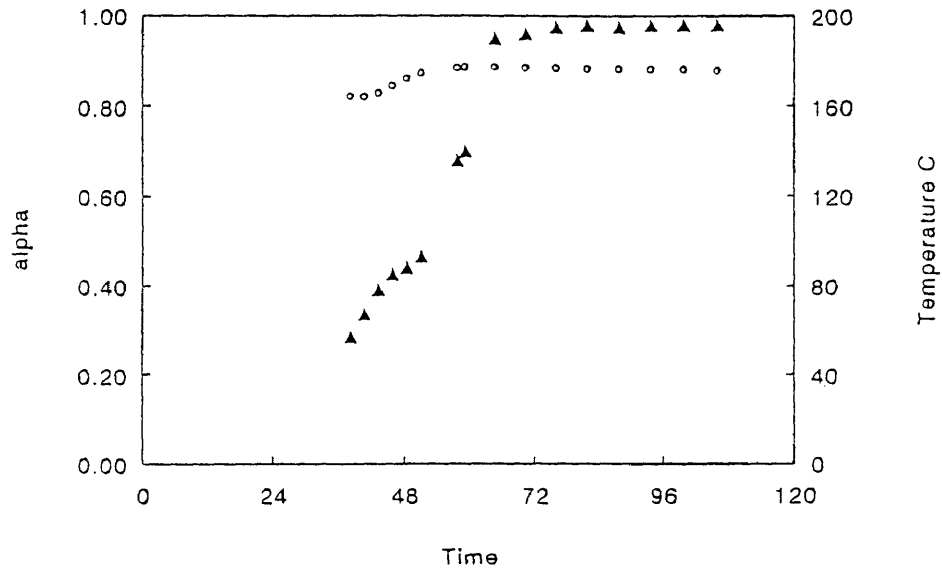


Figure 5.2k

PR500 run dh071394 Probe#6

Degree of Cure (alpha)-M

▲ alpha ○ Temperature

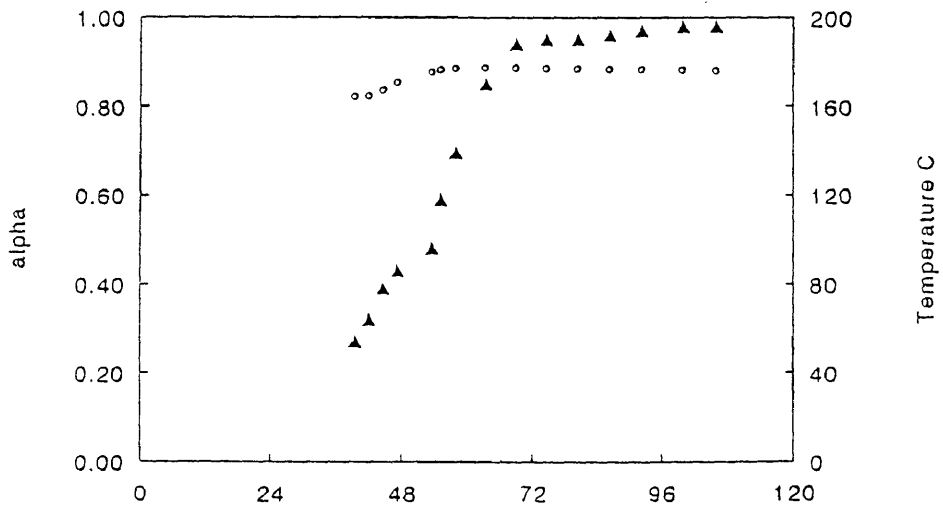


Figure 5.2l

Second RTM Run - DH012795

The wetout times for DH012795 are listed in Table 5.3.

Sensor #	Wetout Time (min)
1	16.1
2	---
3	45.0
4	25.8
5	39.3
6	16.3

Table 5.3

The resin was injected at the front of the plate at a rate of 20 cc/min. Dielectric measurements of the sensors were started at injection. The part fabrication was monitored for approximately 120 minutes. (Figures 5.4a-5.4f) The data was correlated in the same manner as DH071395. (Figures 5.5a-5.5f) Both Mausey and Loos models were used to predict degree of cure. A diagram of the RTM plate is shown below in Figure 5.6.

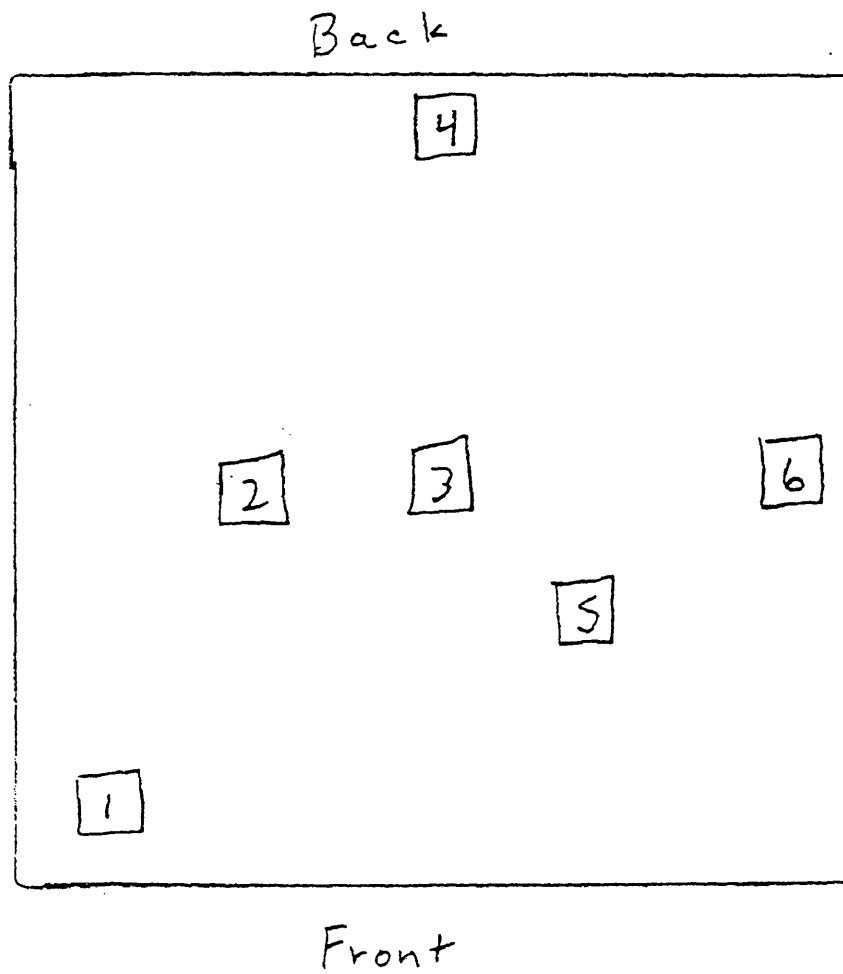


Figure 5.6

Data file: dh012795
Probe: 1

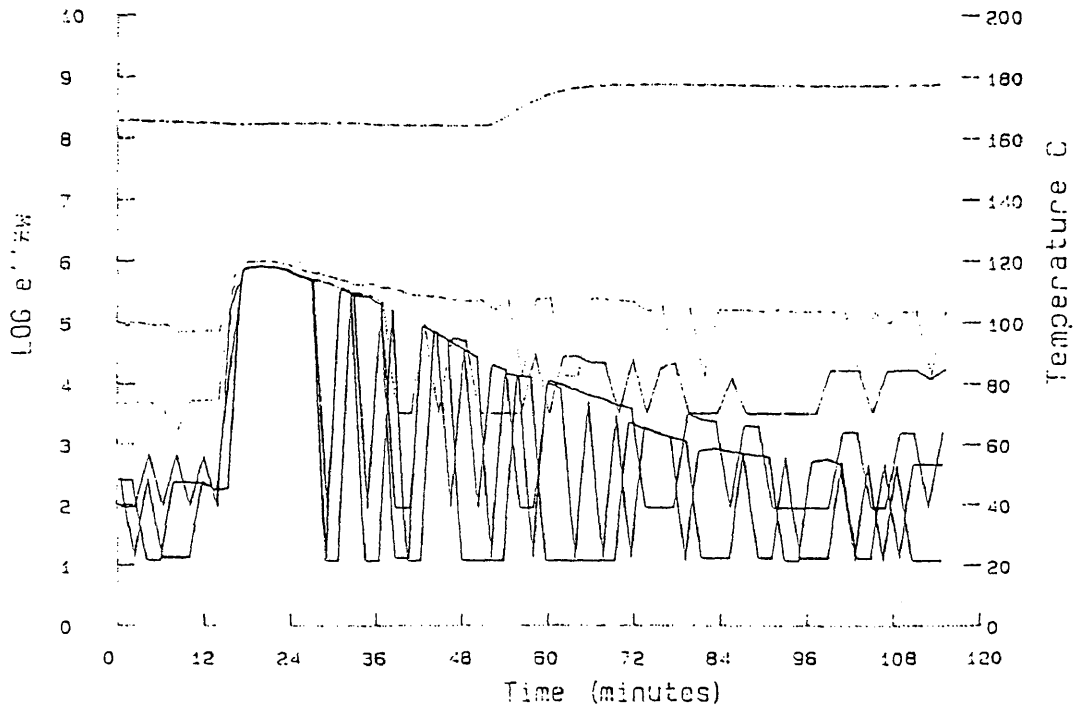


Figure 5.4a

Data file: dh012795
Probe: 2

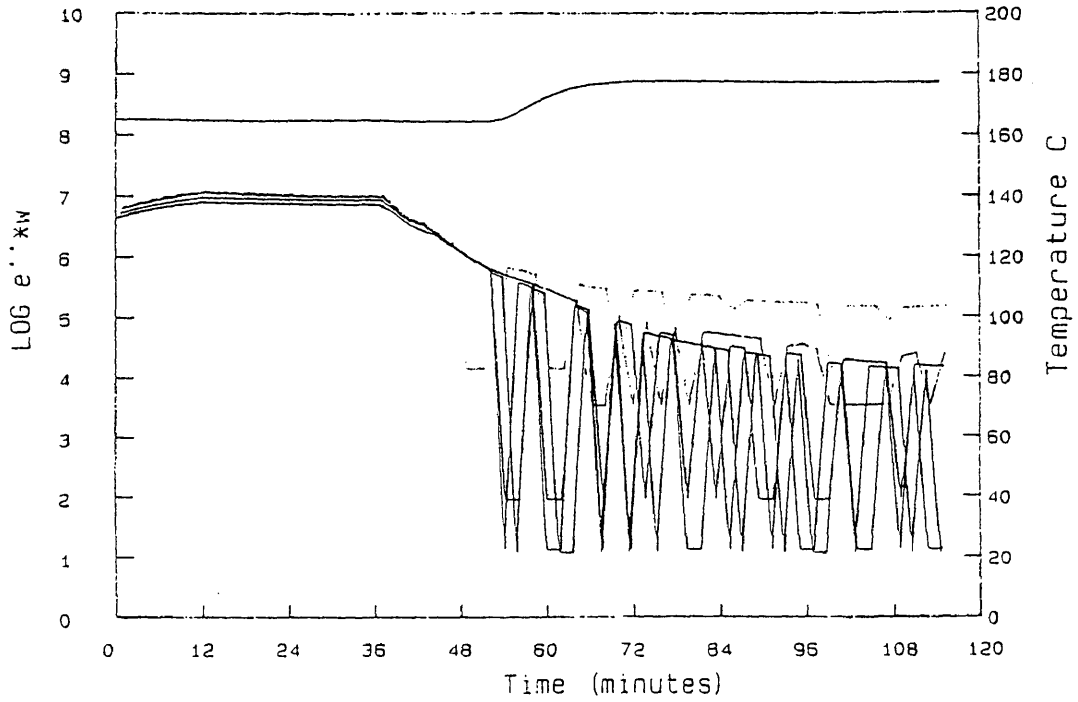


Figure 5.4b

Data file: dh012795
Probe: 3

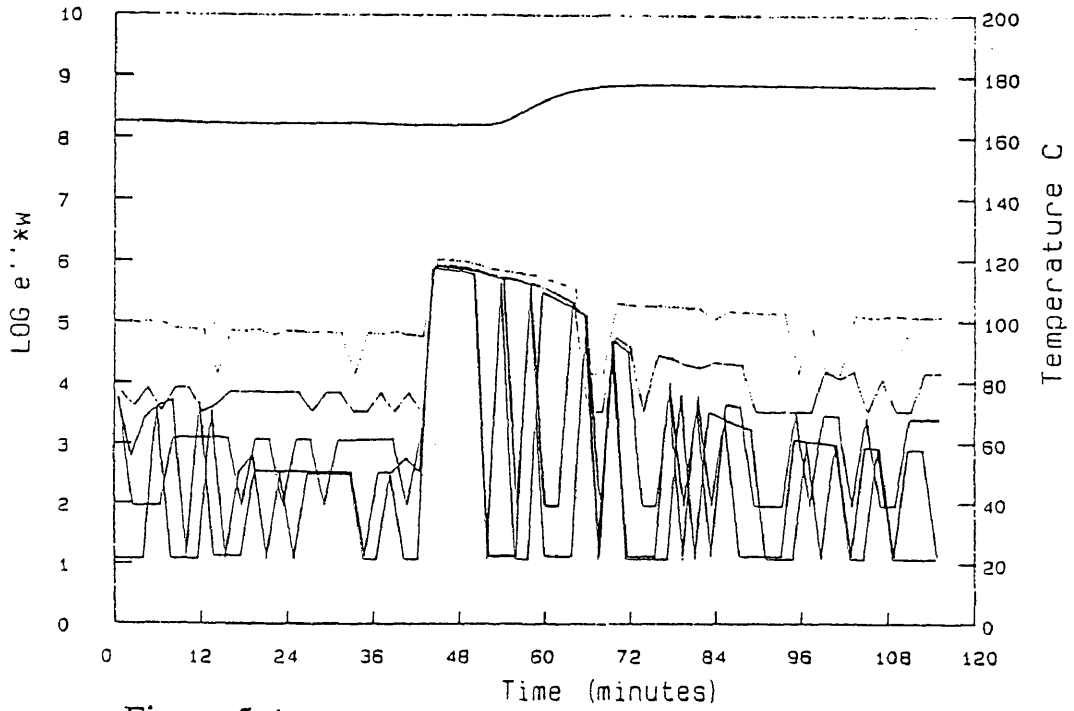


Figure 5.4c

Data file: dh012795
Probe: 4

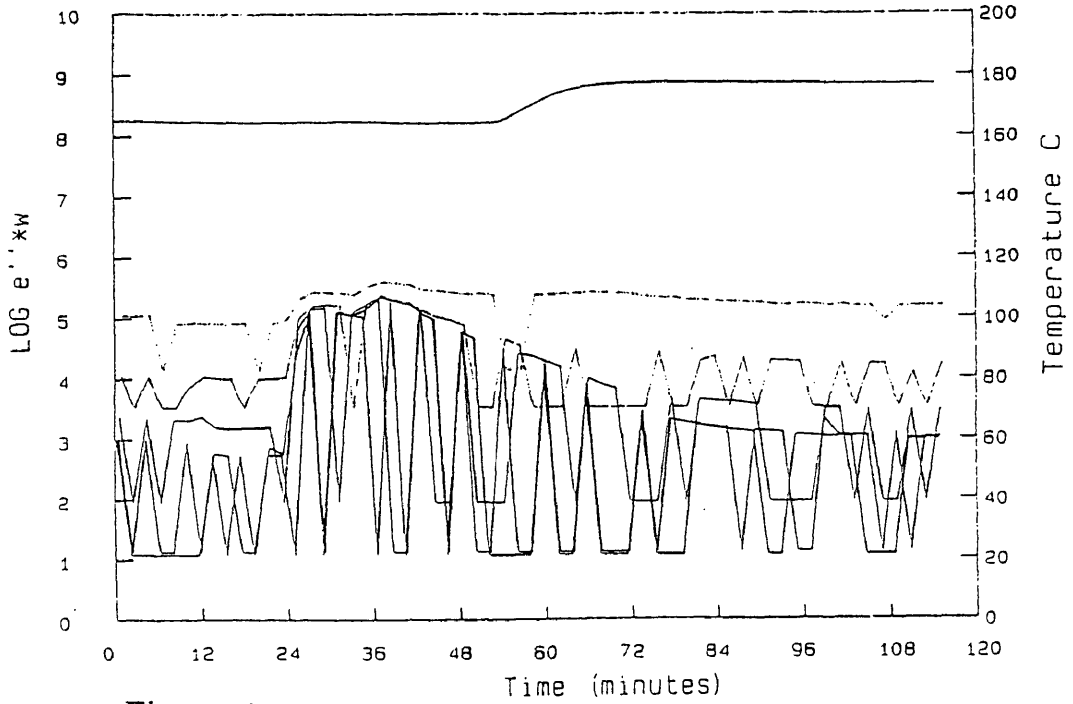


Figure 5.4d

Data file: dh012795
Probe: 5

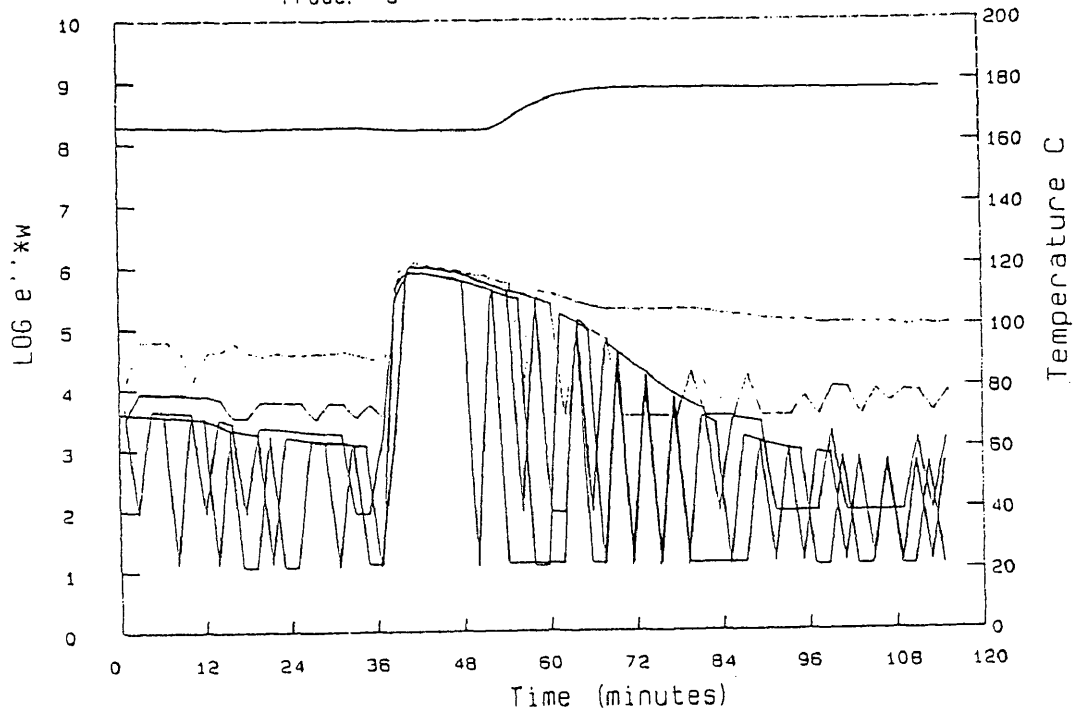


Figure 5.4e

Data file: dh012795
Probe: 6

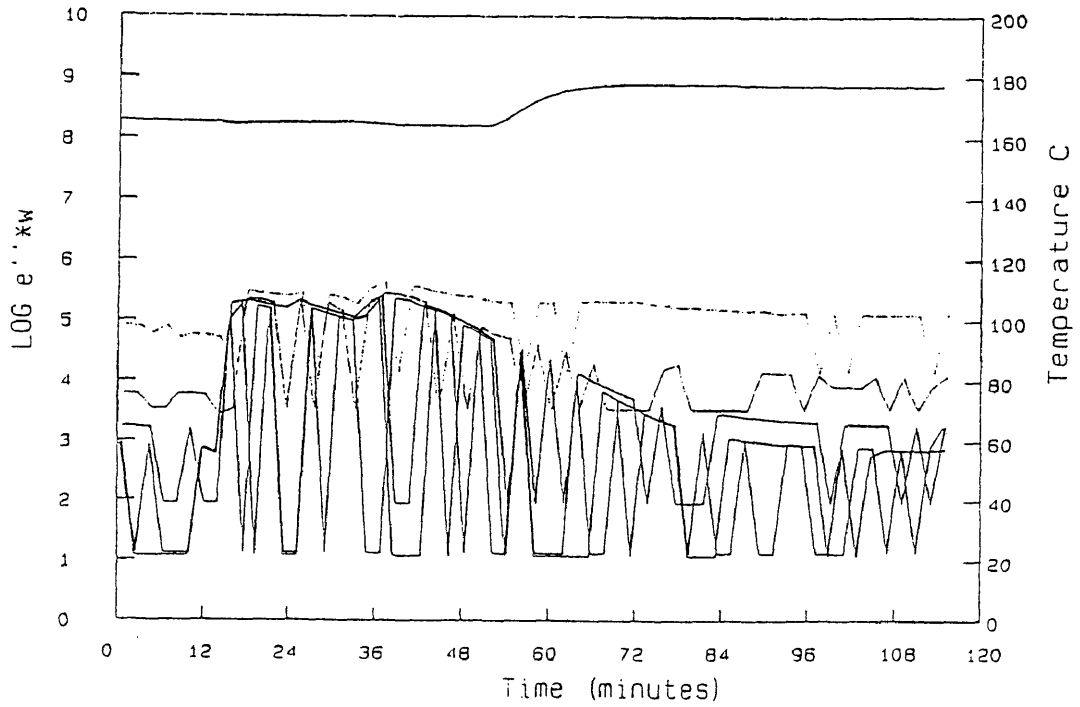


Figure 5.4f

PR500 run dh012795 probe#1
Correlated Viscosity

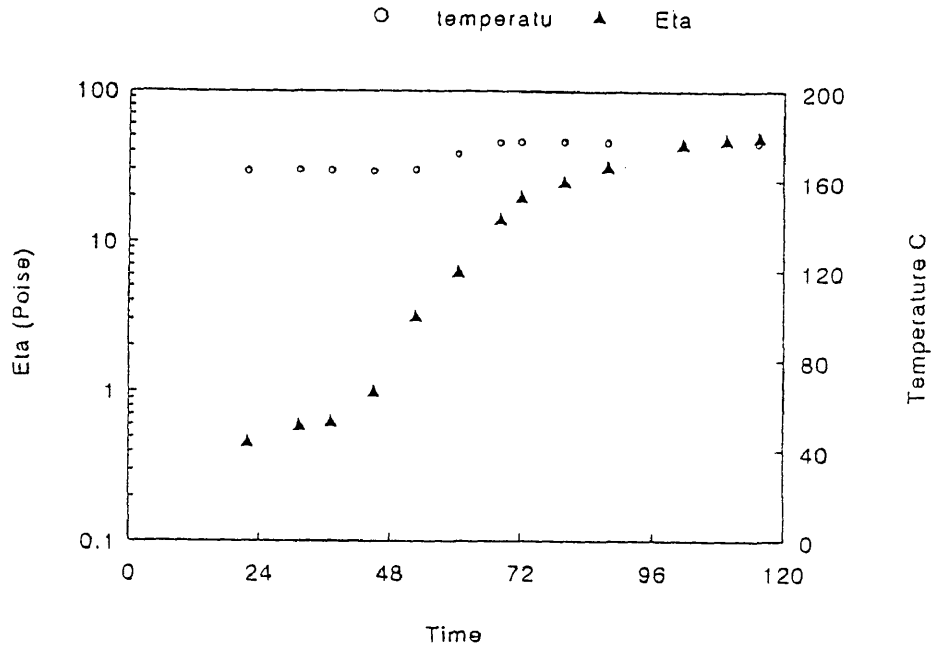


Figure 5.5a

PR500 run dh012795 probe#6
Correlated Viscosity

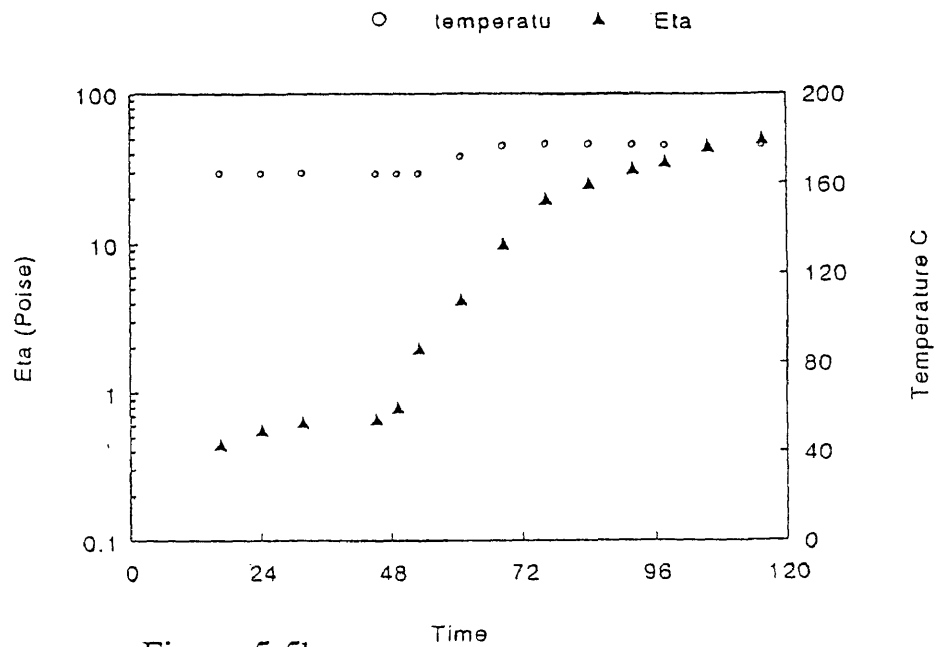


Figure 5.5b

PR500 run dh012795 probe#1

Degree of Cure (alpha)-M

▲ alpha ○ temperature

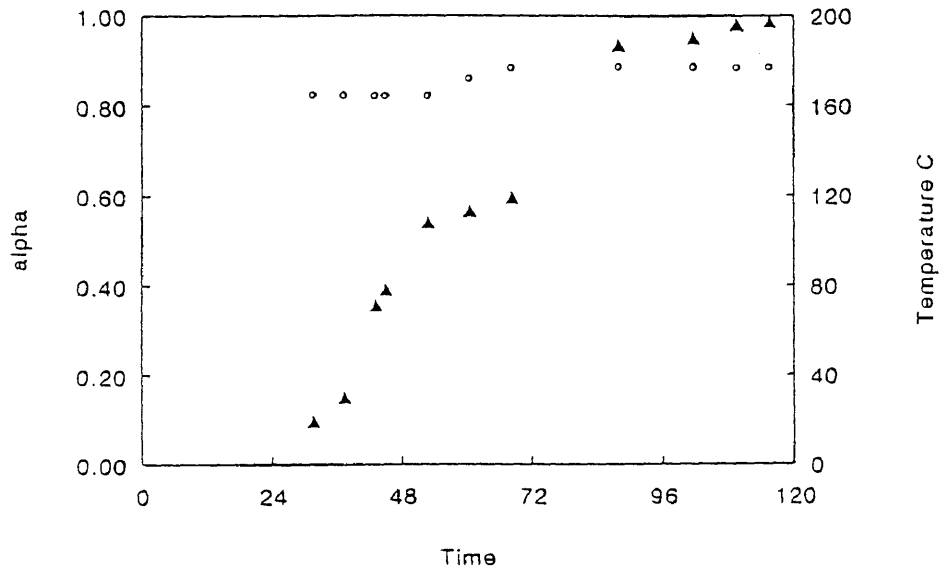


Figure 5.5c

PR500 run dh012795 probe#1

Degree of Cure (alpha)-L

▲ alpha ○ temperature

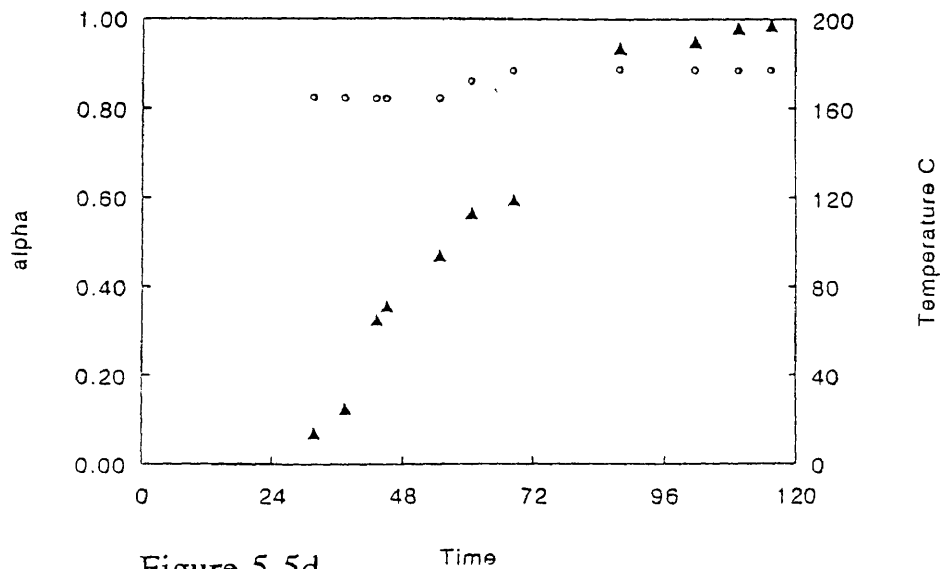


Figure 5.5d

PR500 run dh012795 probe#6

Degree of Cure (alpha)-M

▲ alpha ○ temperature

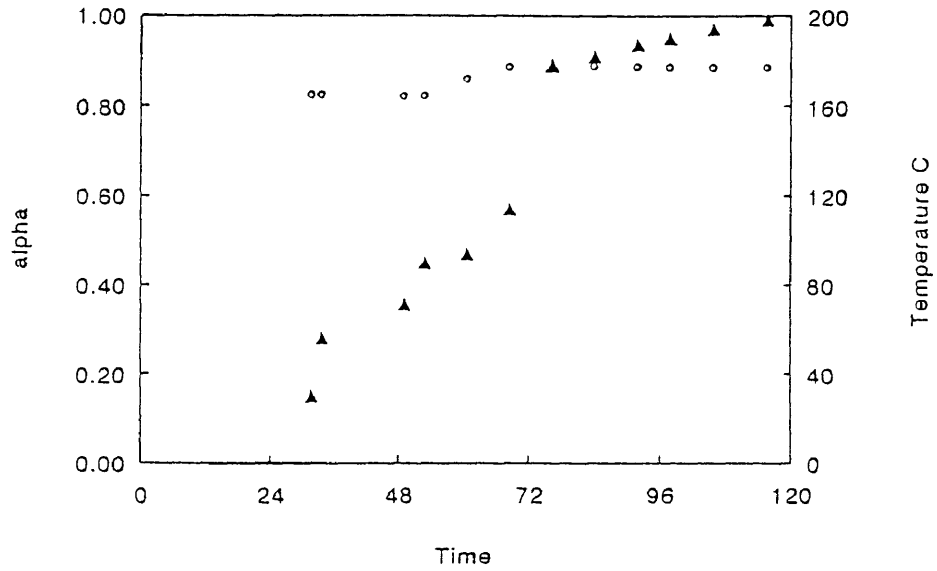


Figure 5.5e

PR500 run dh012795 probe#6

Degree of Cure (alpha)-L

▲ alpha ○ temperature

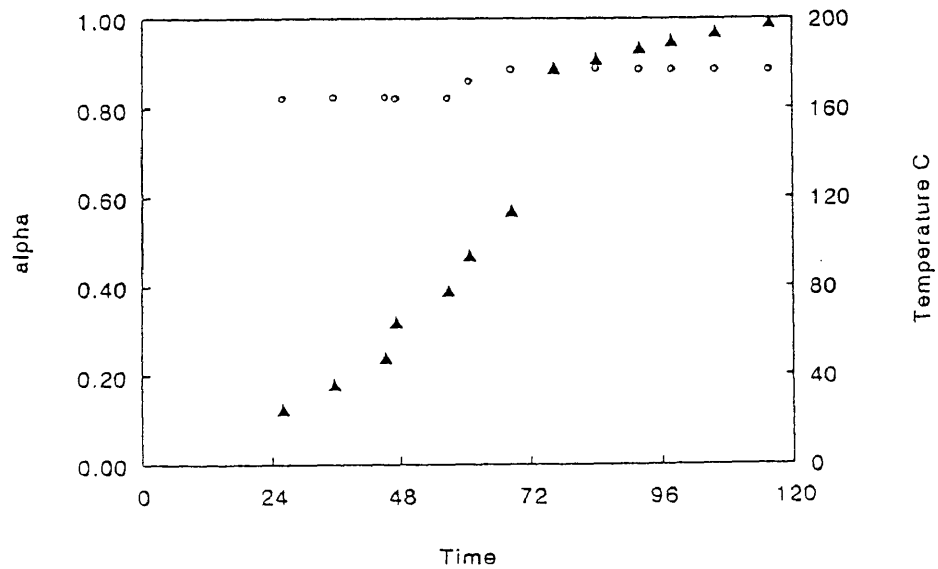


Figure 5.5f

Third RTM Run - DH032495

The wetout times for DH032495 are listed in Table 5.4.

Sensor #	Wetout Time (min)
1	13.5
2	14.9
3	18.9
4	25.6
5	26.9
6	33.7

Table 5.4

The resin was injected at the front of the plate at a rate of 20 cc/min. Dielectric measurements of the sensors were started at injection. The part fabrication was monitored for approximately 120 minutes.(Figures 5.7a-5.7d) The data was correlated the same as DH071395.(Figures 5.8a-5.8h) Both Maussey and Loos models were used to predict degree of cure. The leads on the bridge used to take the dielectric measurements has the capacity to measure only four sensors at a time. Therefore, sensor one shows the wetout for both sensors one and five. Sensor two shows wetout for sensors two and six. Since measurements on sensors one and two are stopped after wetout, degree of cure and viscosity can not be determined. A diagram of the RTM plate used is shown below.(Figure 5.9)

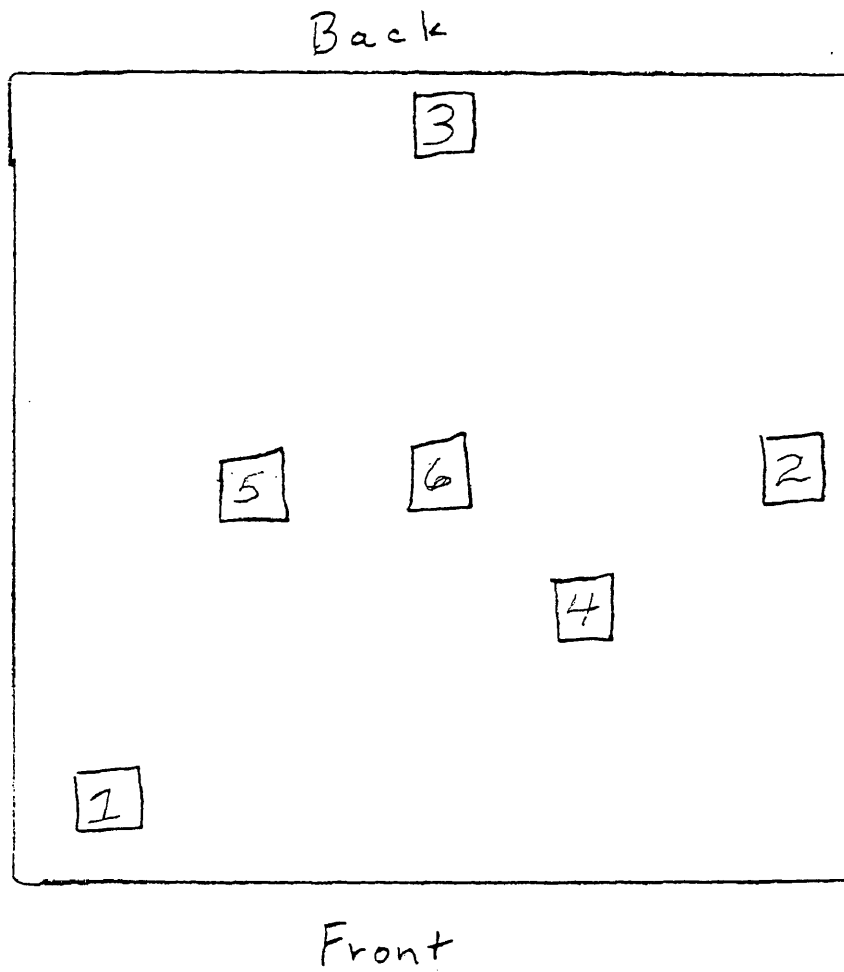


Figure 5.9

Data file: a: dh032495
Probe: 1 and 5

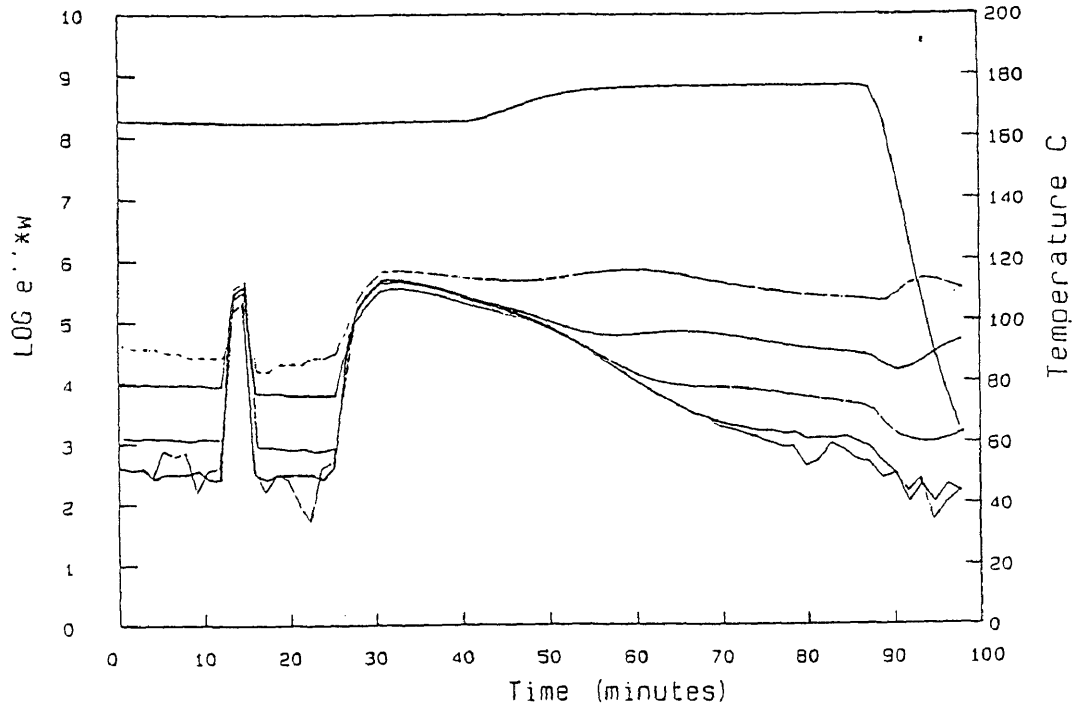


Figure 5.7a

Data file: a: dh032495
Probe: 2 and 6

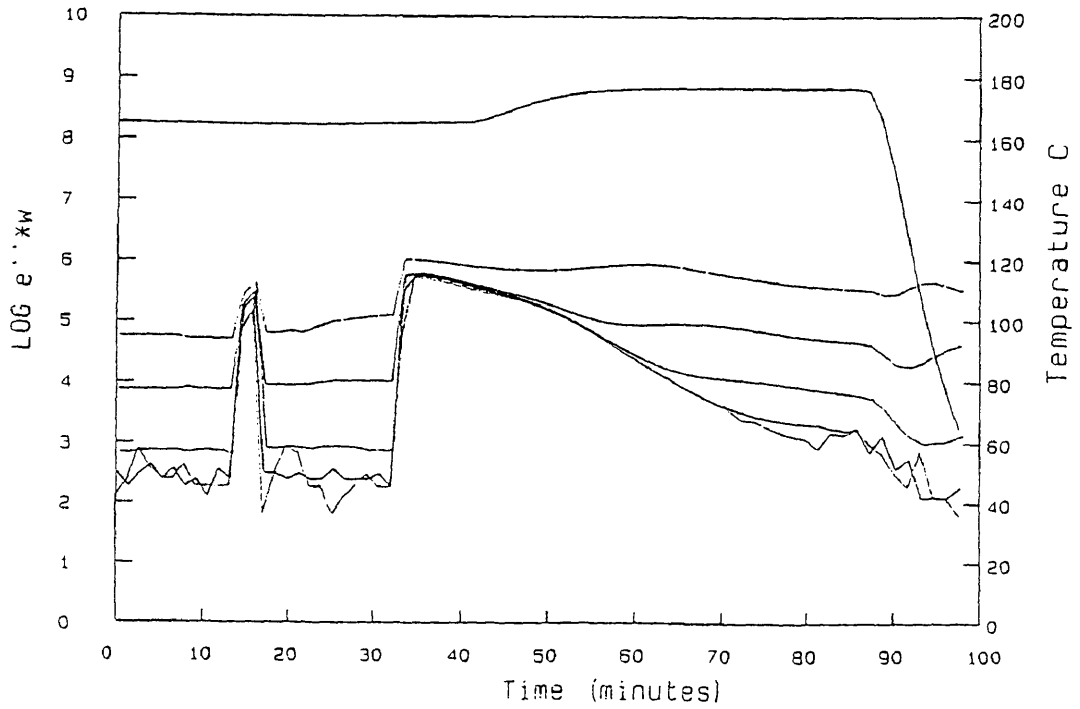


Figure 5.7b

Data file: a:dh032495

Probe: 3

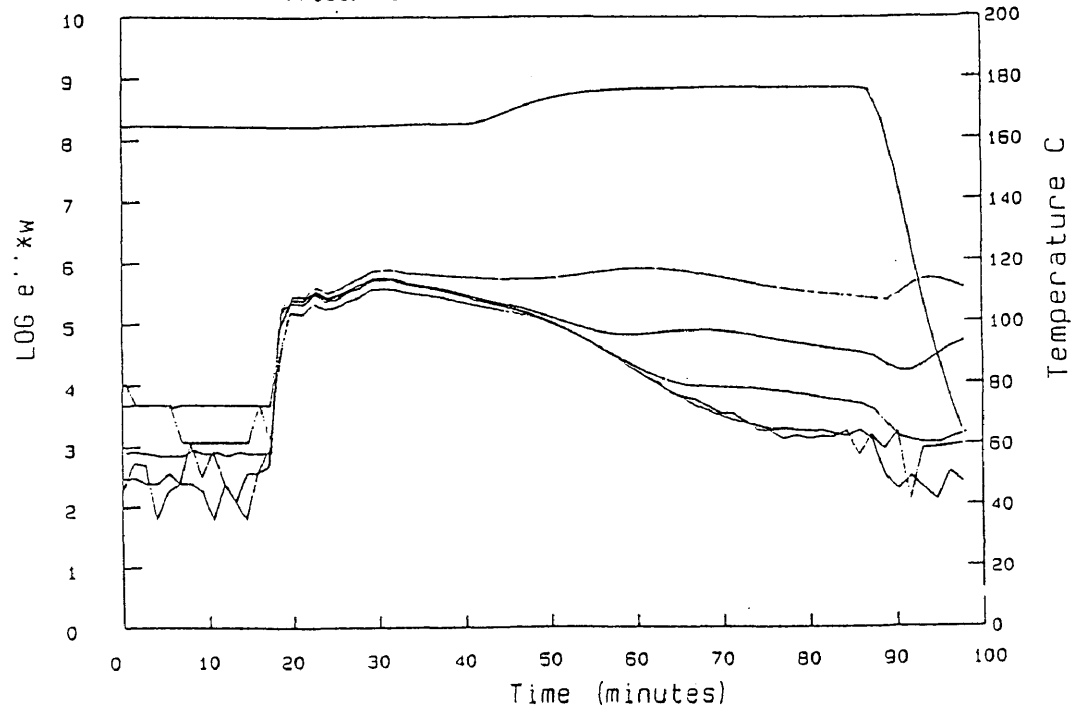


Figure 5.7c

Data file: a:dh032495

Probe: 4

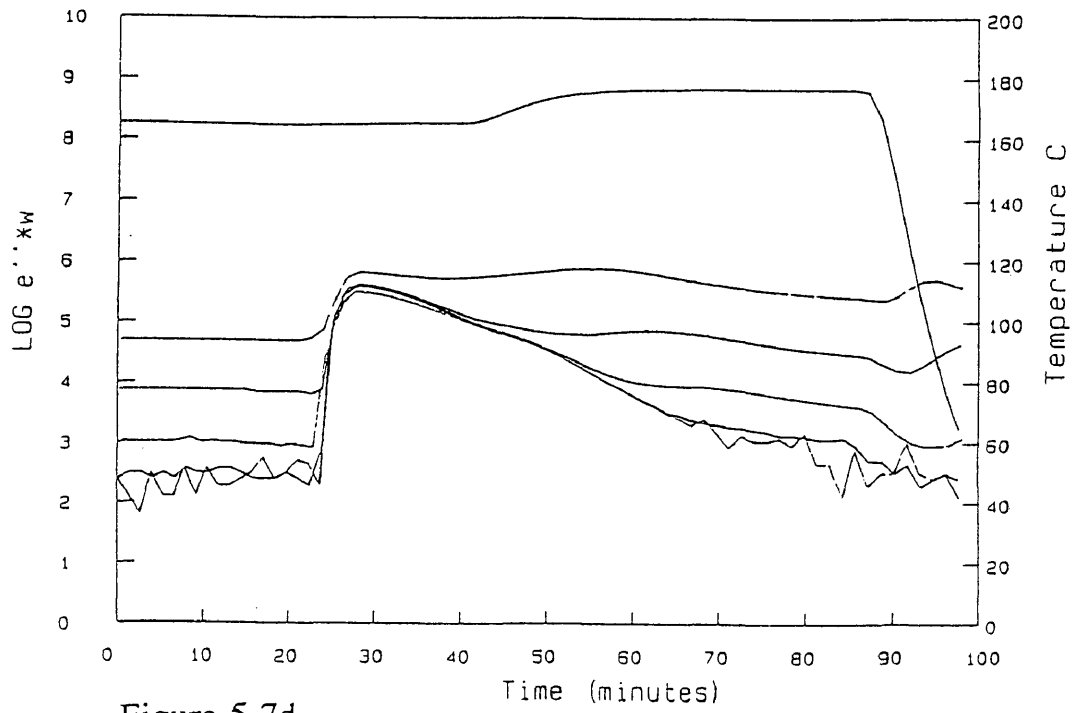


Figure 5.7d

PR500 run dh032495 probe#3

Correlated Viscosity

○ temperaturu ▲ Eta

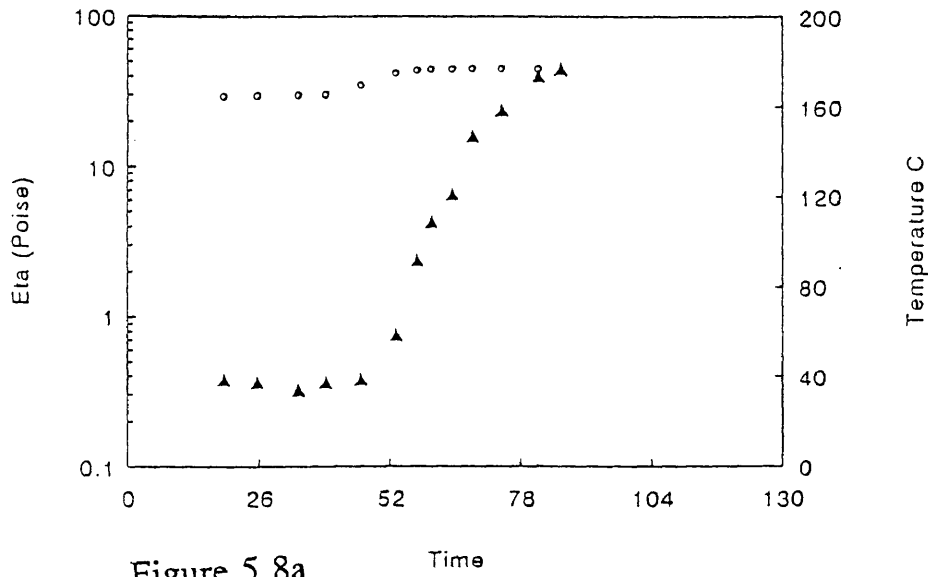


Figure 5.8a

PR500 run dh032495 probe#4

Correlated Viscosity

○ temperaturu ▲ Eta

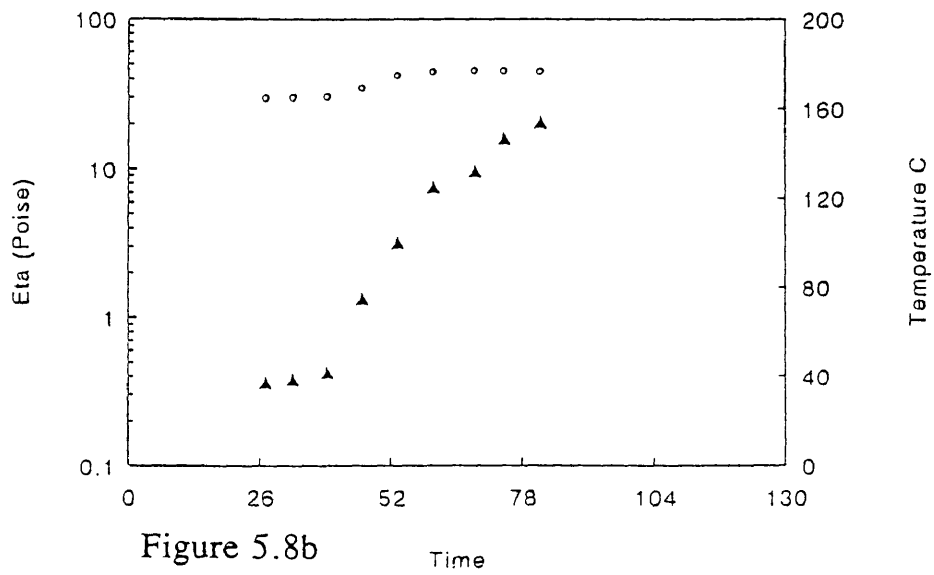


Figure 5.8b

PR500 run dh032495 probe#5

Correlated Viscosity

○ temperatu ▲ Eta

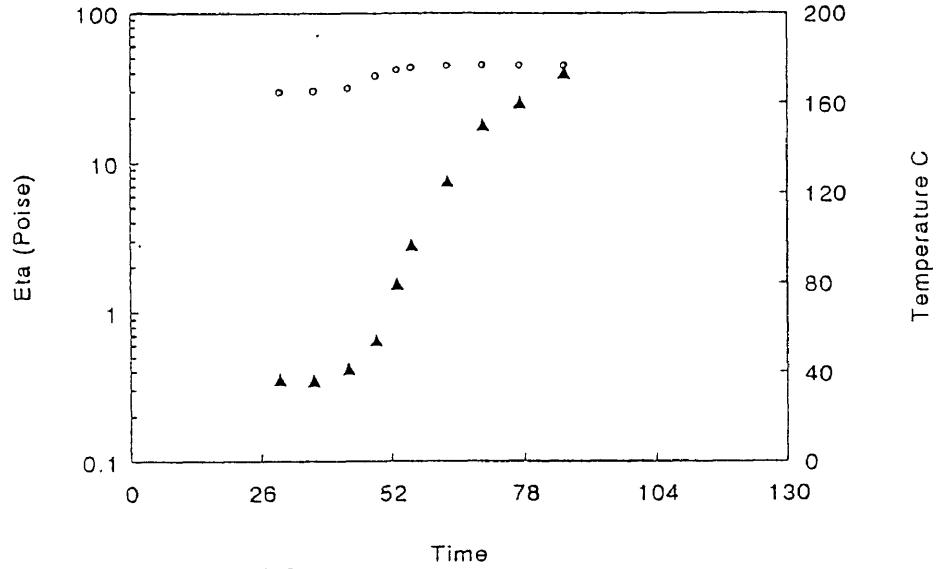


Figure 5.8c

PR500 run dh032495 probe#6

Correlated Viscosity

○ temperatu ▲ Eta

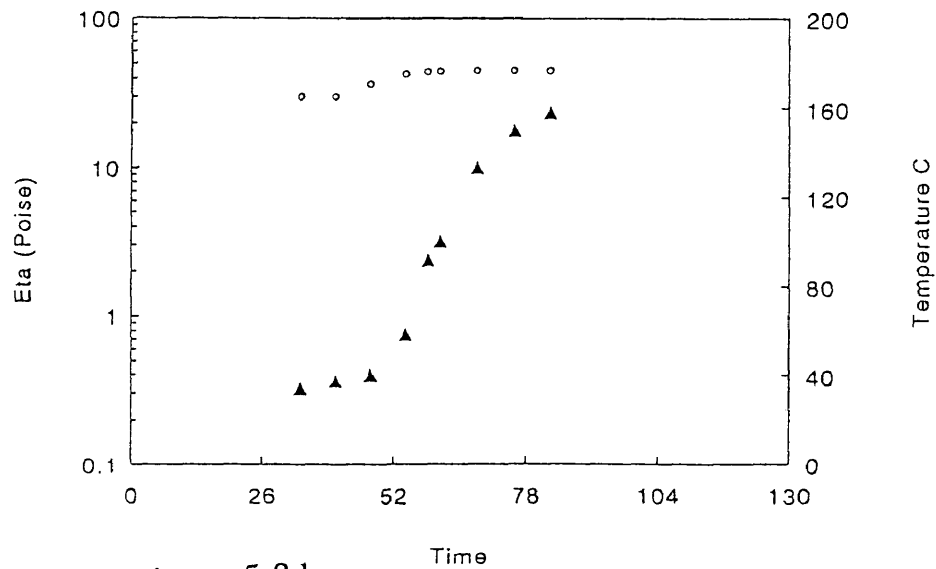


Figure 5.8d

PR500 run dh032495 probe#3

Degree of Cure (alpha)-M

▲ alpha ○ temperature

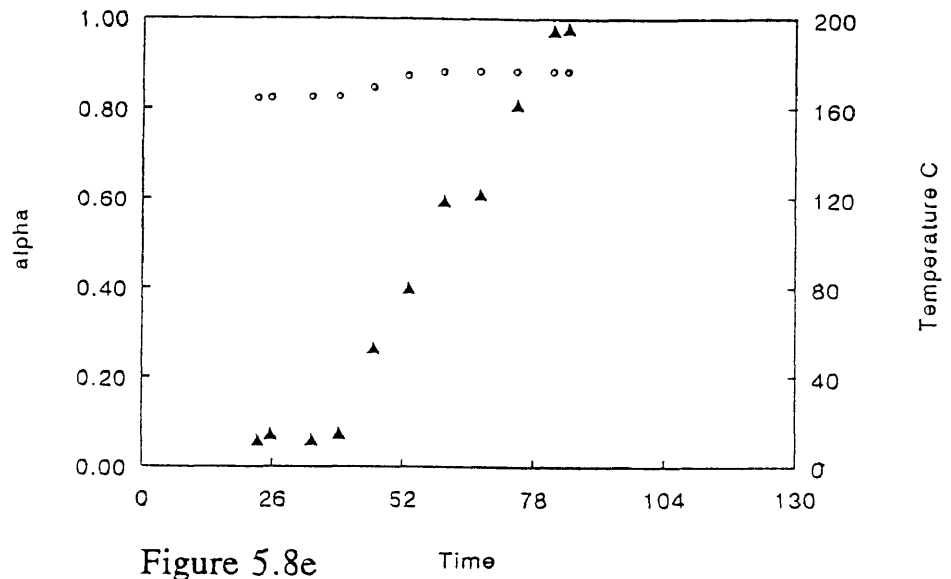


Figure 5.8e

PR500 run dh032495 probe#3

Degree of Cure (alpha)-L

▲ alpha ○ temperature

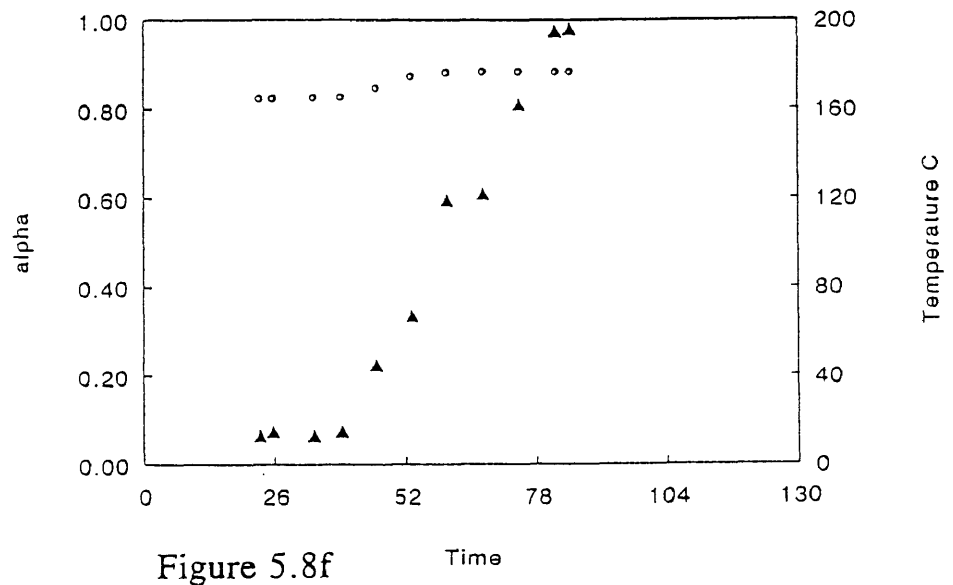


Figure 5.8f

PR500 run dh032495 probe#4

Degree of Cure (alpha)-M

▲ alpha ○ temperature

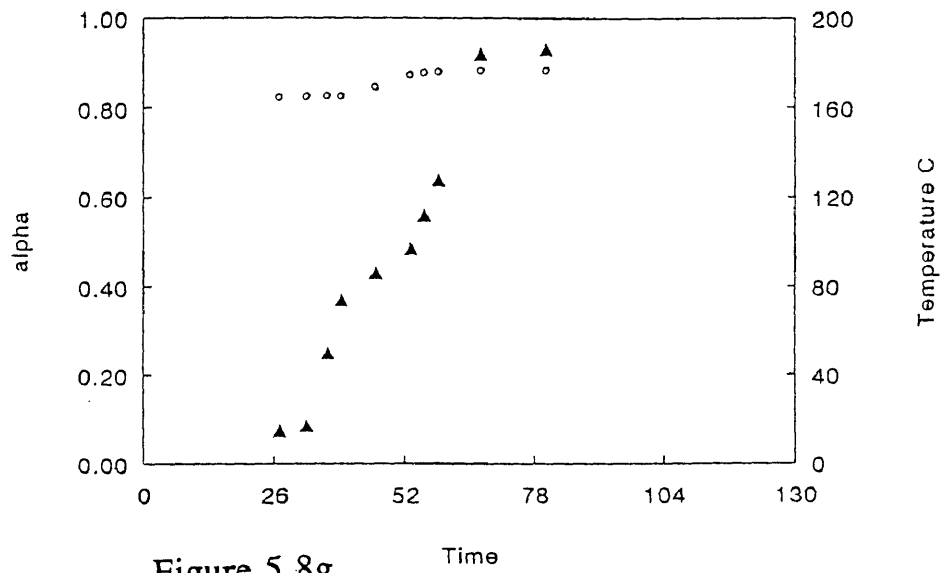


Figure 5.8g

PR500 run dh032495 probe#4

Degree of Cure (alpha)-L

▲ alpha ○ temperature

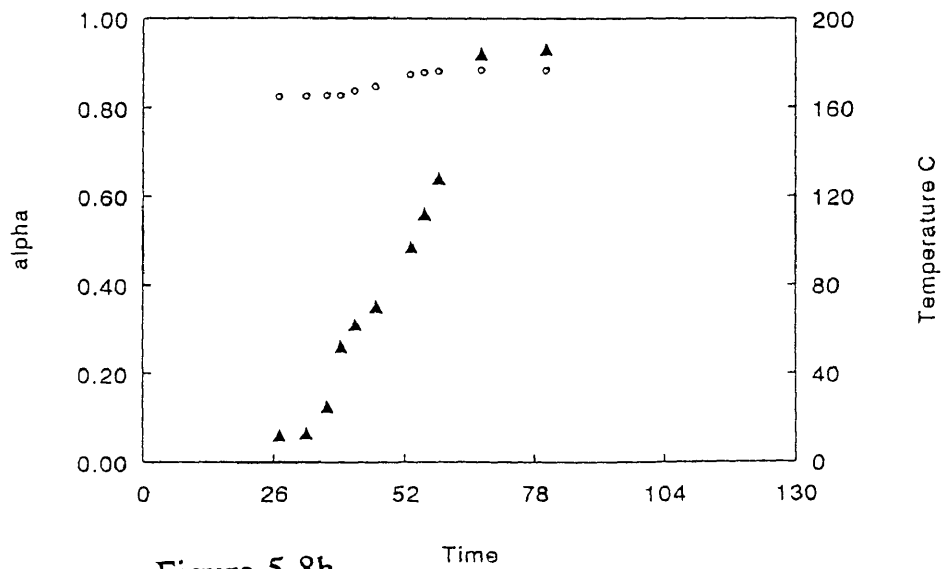


Figure 5.8h

PR500 run dh032495 probe#5

Degree of Cure (alpha)-M

▲ alpha ○ temperature

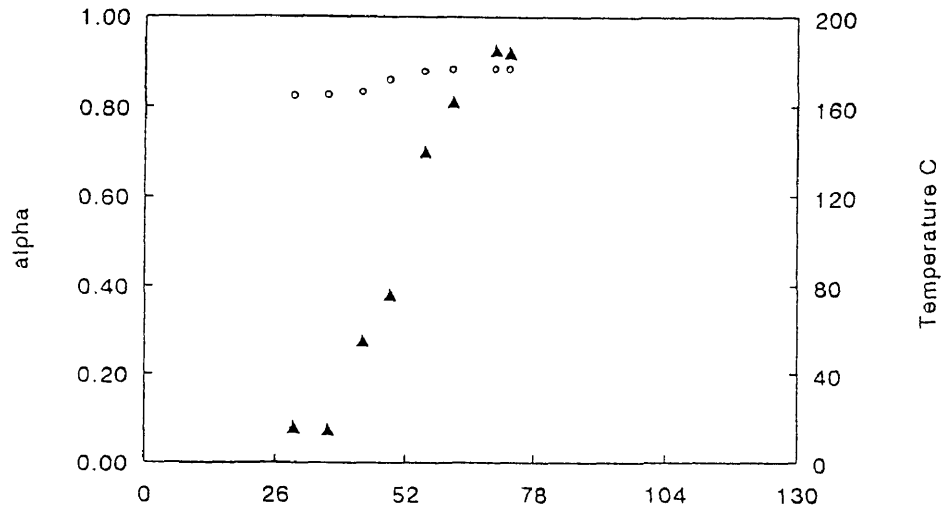


Figure 5.8i Time

PR500 run dh032495 probe#5

Degree of Cure (alpha)-L

▲ alpha ○ temperature

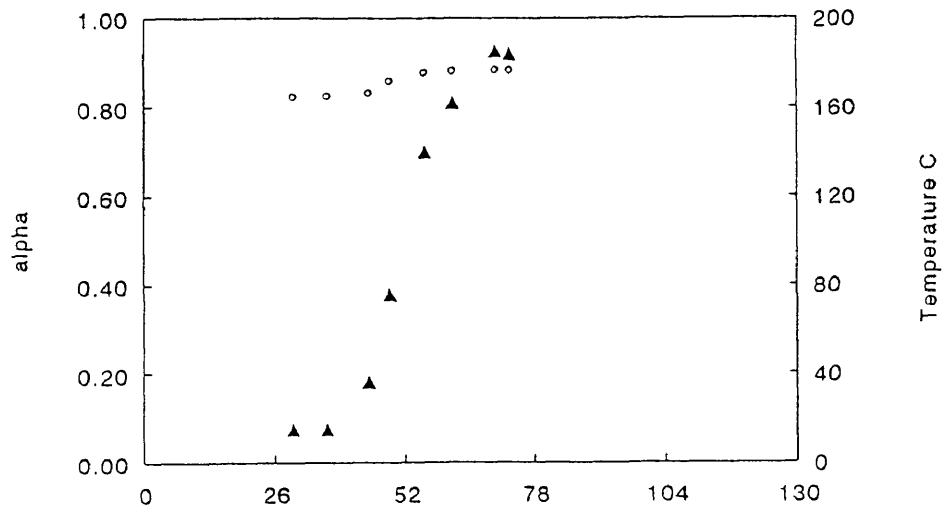
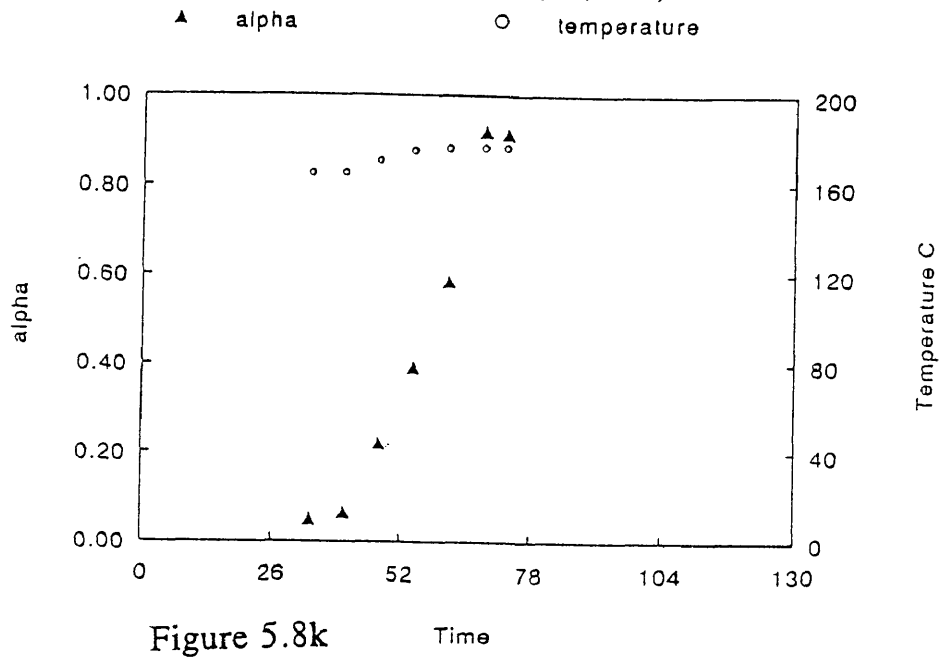


Figure 5.8j Time

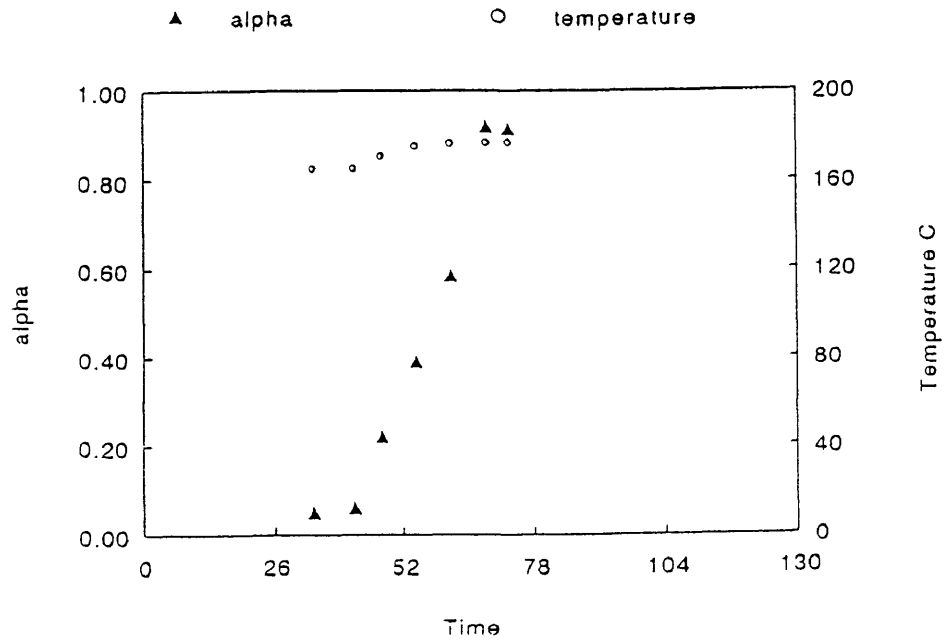
PR500 run dh032495 probe#6

Degree of Cure (alpha)-M



PR500 run dh032495 probe#6

Degree of Cure (alpha)-L



Fourth RTM Run - DH032995

The wetout times for DH032995 are listed in Table 5.5.

Sensor #	Wetout Time (min)
1	18.9
2	32.4
3	33.8
4	53.2
5	46.2
6	36.5

Table 5.5

The resin was injected at a rate of 10 cc/min through the exit port of the plate. Dielectric measurements of the sensors were started at injection. The PR500 resin was injected at a different port during this experiment than in the previous runs. The part fabrication was monitored for approximately 120 minutes. (Figures 5.10a-5.10d) The data was correlated the same as DH071395. (Figures 5.11a-5.11h) Both Mausey and Loos models were used to predict degree of cure. The bridge used to take the dielectric measurements has the capacity to measure four sensors at a time. Therefore, sensor one shows the wetout for both sensors one and five. Sensor two shows wetout for sensors two and six. Since measurements on sensors one and two were stopped after wetout, degree of cure and viscosity can not be

determined. A diagram of the RTM plate is shown below. (Figure 5.12)

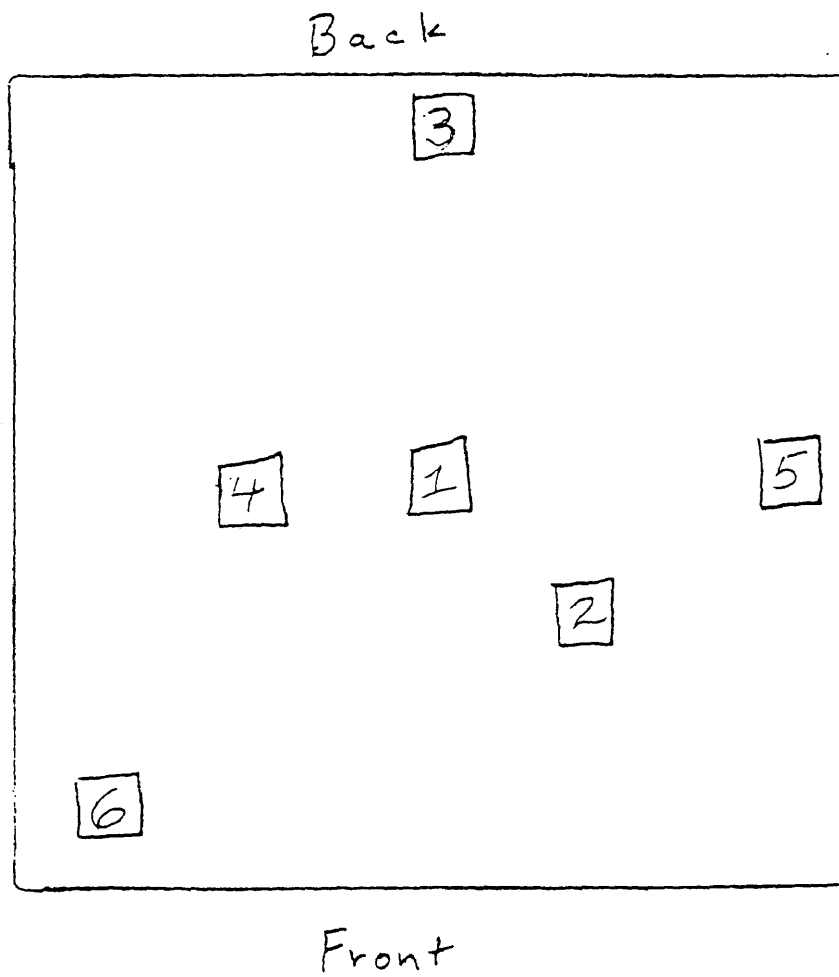


Figure 5.12

Data file: c:\nas32995\dh032995

Probe: 1

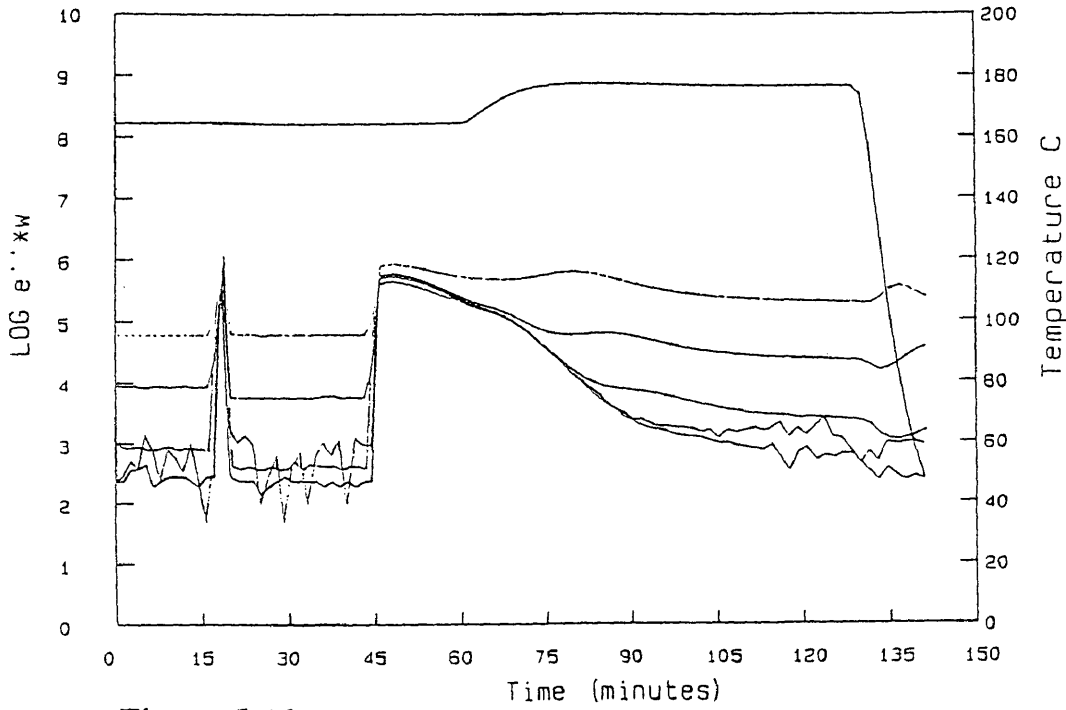


Figure 5.10a

Data file: c:\nas32995\dh032995

Probe: 2

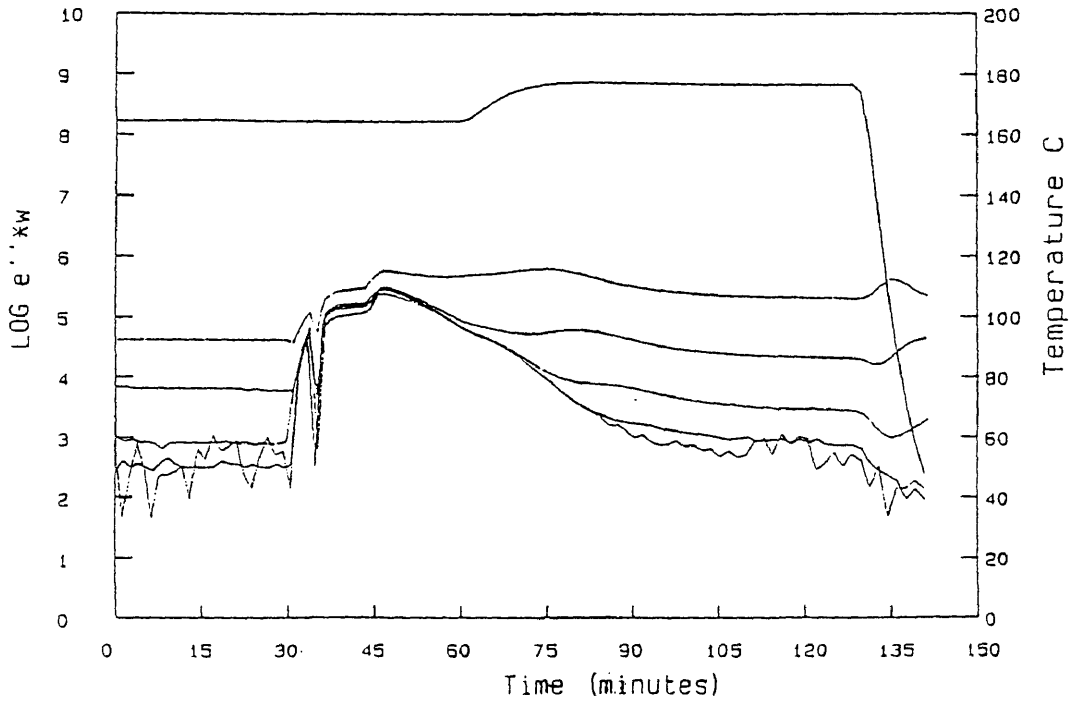


Figure 5.10b

Data file: c:\nas32995\dh032995

Probe: 3

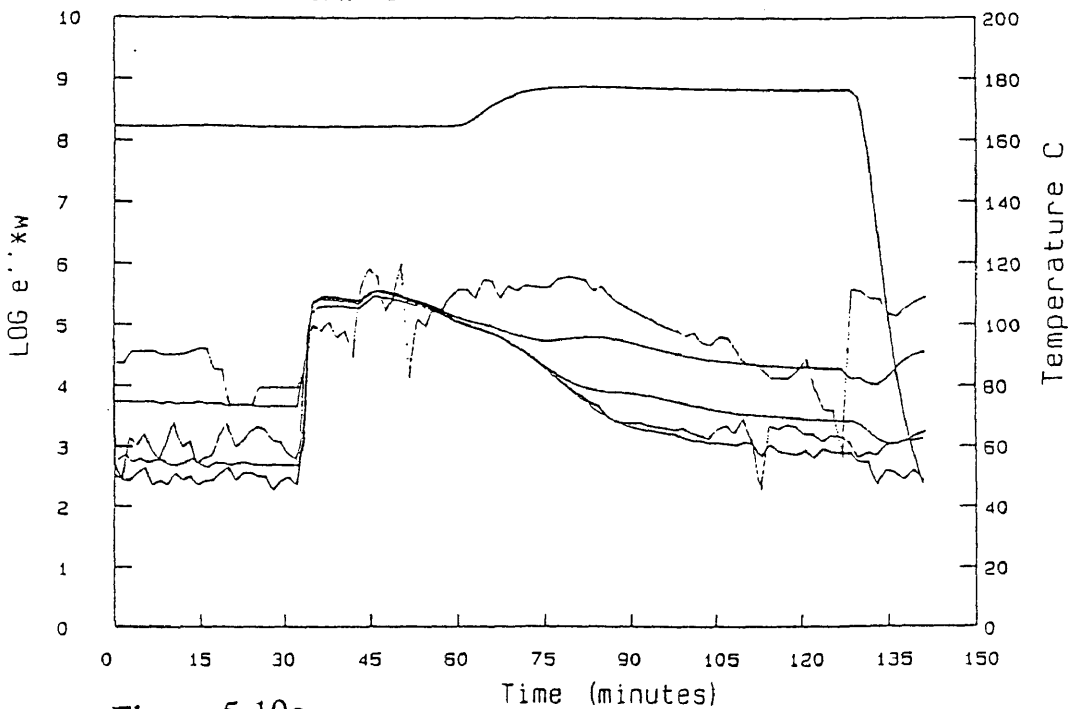


Figure 5.10c

Data file: c:\nas32995\dh032995

Probe: 4

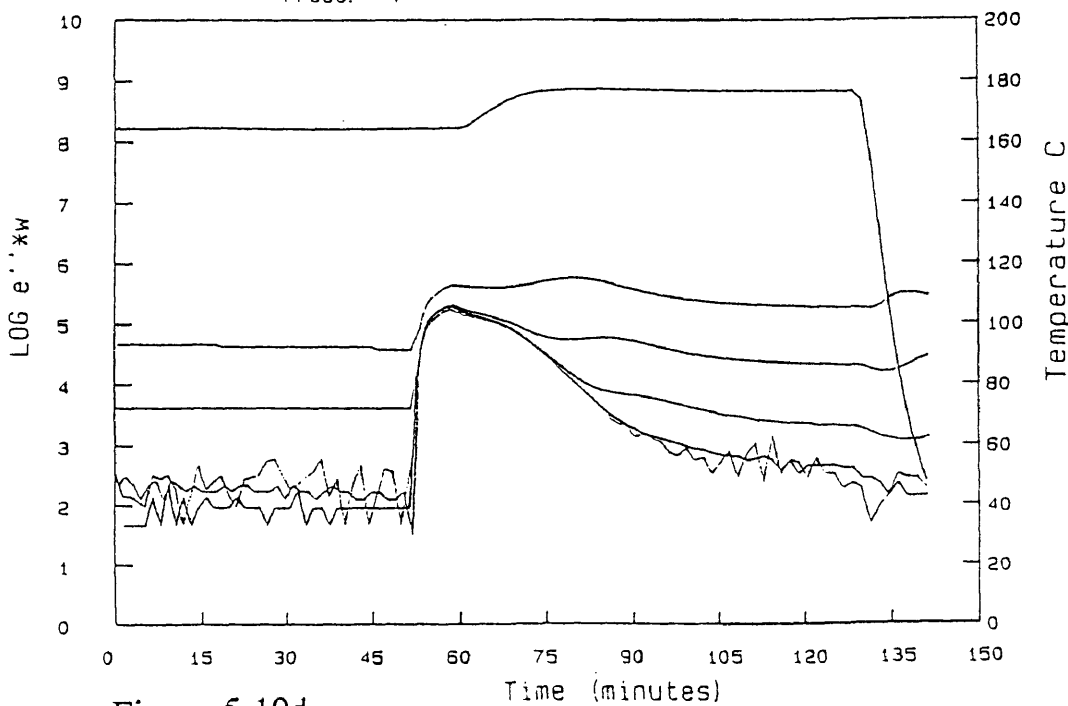


Figure 5.10d

PR500 run dh032995 probe#3

Correlated Viscosity

○ temperatu ▲ Eta

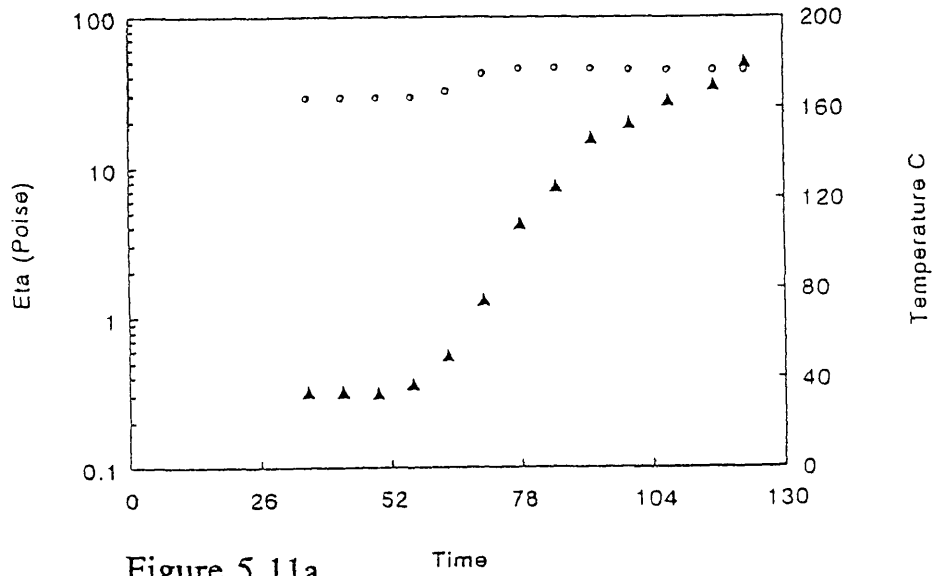


Figure 5.11a

PR500 run dh032995 probe#4

Correlated Viscosity

○ temperatu ▲ Eta

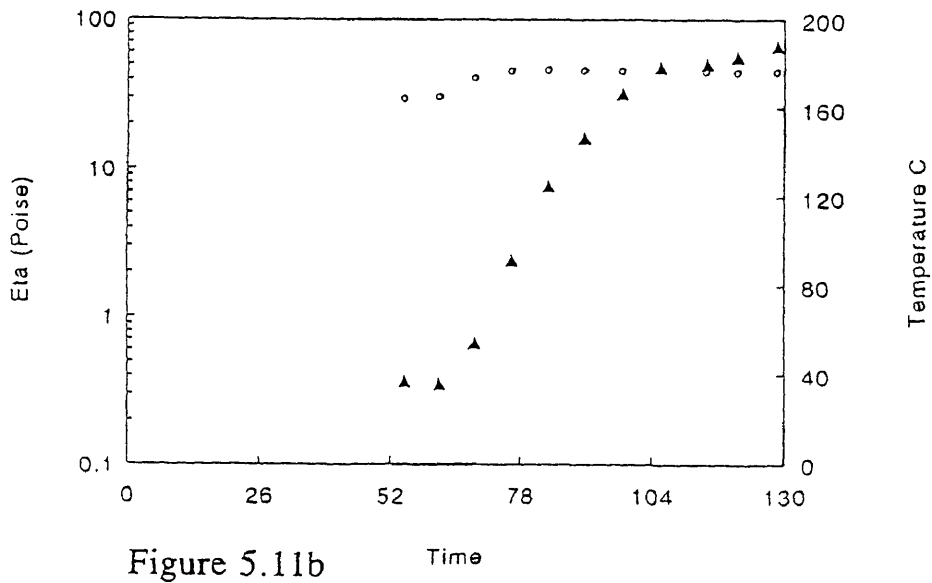


Figure 5.11b

PR500 run dh032995 probe#5
Correlated Viscosity

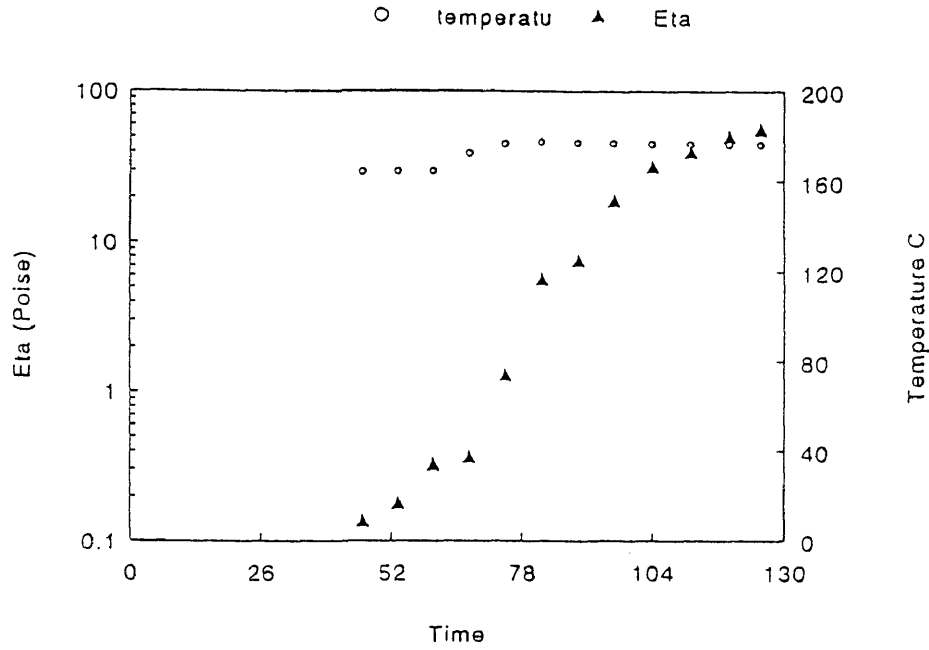


Figure 5.11c

PR500 run dh032995 probe#6
Correlated Viscosity

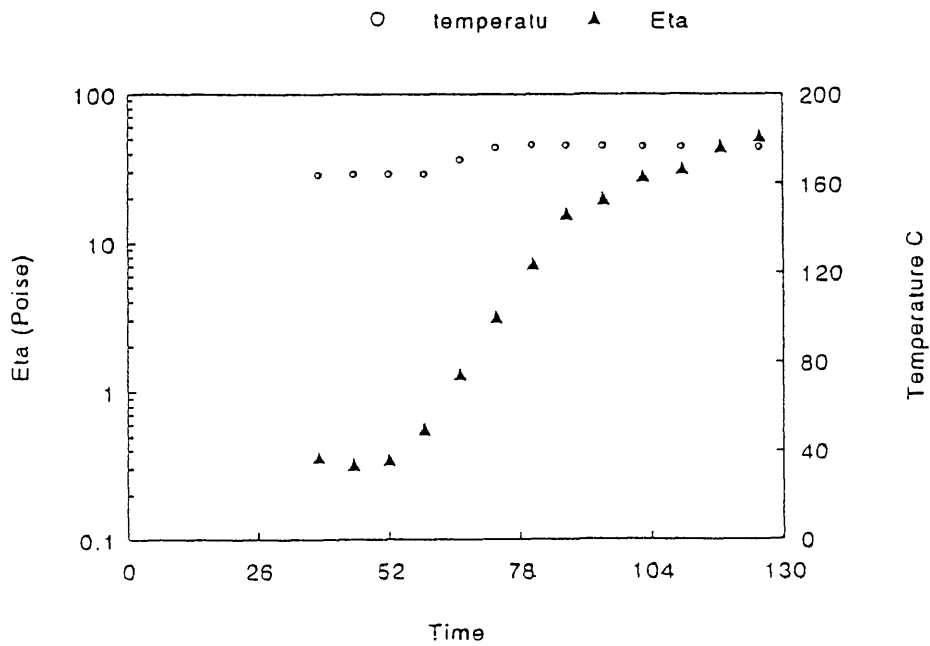


Figure 5.11d

PR500 run dh032995 probe#3

Degree of Cure (alpha)-M

▲ alpha ○ temperature

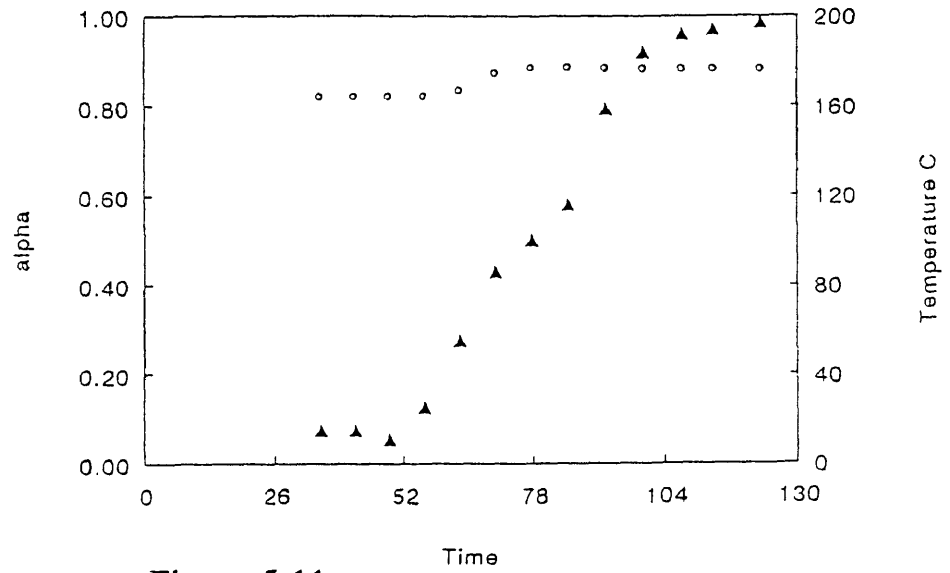


Figure 5.11e

PR500 run dh032995 probe#3

Degree of Cure (alpha)-L

▲ alpha ○ temperature

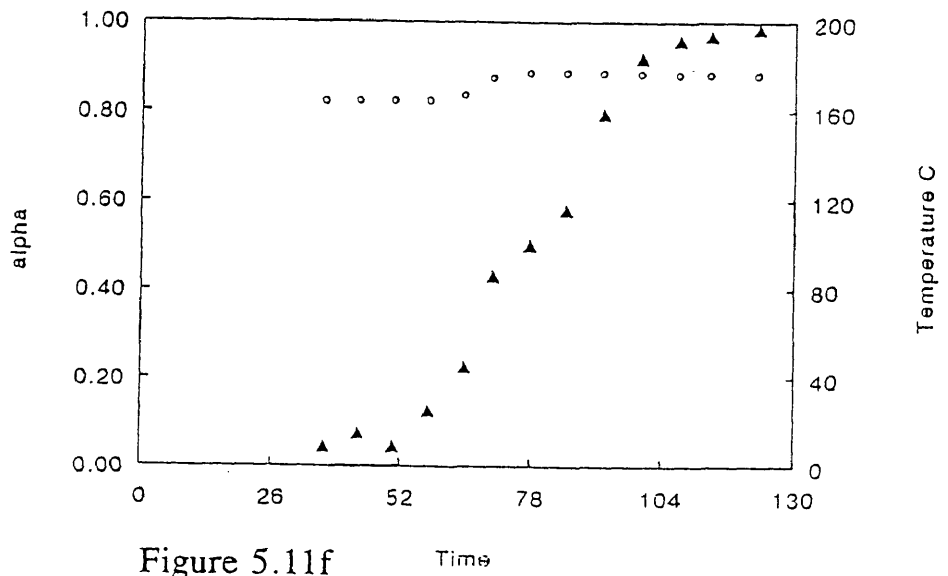


Figure 5.11f

PR500 run dh032995 probe#4

Degree of Cure (alpha)-M

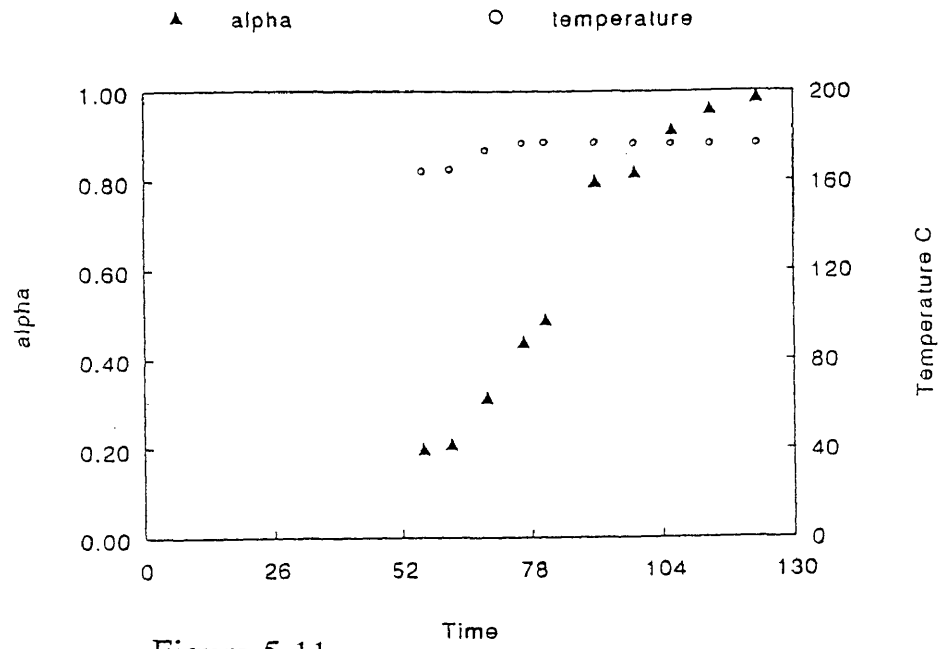


Figure 5.11g

PR500 run dh032995 probe#4

Degree of Cure (alpha)-L

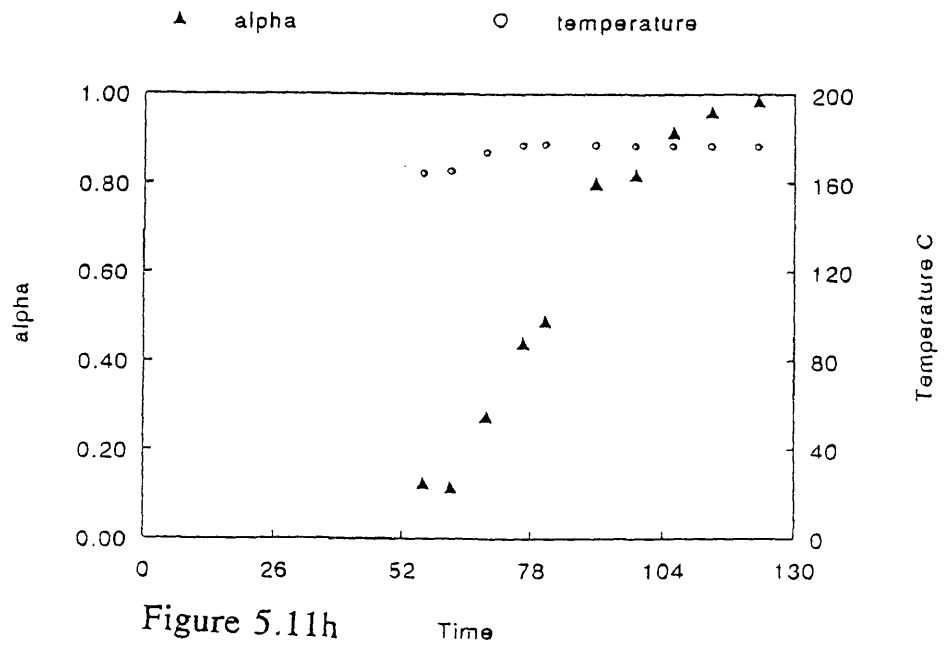


Figure 5.11h

PR500 run dh032995 probe#5

Degree of Cure (alpha)-M

▲ alpha ○ temperature

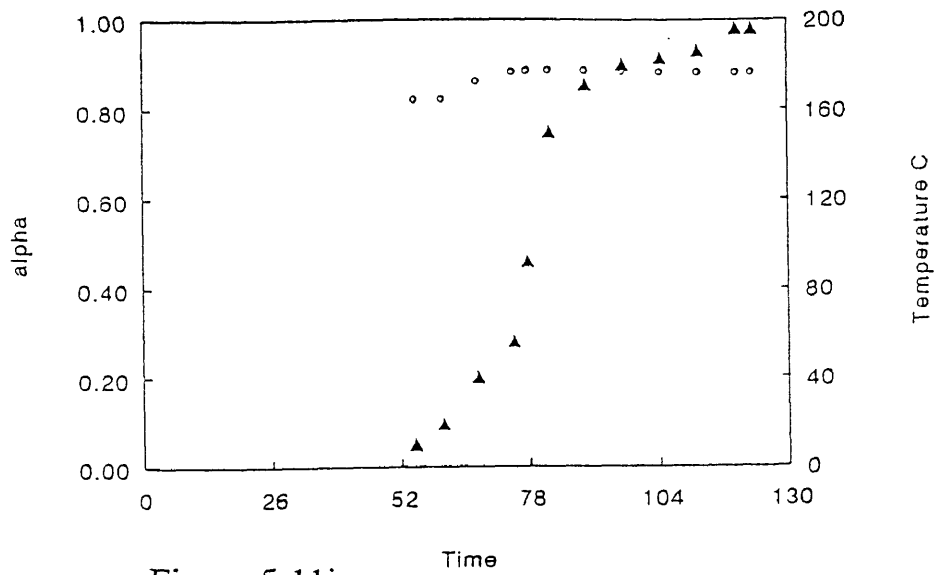


Figure 5.11i

PR500 run dh032995 probe#5

Degree of Cure (alpha)-L

▲ alpha ○ temperature

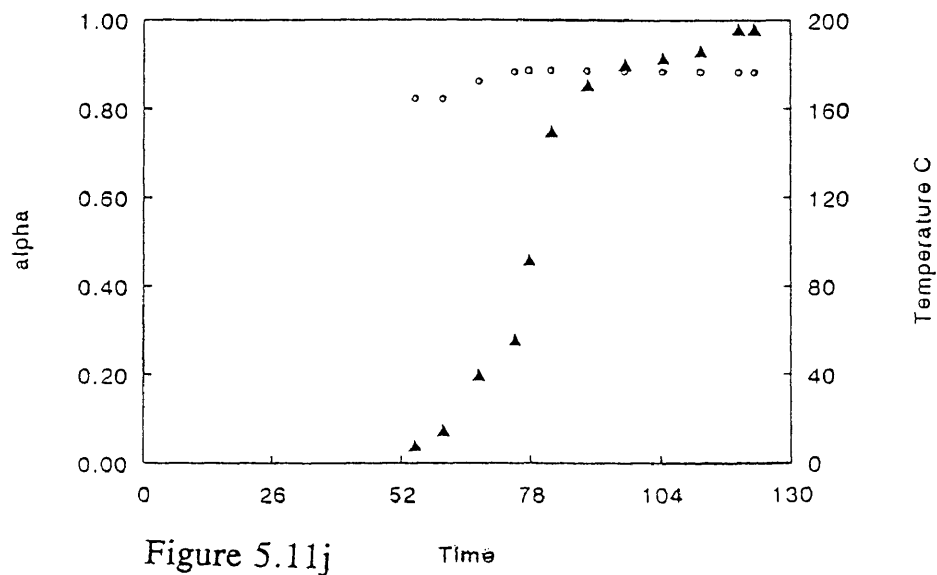


Figure 5.11j

Time

PR500 run dh032995 probe#6

Degree of Cure (alpha)-M

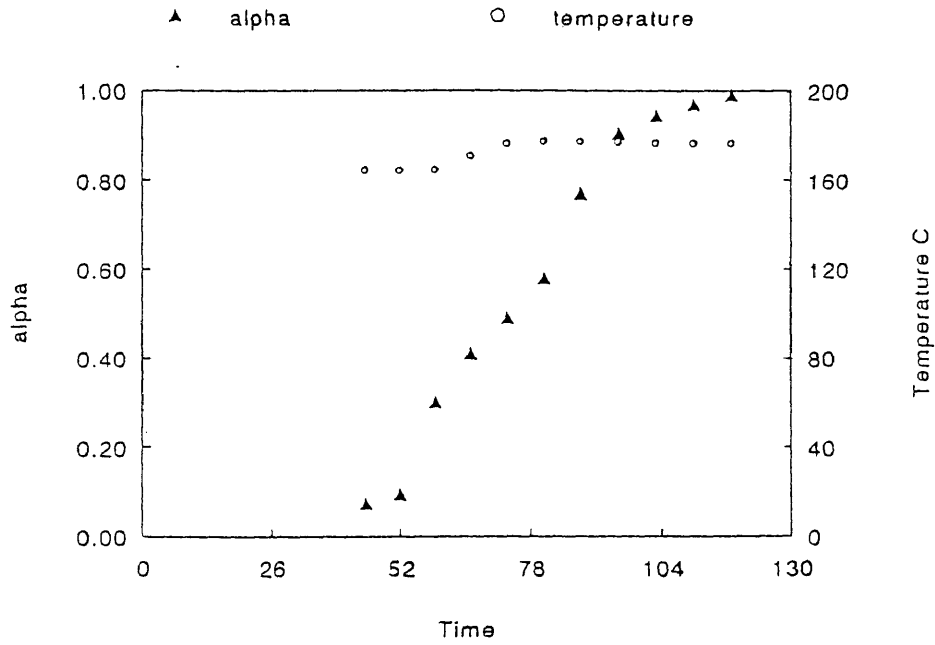


Figure 5.11k

PR500 run dh032995 probe#6

Degree of Cure (alpha)-L

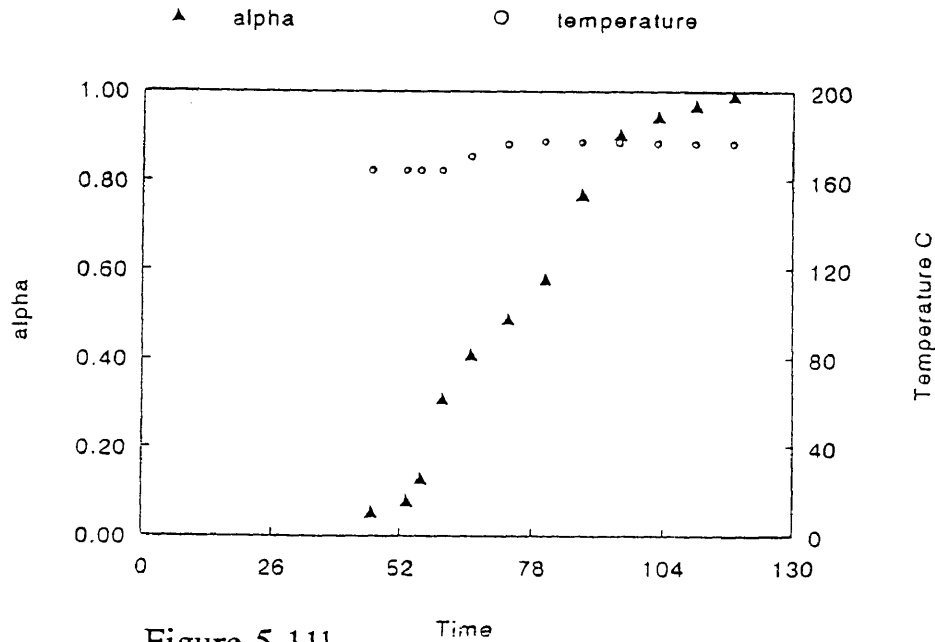


Figure 5.11l

Fifth RTM Run - DH033195

Experiment DH033195 uses a plate with 3 kapton sensors and 2 thermocouples.

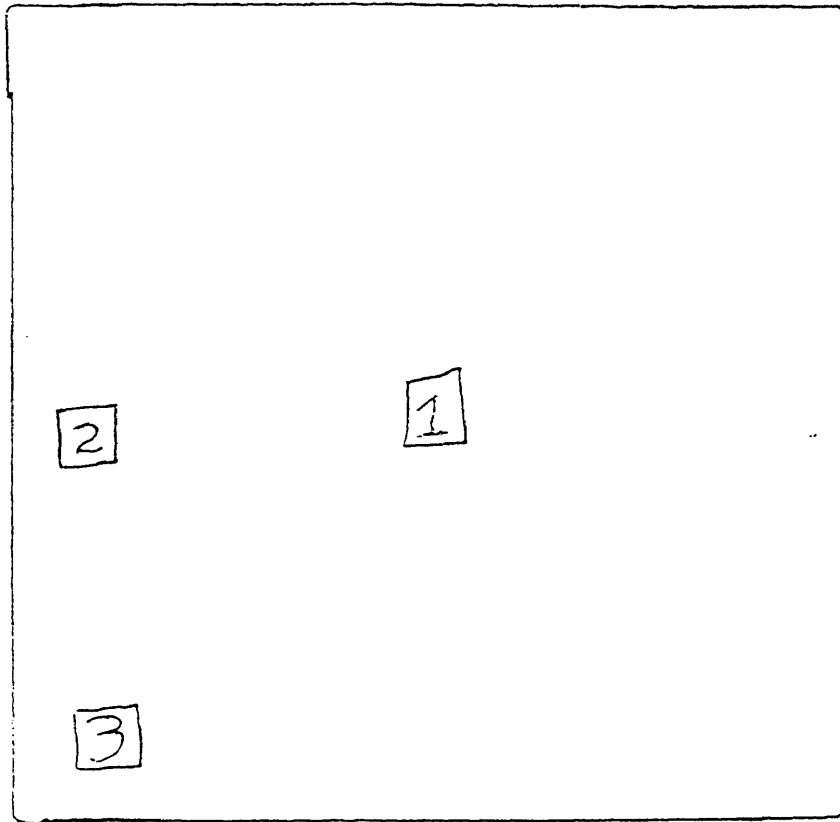
The wetout times for DH033195 are listed in Table 5.6.

Sensor #	Wetout Time (min)
1	13.6
2	34.7
3	---

Table 5.6

The resin was injected at rate of 10 cc/min through the exit port of the plate. Dielectric measurements of the sensors were started at injection. The part fabrication was monitored for approximately 100 minutes.(Figures 5.13a-5.13c) The data was correlated the same as DH071395.(Figures 5.14a-5.14f) Both Maussey and Loos models were used to predict degree of cure. A diagram of the RTM plate used is shown below.(Figure 5.15)

Back



Front

Figure 5.15

Data file: c:\nas33195\dh033195
Probe: 1

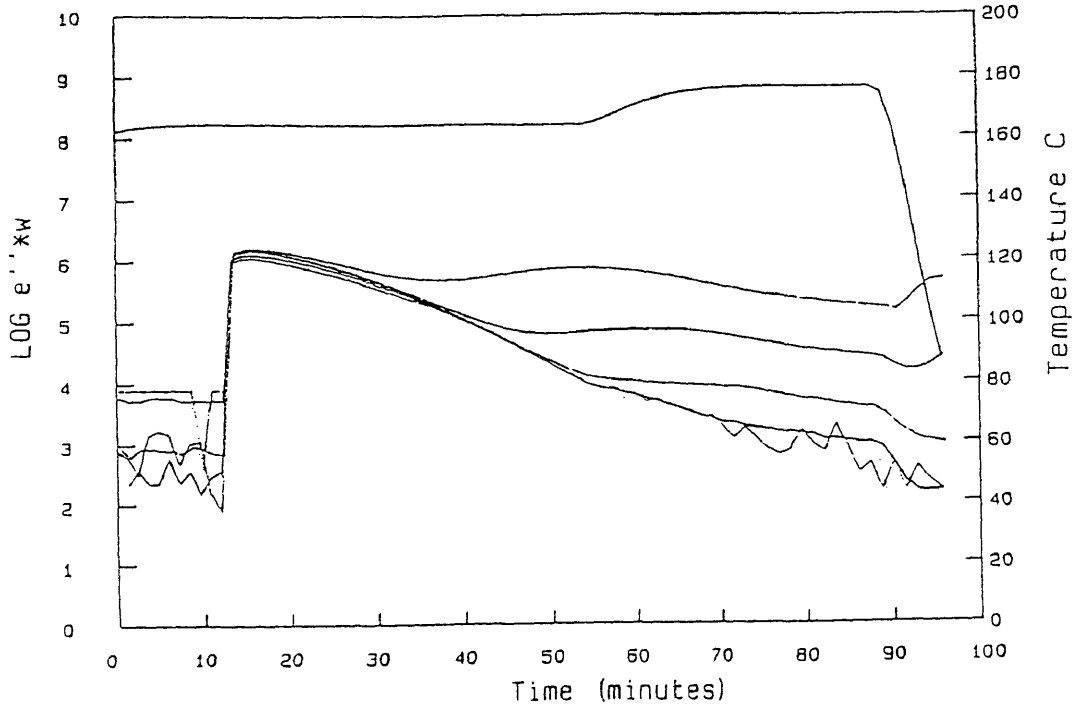


Figure 5.13a

Data file: c:\nas33195\dh033195
Probe: 2

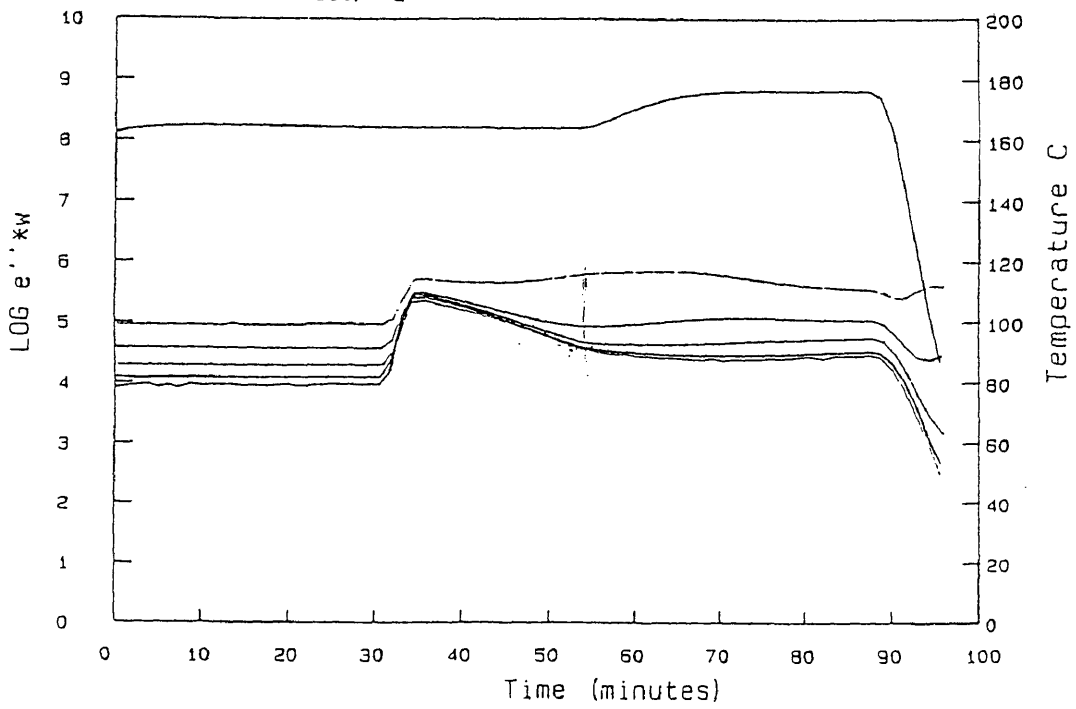


Figure 5.13b

Data file: c:\nas33195\dh033195
Probe: 3

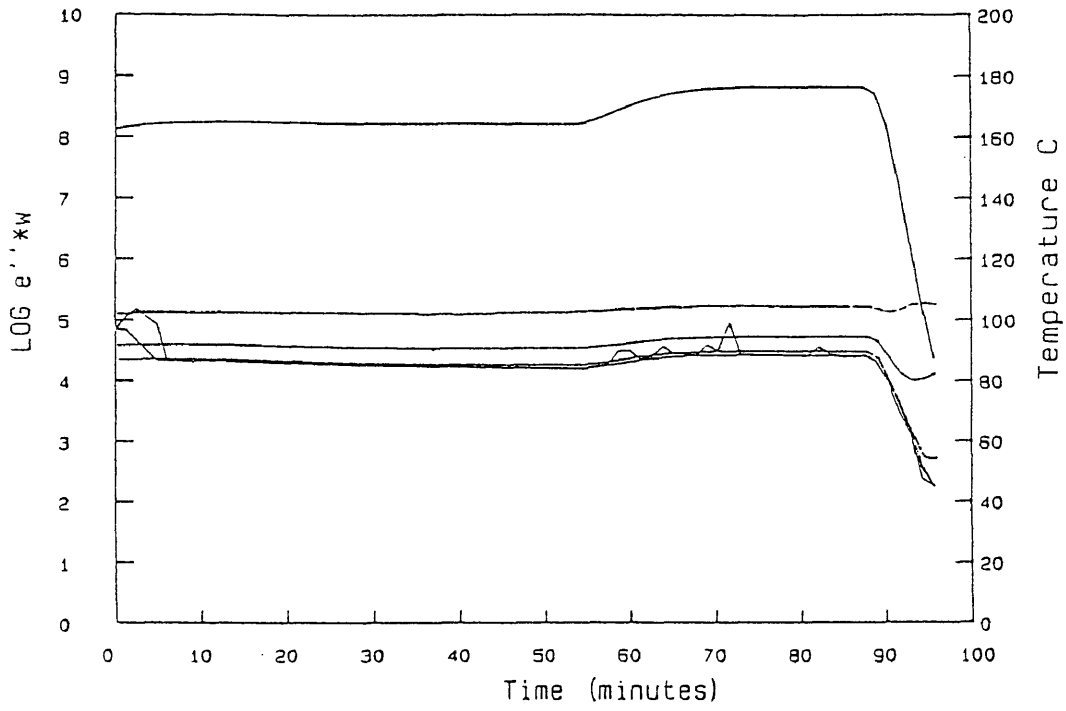


Figure 5.13c

PR500 run dh033195 probe#1

Correlated Viscosity

○ temperatu ▲ Eta

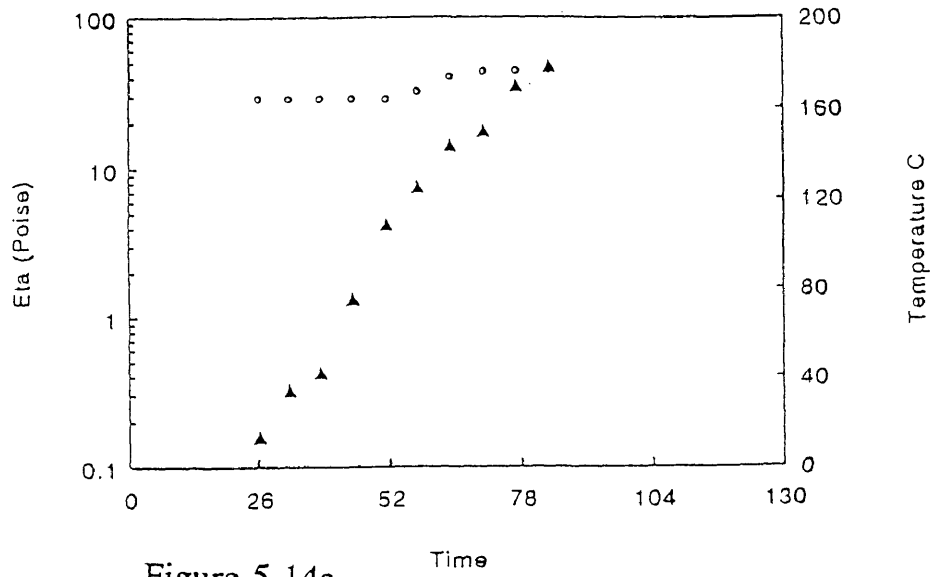


Figure 5.14a

PR500 run dh033195 probe#2

Correlated Viscosity

○ temperatu ▲ Eta

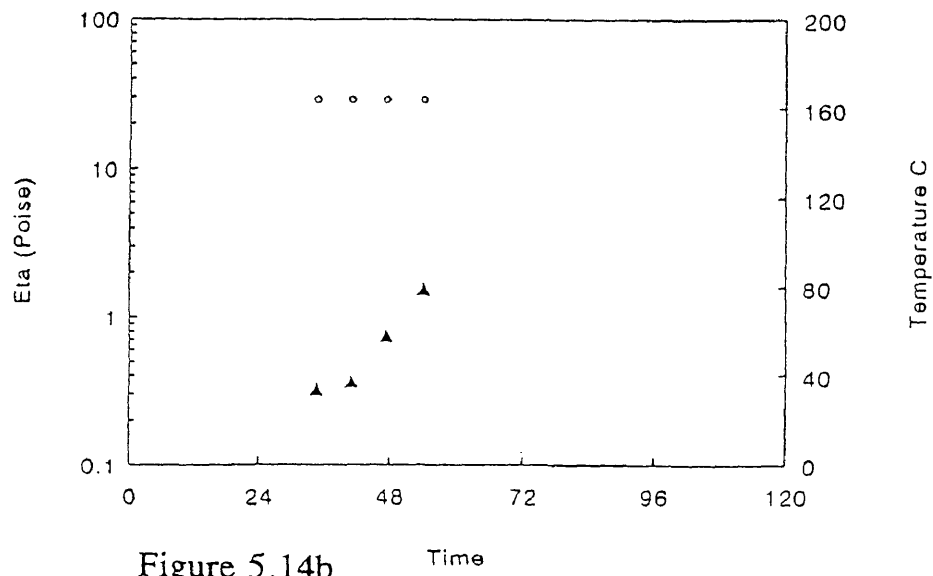


Figure 5.14b

PR500 run dh033195 probe#1

Degree of Cure (alpha)-M

▲ alpha ○ temperature

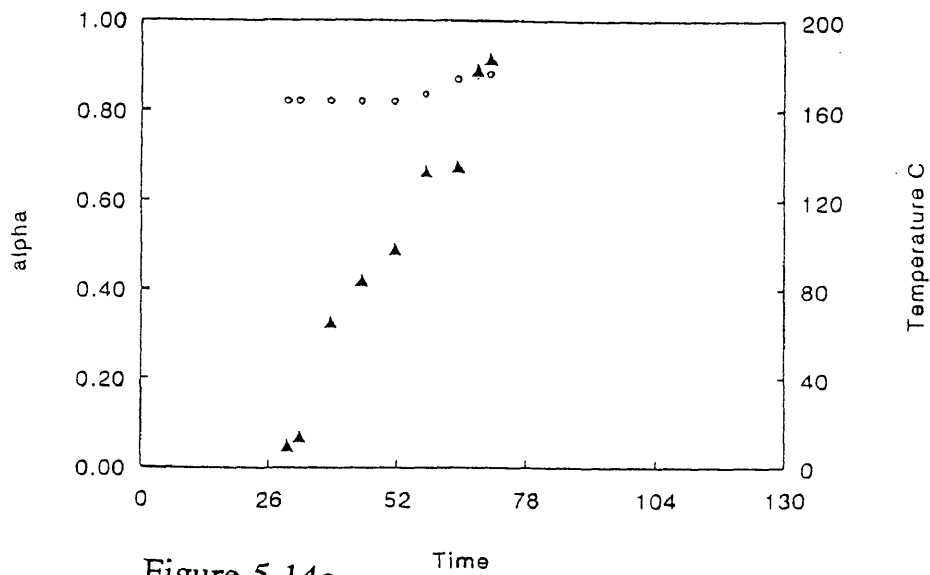


Figure 5.14c

PR500 run dh033195 probe#1

Degree of Cure (alpha)-L

▲ alpha ○ temperature

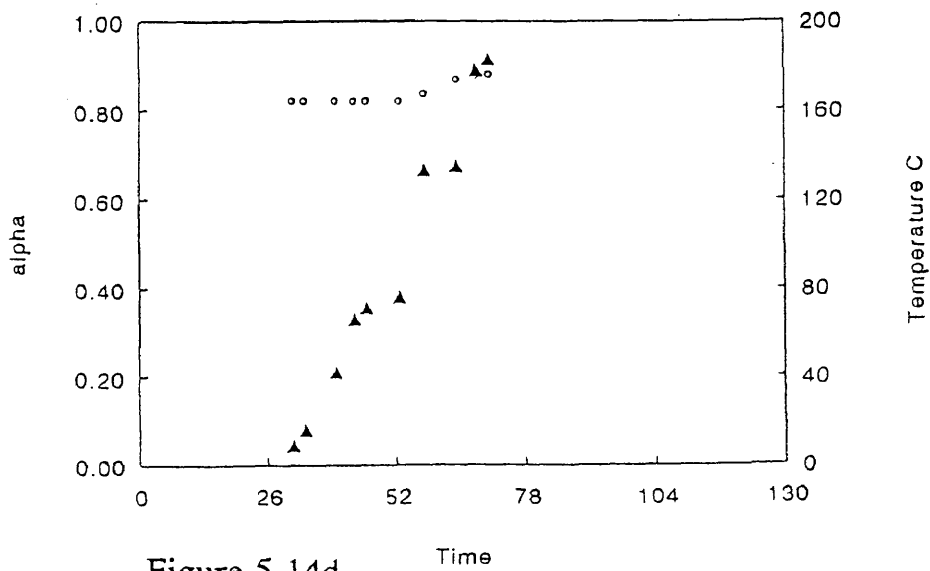


Figure 5.14d

PR500 run dh033195 probe#2

Degree of Cure (alpha)-M

▲ alpha ○ temperature

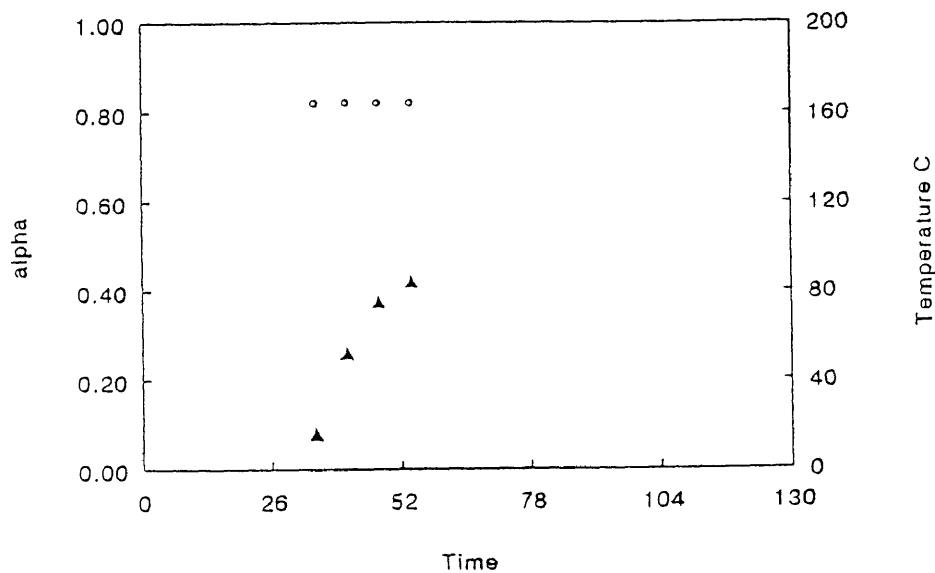


Figure 5.14e

PR500 run dh033195 probe#2

Degree of Cure (alpha)-L

▲ alpha ○ temperature

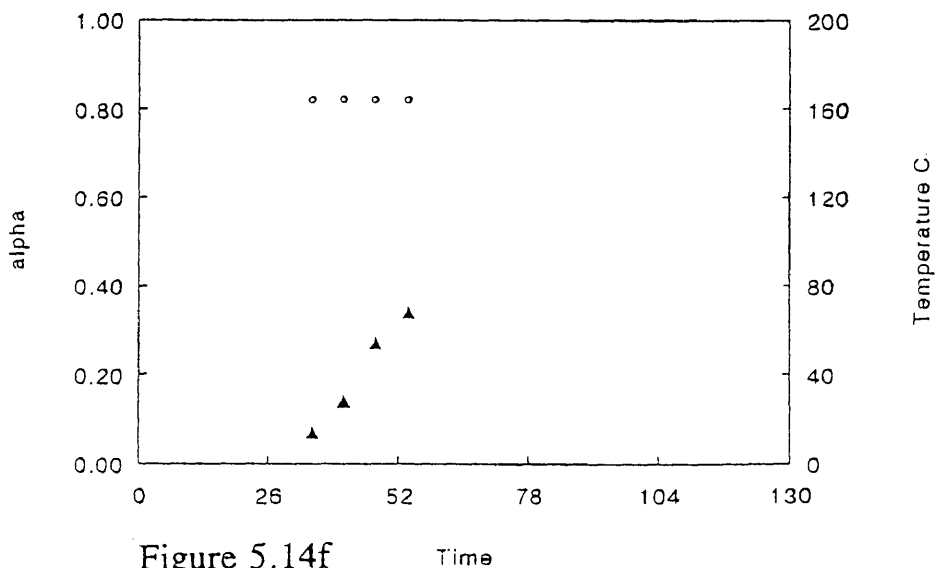


Figure 5.14f

VI. Conclusions

The different injection conditions of the resin transfer molding experiments enable the prediction and verification of many different resin characteristics. DH071394, DH012795, and DH032495 were injected at the front of the plate with a flow rate of 20 cc/min. DH071395 and DH032495 exhibited similar wetout times, while experiment DH012795 took a considerably longer time to reach wetout. During the experiment DH012795, the resin was not degassed. There may have been air trapped in the resin causing the resin to flow slower despite the constant injection rate. This would cause the sensors to take longer to wetout. Experiment DH071394 used a different frame style, frame II, than the other two experiments. The frame had a groove in which the resin was suppose to fill and then flow to the sensors. If this happened, then the sensors would take longer to wetout. Instead, the wetout time was close to that of experiment DH032495. Therefore, the groove did not prolong wetout. No differences between the grooved plate and the non-grooved plate were observed.

DH032995 and DH033195 both had the resin injected at the exit port of the plate. The rate of injection was 10 cc/min for both of these experiments.

DH032995 took longer to wetout than the experiments that had resin injected at the front port. The longer wetout time would require more time to work with the part during the fabrication than the previous style of injecting the resin. DH033195 did not show the same results. More testing would have to be done to assure that injecting the resin from the exit port would require more time to work with the part.

All patterns of injection and flow rates are acceptable because viscosity on all sensors is below one poise at wetout. If there is viscosity buildup before all parts of the plate fully wetout, then that particular flow pattern would be riskier than the other patterns attempted. This situation would result in incomplete resin infiltration of the mold.

The sensors in experiments DH071394 and DH032495 approached full cure at approximately 75 minutes. Experiment DH033195 also showed close to full cure in sensor one at approximately 75 minutes. Full cure in experiments DH012795 and DH032995 was seen at approximately 105 minutes. Despite the injection pattern, the late cure in DH012795 again was probably seen because the resin was not degassed. DH033195 used resin that had been heated prior to this experiment. This led to the conclusion that the resin had advanced prior to this experiment giving an earlier cure time.

The flow of the resin did not seem to have an effect on the wetout of the resin. When the rate was doubled, wetout time should decrease by one-half. This pattern

was not observed. The increase in flow may have led to a resistance, therefore not causing a decrease in wetout time.

It was found that for all injection plans the viscosity remained low until complete infiltration of the plate and full cure was nearly attained. Experiments DH012795 and DH032995 gave the longest wetout times. Therefore, the mold required more time to be infiltrated. From this study, the optimal conditions of PR500 injection in the RTM are the front port of the plate with a steady flow of 20 cc/min. Although the resin cured faster under these conditions, the time and pattern of curing is more consistent.

VITA

Rhonda Michelle Barksdale

Rhonda Michelle Barksdale was born in Lynchburg, Virginia, June 20, 1972. She graduated from Randolph Henry High School, Charlotte Court House, Virginia as salutatorian in June 1990. She earned a Bachelors of Science degree in Chemistry at the College of William and Mary in Williamsburg, Virginia in May 1994. Afterwards, she enrolled in the Chemistry Graduate Program as a candidate for a Master of Arts at the College of William and Mary and fulfilled requirements in August 1995.